C O N T E N T S

KZESO IS 90!
(Interview with the head of PrJSC KZESO Mikitin Ya.I.)

This year we celebrate 90 years from the day of establishment of KZESO — acknowledged world leader in the field of creation and manufacture of suspended and stationary rail welding machines. In respect of a jubilee the editorial board initiated an interview with a Head of Board of Private Joint Stock Company «Kakhovka Plant of Electric Welding Equipment», Hero of Ukraine Mikitin Ya.I., which we believe will be interesting to the readers.

Yarosvav Ivanovych, please, tell how the plant was founded, what stages of its establishment and development can be outlined?

On September 1, 1929, Kakhovka Artisan-Industrial School (till 1914 it was a plant of agricultural equipment of merchant I. Gurevich), which provided training of the basics of metal and woodworking, manufactured and repaired different agricultural equipment, started on its territory commercial production of piston rings for tractor engines. We assume this date as a Plant's birthday.

In the beginning of the 1950th Kakhovka Plant «Avtotraktorodetal No.22» was renamed as Kakhovka Repair-Mechanical Plant and its activity came under the administration of «Dniprobud», which at that moment took part in construction of Kahovka HPP. At the same time, there was reconstruction of the enterprise following the set general plan, its area was expanded, engineering buildings, boiler house, storehouses were constructed, new lines were laid. The result of these reforms was increase of number of subdivisions, engineer specialists and the main thing was a real perspective of transformation of plant into multibusiness enterprise.

«Welding» history of KZESO has started from 1959, when by the initiative of B.E. Paton specialization of the Plant was changed and it started output of electric welding equipment. Was it a happy coincidence — choice of a small plant from Ukrainian province for manufacture of new welding equipment?

A life-changing for the Plant governmental decree No. 624 «On further implementation into production of welding engineering» was issued on July 5 (August 15) 1959 following a request of E.O. Paton Electric Welding Institute (PWI) and personally its Director B.E. Paton, who managed to see in a small machine-building enterprise on the South of Ukraine the potential for mastering new type of production. The Plant equipped by that time with novel production equipment, competent staff and oriented on implementation of modern technologies, was ready to become an area for fulfillment of governmental program on manufacture of welding equipment.

On January 1, 1960 Kakhovka Mechanical Plant was renamed as the Plant of Electric Welding Equipment. At that time, still Soviet enterprise started to demonstrate their products at international exhibitions, namely A482 automatic machine in Swedish city Goteborg, automatic device ABS with power supply in Dutch city Utrecht.

What did cooperation with PWI give to the Plant?

In January 1964 Kakhovka Plant of Electric Welding Equipment created a branch of research design —

technological bureau of PWI of the National Academy of Sciences of Ukraine. The main aim is to provide as soon as possible implementation into production of the achievements of science and technology, strengthen the connections of scientific and design organizations with production for successful mastering of new welding equipment. Created at that time powerful tandem of science and production became a starting point in modern success of KZESO. An engineering center was created at the Plant to mobilize engineering findings. Its work in tight cooperation with PWI (in particular, with department No.26 headed by Acad. of the NAS of Ukraine S.I. Kuchuk-Yatsenko) significantly reduced the terms necessary to realize technical ideas. The breakout to the world market was, first of all, possible due to the fact that we in proper time understood that in order to be competitive it is necessary to have modern science, qualified staff, first-rate ideas, novel technologies and well-equipped production.

Development of rail welding machines requires complex efforts in design, construction and creation of welding technology, etc. How did you manage to form a team for solution of such complex tasks? How do you attract youth to the Plant?

We always present our Plant as a high-tech enterprise that, certainly, stipulates presence of professional staff at each step of manufacture of welding equipment. Today, approximately 50 % of workers have professional technical education and almost 25 % are the specialists with higher education. This allows solving different technical problems; accept the challenges of continuous technological development. Our designers, technologists, engineers constantly improve their qualification level, master new programs for designing.

I would like to notice that a lot of family dynasties work at our enterprise. No matter how pathetic it may

be, but experience of manufacture of welding equipment hands on from grandfathers to grandsons. Today, at the end of second decade of the XXI century, our veterans, started their carrier at Kakhovka Plant back in 1960th, have still been working together with young specialists.

How the Plant provide for the needs in labor and engineering force?

The enterprise has implemented the system for training of staff of almost all trade jobs. Experienced specialists explain theoretical material and practical lessons take place under conditions of real production. To get the specialists with higher education we send inquires to technical universities of our region. Besides, around 100 people graduated from higher education institutions by assignment from the enterprise.

Ukrainian rail welding machines of «KZESO» type work on 5 continents in more than 100 countries. What helps you long years to keep the leading positions in the world market? What tasks should be fulfilled due to activity of competitors from China and other countries and output of counterfeit goods?

Annual mastering of new and new types of welding equipment has become typical for the scientists of PWI and Kakhovka machine-building engineers. Up-to-date science and modern production created an inseparable tandem, which is the locomotive that leads the Plant to set aim, namely to be a leader in its field in the world market, not simply move with the requirements of times, but think long-term and pass ahead the competitors by a step or even two.

For the last decade we a lot of times faced with the examples of copying of our products, attempts to issue welding equipment under «KZESO» trademark at different territories. Of course, these are unpleasant moments, but our analysis of such cases shows that these counterfeit goods do not work at all or have totally low indices of efficiency and operation life. I feel sorry for such clients, which trying to save, or being led into confusion, buy counterfeit goods and very soon face with a lot of problems.
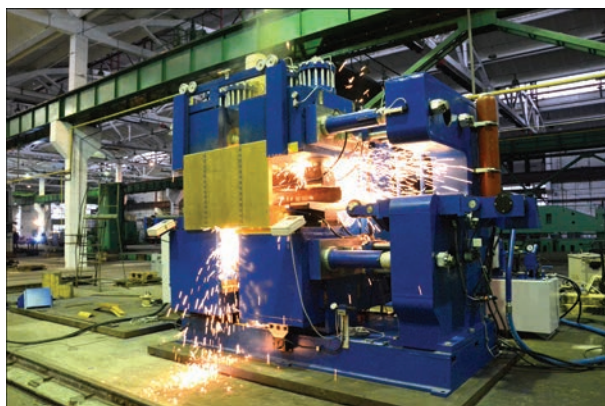
KZESO produced more than 3000 rail-welding machines, about 80 % of which were supplied abroad. When foreign deliveries began, who initiated them?

K922 machine,
Chengdu, Shenzhen, China

The first deliveries abroad were made to France (1971), Japan, Austria (1973), Sweden, Poland, Czechoslovakia, Hungary, USA, Cuba, Romania (1975) and the PWI was the initiator of these deliveries.

How do you form a stock of orders and how wide is sales geography?

A stock of our orders is formed in different ways taking into account specifics of our products and terms of its manufacture. There are regular clients, with whom

it is enough to discuss volume of order and specification, because they work with us for decades and sure in quality of equipment and decency of fulfillment of contract terms from the enterprise side. Every year we have new clients, which necessarily come to Kakhovka, to see production facilities, personally discuss conditions of future contracts. We are happy about renewal of active cooperation with «Ukrzaliznytsia». If during the last 10 years the Plant has manufactured more than 90 % of welding machines and complexes to export in the countries of the far abroad, then now at last we started to get orders of equipment for construction and repair of Ukrainian rails.

K920 machine,
Kuala-Lumpur, Malaysia

The enterprise has a marketing department, where young and progressive specialists analyze and study new markets and push forward our unique products in new directions. Certainly, we every year take part in international exhibitions and specialized events that also opens new possibilities for further development of KZESO. Wining confidence of customer and complete fulfillment of its needs and wishes is one of our principles in competition for leadership and stock of orders.

Welding machines of «KZESO» trademark work on all five continents, in more than 100 advanced countries of the world.

Which problems does the Plant face with in the epoch of 4th industrial revolution due to implementation of digital technologies in all spheres of activity? How do you imagine the direction of further development of rail welding machines?

The equipment will always change. Everything keeps up with the development of science. Concord existing between the advanced science, presented by PWI, and modern engineering enterprise, KZESO, give the best results in fulfilment of time requirements, and, certainly, our clients.

K945 machine,
Wales, Great Britain

As for development of rail welding equipment, it is necessary to note, that machines and complexes of KZESO are already the equipment of future. By the determination of Russian Acad. S. Glaziev, one of the authors of theory of technological setup, «KZESO» rail welding machines fulfil the requirements of the highest 6th technological setup, i.e. being the equipment of XXI century. Use of the elements of artificial intelligence in the recent models of KZESO machines for welding of rails in combination with modern computer equipment and specially developed software allows performing preliminary testing of butt joint, set corresponding mode of welding, follow the welding progress and remove disadvantages, use the algorithms for verification of quality and ultrasonic testing of each butt joint being welded, develop e-passport of welding.

I may definitely say that KZESO is the manufacturer of modern welding machines and complexes, which already use technologies of future that will be still relevant for many years. And we move forward, improve and with confidence in own forces look in the future.
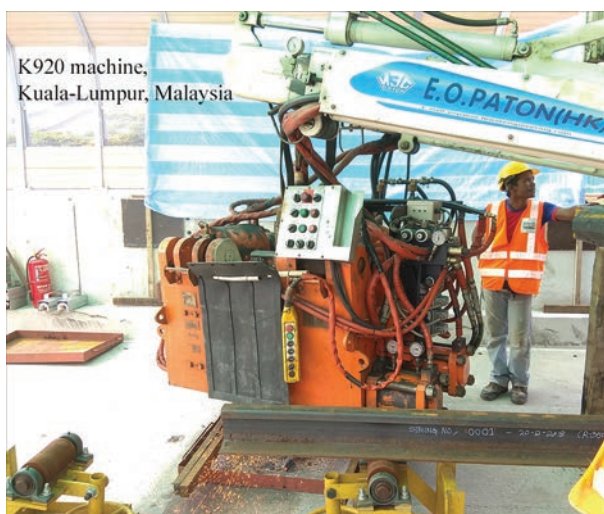
Interview was recorded by
Oleksandr Zelnichenko

MULTIFUNCTIONAL ROBOTIC COMPLEX
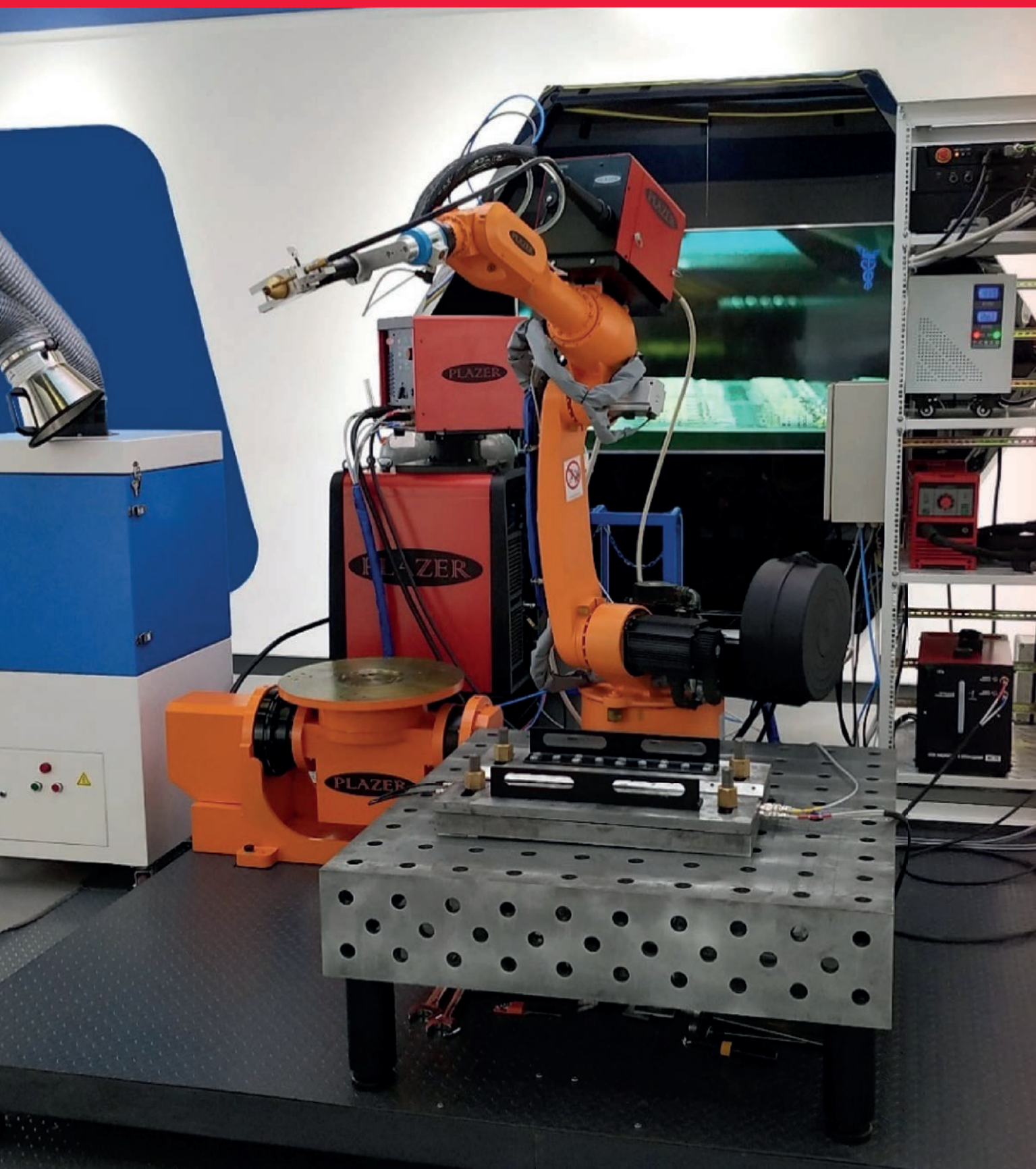
E.O. Paton Electric Welding Institute
11 Kazimir Malevich Str., 03150, Kyiv, Ukraine
Tel.: + 38 (044) 205-25-16, 205-25-40
E-mail: vn@paton.kuev.ua, vnkorzhyk@qq.com

FOR PLASMA-ARC WELDING

Performable technologies:

- Pulsed-arc consumable electrode (filler wire) welding
- TIG welding with filler wire feed
- Plasma welding with and without filler wire
- Plasma spot welding with and without filler wire feed
- Welding in «soft plasma» mode with filler wire feed
- Hybrid plasma-MIG consumable electrode welding

Characteristics of welding robot

Work area, mm 1420

Number of axes 6

Lifting capacity of the «wrist», kg................................ 10

Lifting capacity of the «elbow», kg.............................. 12

Maximum positional repeatability error, mm 0.02

Maximum path error, mm.. 0.10

Welded joints of aluminium AMg5 alloy

Plasma
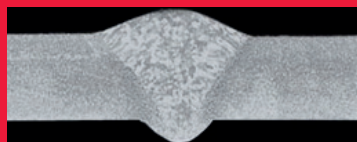
MIG
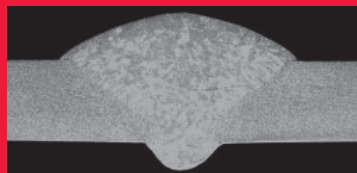
TIG
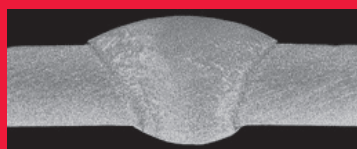
**Seam welding
of 4 mm sheets**
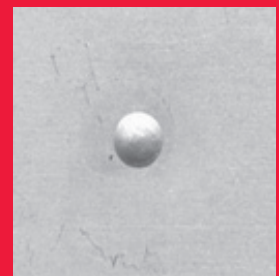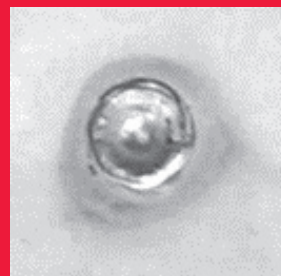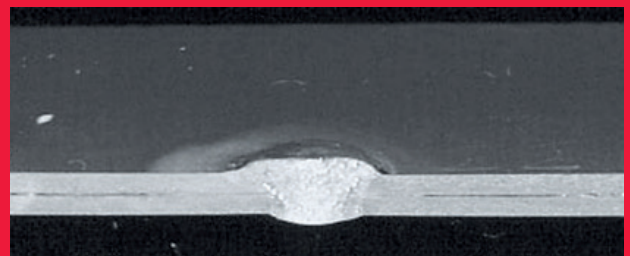
Plasma spot welding of 1 + 1 mm sheets

PLAZER®

BEGINNING OF THE ERA
OF SPACE WELDING TECHNOLOGIES

Academician B.E. Paton

In October 16, 1969, for the first time in the world on the «Soyuz-6» space vehicle the USSR pilot-cosmonauts Georgy Shonin and Valery Kubasov conducted experiments on welding and cutting in open space using the universal automated unit «Vulkan».

Sergei Pavlovich Korolev, creator of practical cosmonautics, already in the early 1960s, specified the task before the E.O. Paton Electric Welding Institute to develop a program of experiments to perform welding and cutting in space. This research program, the ultimate aim of which was the creation of welding equipment and technologies for joining materials in space using welding, began to be realized in 1964, and in October, 1969, the experiments were conducted.

Georgy Stepanovich Shonin (1935–1997) —
USSR pilot-cosmonaut, Hero of the Soviet Union

In 1957, he graduated from the Yeisk Naval Aviation School. He served in the Soviet Navy. In 1960, he was selected to the cosmonaut corps. In 1968, he graduated from the N.E. Zhukovsky Air Force Engineering Academy, Candidate of Technical Sciences. In October 11–16, 1969, he made a space flight as the commander of the «Soyuz-6» space vehicle. Since November, 1990, G.S. Shonin was reserved.

Valeri Nikolayevich Kubasov (1935–2014) —
USSR pilot-cosmonaut, twice Hero of the Soviet Union

In 1958, he graduated from the Moscow Aviation Institute. In 1958–1966, he worked at the RSC «Energia». He was involved in designing of manned space vehicles. In 1966–1993, he was on the rolls in the cosmonaut corps. He made three flights into space (1969, 1975, 1980). In October, 11–16, 1969 he made the first space flight as a flight engineer of the «Soyuz-6» space vehicle (in the crew with Georgy Shonin). During the flight, for the first time in the world an experiment on welding in space was conducted. After leaving the cosmonaut corps, he continued his work in the RSC «Energia», and since 1997 he was a research adviser.

Automated welding unit
«Vulkan»

The automated welding unit «Vulkan», in which experiments on welding and cutting in open space were conducted, was designed and manufactured at the E.O. Paton Electric Welding Institute.

In creation of the unit leading scientists, designers, technologists, assemblers of equipment and testers of the Institute took part. A great help in creating the unit was provided by the specialists of the S.P. Korolev RSC «Energia». It allowed performing fusion welding in three different methods: by a low-pressure arc with a consumable electrode, by a constricted low-pressure arc with a hollow cathode and an electron beam. The unit «Vulkan» consisted of two compartments. In a one (nonsealed) of them, devices to perform each of the mentioned welding methods and a rotating table with samples to be welded were located. During operation, in that compartment a low pressure — space vacuum was maintained. In another (sealed) compartment, an autonomous battery power source, a secondary power source (SPS was designed by the Institute of Electrodynamics of the NAS of Ukraine), control units and measuring instruments were installed. The unit was equipped with a remote con-

trol. The mass of the equipment is about 50 kg. The power of welding devices for different methods ranged from 0.6 to 1.0 kW.

The unit «Vulkan» was located in the airlock compartment of the «Soyuz-6» space vehicle. For the period of experiments, that compartment was depressurized. Inside the pressure was maintained close to the outboard pressure of $1 \cdot 10^{-4}$ mm Hg. During the experiment, the crew was in a sealed return compartment, separated from the airlock compartment by a closed hatch.

Outer space, where manned space vehicles and stations fly, differs from the conditions on Earth by a number of so-called outer space factors and, first of all, by microgravity and space vacuum. Experiments on welding in space were a completely new direction among the works performed by our Institute. Therefore, when the directions of works on welding in space were determined, different types of welding both in the solid phase as well as fusion one were considered. But the most flexible and widespread types of welding works in space for performing possible assembly and repair-restoration operations are the methods of fusion welding. To apply welding methods that require the use of

Kubasov V.N. and Shonin G.S. with the unit «Vulkan» before flight at the «Soyuz-6» space vehicle (1969)

gases in outer space is very difficult. Outer space is a completely open infinite volume. Therefore, gas molecules are rapidly removed into outer space. Great difficulties also arise when using the method of arc welding with a consumable electrode in space. As the pressure of surrounding atmosphere de-creases, the nature of arc discharge is changed. At low pressure, the plasma-forming substance is no longer gas, but fumes of filler and welded materi-als. Although the pressure of fumes in the region of the arc column is higher than the surrounding one, it is not enough to obtain a localized arc discharge. A great influence on the process of arc welding with a consumable electrode is exerted by microgravity. It complicates the transition of molten electrode metal into the weld, and the metal droplets located on the electrode can reach very large sizes. The problems discussed above are practically absent in electron beam welding. Space vacuum only contributes to a high-quality performance of electron beam welding, and microgravity does not significantly affect this process.

The carried out experiments made it possible to es-tablish that the most suitable type of welding in outer space is electron beam welding. It was found that during prolonged zero gravity and space vacuum, the processes of welding and cutting with an elec-tron beam proceed stably and the necessary condi-tions for normal formation of welded joints and cuts are provided. Thus, the experiments carried out in

Paton B.E. and Kubasov V.N. near the unit «Vulkan»

Set of the «Universal» equipment for manual electron beam welding

the unit «Vulkan» provided a wealth of information that allowed creating new models of space welding equipment in future and develop technologies for welding in space.

The carried out experiment started the era of space welding technologies.

The works on creation of equipment and technologies for welding in outer space were continued.

Universal manual tool (URI)

During the work in outer space on board a space vehicle, the most unexpected situations may arise that require the use of welding and related technologies, and often the type and scope of operations will have to be determined by cosmonauts directly in situ. They will have to work in different areas of a space vehicle and deal with different structural materials. For these purposes, at the E.O. Paton Electric Welding Institute a universal working tool (URI) was created. The tests of URI in outer space were carried out aboard the «Salyut-7» station by cosmonauts S.E. Savitskaya and V.A. Dzhanibekov. The carried out experiments on welding, cutting, brazing and coating showed good results and confirmed a high efficiency of the URI equipment in outer space.

The next generation of equipment for welding in outer space was the creation of the «Universal» equipment. Its main difference from the URI was the more than double increase in output power. In addition, a number of basic components was modified, which provided an increase in reliability of the tool. The «Universal» complex passed comprehensive on-land tests and was recommended for the use as a standard tool at orbital manned stations. Unfortunately, for a number of objective reasons, the «Universal» complex was not tested in outer space, although it was supposed to be tested both on board the space shuttle «Columbia» as well as at the «Mir» station.

Analysis of the results of on-land technological experiments, conducted using the «Universal» equipment showed that it can be used to weld aluminum and titanium alloys, as well as stainless steel of up to 1.5 mm thickness.

Hand electron beam tool of a new generation

At present, at the E.O. Paton Electric Welding Institute the works on creation of the next generation of electron
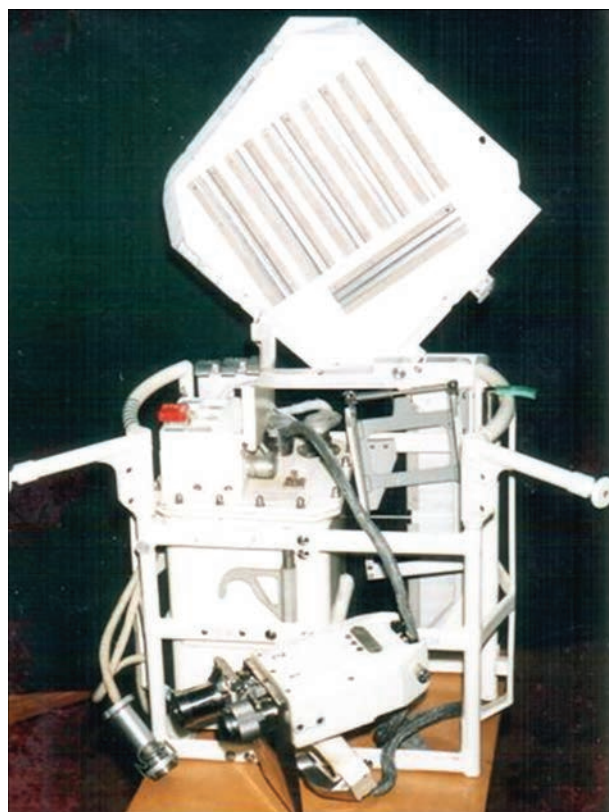
beam tool for welding in outer space are carried out, which includes triode electron beam gun, separated from high-voltage power source. The separation of electron beam gun from power source and the use of flexible high-voltage cable with small-sized high-voltage connector for this purpose makes it possible to significantly reduce the dimensions and weight of the tool, increase its maneuverability when carrying out technological processes in outer space, increase the duration of continuous operation and operational reliability, as well as to facilitate the replacement of tools for different technological purposes directly outboard the space vehicle.

In electron beam tool of a new generation, the power was significantly increased — up to 2.5 kW, which allows welding aluminum and titanium alloys, as well as stainless steel with a thickness of 6 mm. The electron-optical gun system allows obtaining a sharply focused beam with a diameter of not more than 0.6 mm. The mass of the gun is 2.5 kg (twice lower than in the «Universal»). The life of cathode is significantly increased and is equal to 30–40 h. The replacement of a worked out cathode unit can be performed in orbit during 5–10 min. The tool is provided with the possibility to operate not only in manual but also in automatic mode using robotic devices or manipulators.

Recently, all over the world the works related to exploration of the Moon are carried out. At the E.O. Paton Electric Welding Institute, the equipment is developed to perform electron beam welding under the conditions of the Moon surface when creating long-term lunar bases and infrastructure for these constructions. Taking into account special physical conditions on the Moon surface, first of all, ultrahigh vacuum (up to 10^{-13} mm Hg), the necessary sealing of joints can be reliably secured only by welding. Therefore, the creation of welding equipment and technologies for assembly and repair-restoration works on the Moon surface is very relevant during its exploration by a human. In addition to ultra-deep vacuum, there are other physical features on the surface: a sharp change in temperatures from +140 °C at day-time to –170 °C at night, reduced gravity (1/6 of gravity on Earth), lunar dust (regolith), etc. All these features should be taken into account when developing both welding equipment as well as when creating auxiliary devices — workplace of the operator. In the developed design of a gun the conditions for electron beam formation in an ultra-deep vacuum were taken into account, which differ significantly from those in on-land vacuum installations and in near-Earth space, where space vehicles and manned space stations fly.

We are convinced that space welding equipment and technologies, the foundation of which was laid 50 years ago by the «Vulkan» experiment, will find application in different projects during construction of industrial complexes on Earth orbit, exploration of the Moon and flights to other planets, and also on the study of fundamental space phenomena.
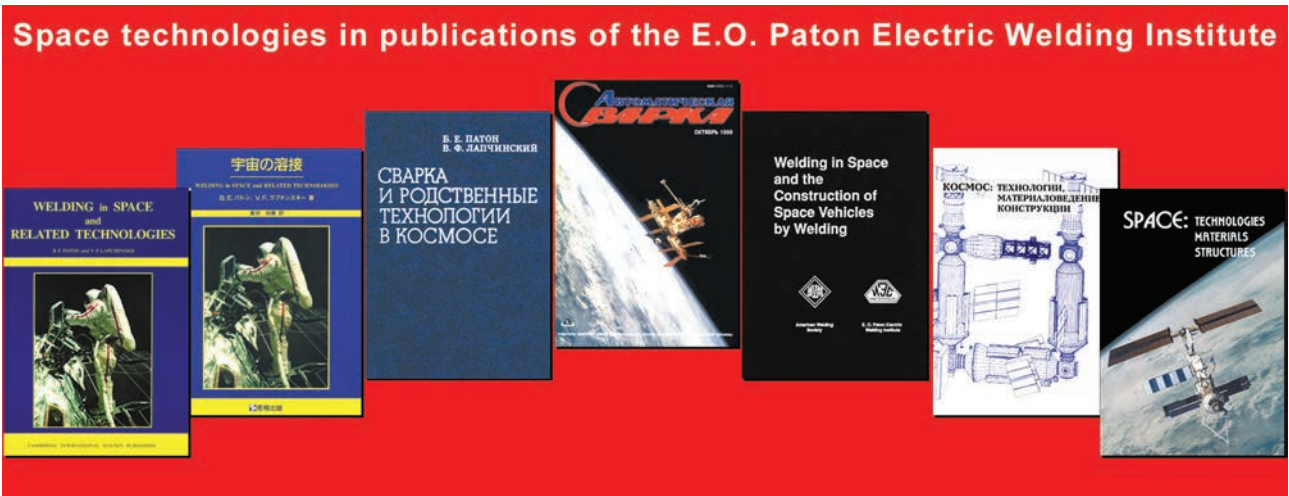
HYBRID LASER-MICROPLASMA WELDING OF SHEET Ti–Al–V TITANIUM ALLOY*

I.V. KRIVTSUN[1], **V.Yu. KHASKIN**[2], **V.M. KORZHYK**[1,2], **I.M. KLOCHKOV**[1], **V.V. KVASNYTSKYI**[3],
O.A. BABICH[1,2], **CAI DETAO**[2], **LUO ZIYI**[2] and **HAN SHANGUO**[2]

[1]E.O. Paton Electric Welding Institute of the NAS of Ukraine
11 Kazymyr Malevych Str., 03150, Kyiv, Ukraine. E-mail: office@paton.kiev.ua
[2]E.O.Paton Chinese-Ukrainian Welding Institute, Guangzhou, China
[3]National Technical University of Ukraine «Igor Sikorsky Kyiv Polytechnic Institute»
37 Peremohy Prosp., Kyiv-56, Ukraine

The process of hybrid laser-microplasma welding of sheet Ti–Al–V titanium alloy of TC4 grade (up to 3.0 mm) was studied. The recommended technological parameters and conditions of laser-microplasma welding in an argon medium, physical and mechanical properties of welded joints were determined, and the presence of hybrid effect was established. 5 Ref., 3 Tables, 7 Figures.

***K e y w o r d s :** laser-microplasma welding, Ti-Al-V titanium alloy, heat input, strength, elongation, hybrid effect*

Welded products from sheet titanium alloys are becoming ever wider accepted in modern industry. Such products are characterized by high strength under the impact of mechanical loads, light weight and high corrosion resistance under operation conditions. Examples of such products can be structures which are applied in aerospace, nuclear, chemical and food industries, and marine engineering when operating in marine climate or at higher humidity (for instance, tanks, filters), etc. A wide range of such structures are made of titanium alloys up to 3.0 mm thick with application of butt welded joints. As a rule, resistance, argon-arc or electron beam welding are used to solve such tasks [1].

However, such welding processes often do not completely meet the requirements as to cost-effectiveness and adaptability to fabrication of such structures and by far not always allow making the physical and mechanical characteristics of welded joints as similar as possible to those of base metal. High requirements as to geometrical accuracy of products from sheet titanium alloys require application of measures and joining technologies, which provide the minimum level of residual welding deformations. One of the best welding methods today in terms of minimizing the residual

deformations, and producing high-quality and durable welded joints of such alloys is electron beam welding [2]. Recently, however, there have been attempts to replace this method by laser welding, as a more efficient one that does not require application of vacuum chambers [3]. This method, however, has not yet become widely accepted, because of comparatively high cost of laser equipment. One of the ways to reduce the cost of laser equipment is lowering the radiation power due to its partial replacement in the welding process by plasma-arc component. Such a process is called hybrid laser-plasma welding [4]. Application of the process of hybrid laser-plasma welding at preservation of quality characteristics of welded joints on the level of those in laser welding opens up a prospect for creation of a new advanced welding technology. Therefore, this work is devoted to studying the capabilities of hybrid laser-microplasma welding of sheet titanium alloys, in the case of a rather widely accepted alloy of Ti–Al–V alloying system of 1.0 and 3.0 mm thickness and is actual.

The objective of the work is optimization of basic techniques of hybrid laser-microplasma welding of sheet Ti–Al–V titanium alloy of TC4 grade (VT6 analog), selection of recommended technological param-

Table 1. Chemical composition (wt.%) of TC4 alloy produced in PRC (VT6 analog)

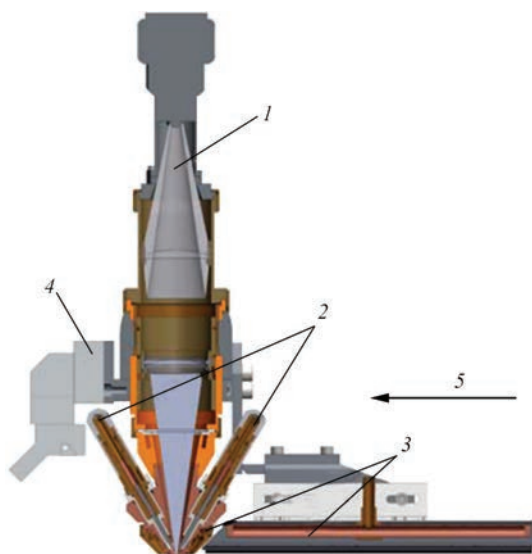| Ti	Fe	C	Si	V	N	Al	Zr	O	H	Additives
86.45–90.9	≤0.6	≤0.1	≤0.1	3.5–5.3	≤0.05	5.3–6.8	≤0.3	≤0.2	≤0.015	Other — up to 0.3

Figure 1. Diagram of integrated plasmatron and experiment performance: *1* — laser radiation feeding of power P = 0.3–1.2 kW; *2* — cathode assemblies; *3* — gas shielding; *4* — fastening to robot arm; *5* — welding direction

eters of the process and welding conditions, as well as determination of physical and mechanical characteristics of the produced joints.

Technological studies of the process of hybrid laser-microplasma welding of the mentioned titanium alloy were conducted using a unit described in [5], the circuit of integrated hybrid plasmatron of which is given in Figure 1. Disk laser with radiation wavelength λ = 1.03 μm was used during the experiments, the power of which was changed in the range of 0.3–1.2 kW. Focal spot diameter was equal to about 0.4 mm. In the integrated coaxial direct action plasmatron of original design applied for studies the laser radiation was combined with the constricted low-ampere arc of up to 2.3 kW power [5]. In this plasmatron the focused laser radiation and constricted arc were output jointly through a common nozzle of 2.5 mm diameter to the sample being welded, which
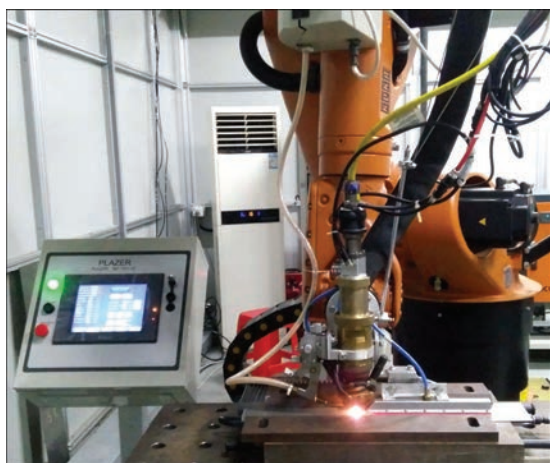
Figure 2. Process of laser-microplasma welding by integrated plasmatron, fastened on the arm of KUKA KR30HA robot
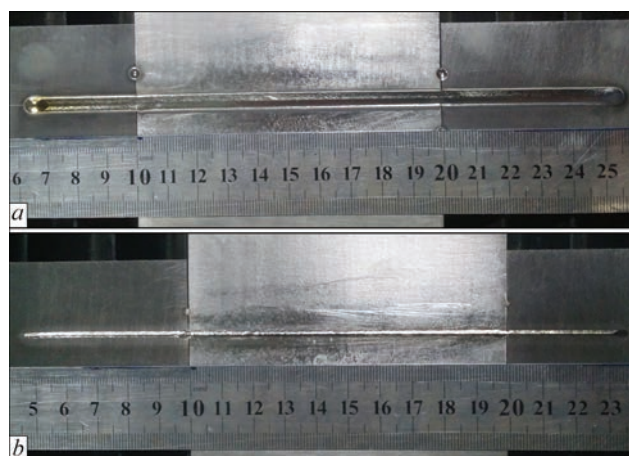
Figure 3. Appearance of plates of TC4 titanium alloy (δ = = 3.0 mm) butt welded without a gap between the edges by laser-microplasma process (radiation power P = 1.0 kW, welding current I = 50 A, voltage U = 26 V, welding speed v = 36 m/h): face (*a*) and reverse (*b*) side

was located at approximately 3 mm distance from the nozzle tip. The focal plane of laser radiation was positioned at the depth of approximately 0.5 mm relative to sample surface. Straight polarity continuous arc was used in the experiments. The arc current in integrated microplasmatron was smoothly adjusted up to 80 A at up to 28 V arc voltage. Sheets of TC4 alloy of (200–300)×100×δ mm dimensions, where δ = 1.0 and 3.0 mm (Table 1) were used as samples for butt welding and bead deposition. Movement of integrated plasmatron relative to the sample being welded was performed by an anthropomorphic robot KUKA KR30HA (Figure 2).

Conducted experiments demonstrated the high stability of the process of laser-microplasma welding. Positive results were obtained (Figures 3, 4) in the case of hybrid butt welding of sheets of TC4 titanium alloy (δ = 1.0 and 3.0 mm) with up to 0.1 mm gap between the edges being welded. Here, the speed of the hybrid process was 30 to 40 % higher than that of laser welding and approximately two times higher than that of plasma welding (Table 2).

Performance of a number of experiments enabled determination of parameters of the modes of sound (absence of undercuts, lacks-of-penetration and sag-

Figure 4. Macrostructure of a butt joint of TC4 titanium alloy (δ = 3.0 mm), produced by laser-microplasma welding in argon

Table 2. Modes and results of laser, plasma and laser-microplasma welding of TC4 titanium alloy in argon

Batch No.	δ, mm	Radiation power, W	Welding current, A	Arc voltage, V	Welding speed, m/h	Heat input, J/mm	Result
1	1.0	600	40	24	60	80	Hybrid welding, penetration, presence of undercuts
2	1.0	600	40	24	51	100	Hybrid welding, penetration, good weld formation, absence of undercuts
3	1.0	600	–	–	30	70	Laser welding, penetration, presence of undercuts
4	1.0	–	40	24	24	115	Microplasma welding, penetration
5	3.0	1200	50	26	42	190	Hybrid welding, penetration, presence of undercuts
6	3.0	1000	50	26	36	200	Hybrid welding, penetration, good weld formation, absence of undercuts
7	3.0	1000	–	–	24	150	Laser welding, penetration, presence of undercuts
8	3.0	–	50	26	18	210	Microplasma welding, penetration

Table 3. Modes and result of hybrid laser-microplasma welding of a sound joint of TC4 titanium alloy (δ = 3.0 mm)

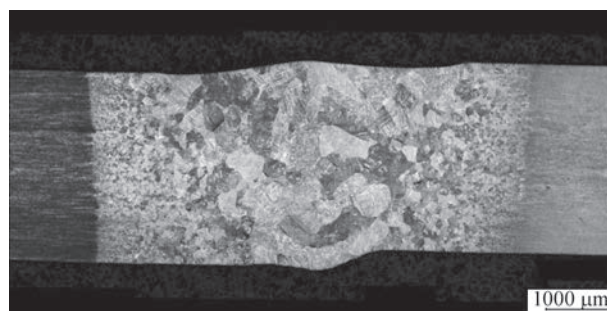| Mode of laser-microplasma welding			
Laser power P, W	1000	Welding speed v, m/h	0.6
Arc current I, A	50	Distance from the part to the nozzle, mm	3
Plasma gas flow rate (argon) Q_{pl}, l/min	10	Flow rate of additional shielding gas (argon), $Q_{ad. sh}$, l/min	20
Shielding gas flow rate (argon) Q_{sh}, l/min	10	Flow rate of gas (argon) for weld root shielding Q_{rev}, l/min	20
Dimensions of the produced weld			
Width of face (top) side of the weld, mm	4.8	Width of weld reverse side (root), mm	1.5
Face side convexity, mm	0.1	Convexity of weld reverse side (root), mm	0.2

ging of the weld) hybrid butt welding of TC4 titanium alloy sheets with protection of the weld pool and hot (more than 200 °C) part of the weld by argon (Table 3). These parameters were used to produce welded joints of TC4 alloy 1.0 and 3.0 mm thick, from which samples of XIII (XIIIa) type were later cut out (GOST 6996–66) to perform mechanical testing.

Three series of 3 samples each were cut out in order to perform mechanical testing of base and welded joint metal of TC4 alloy (δ = 1.0 and 3.0 mm) butt

welded by laser-microplasma method in argon atmosphere. Tensile testing machine of MTS Criterion 45 type was used to perform static tensile testing of butt welds to determine the ultimate strength σ_t (MPa) and relative elongation δ (%). Results measured for each test series were averaged. The obtained averaged values were used to plot the respective diagrams (Figure 5). The derived results demonstrated that the strength of joints of titanium alloy TC4, produced by hybrid laser-microplasma welding, is equal to approximately 85–90 % of base metal strength, relative elongation of the thus welded samples is not much higher than 40 % of that of base metal (δ ≈ 4.5 for the joints
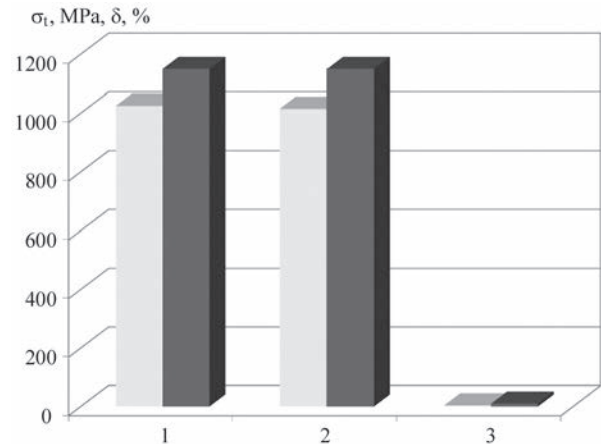
Figure 5. Comparative results of mechanical testing of samples of TC4 titanium alloy (light grey colour) welded by laser-microplasma method and base metal (dark-grey colour) at their static tension: 1, 2 — averaged ultimate strength σ_t (MPa) for samples of 1.0 (*1*) and 3.0 (*2*) mm thickness; 3 — relative elongation δ (%) for all the cases
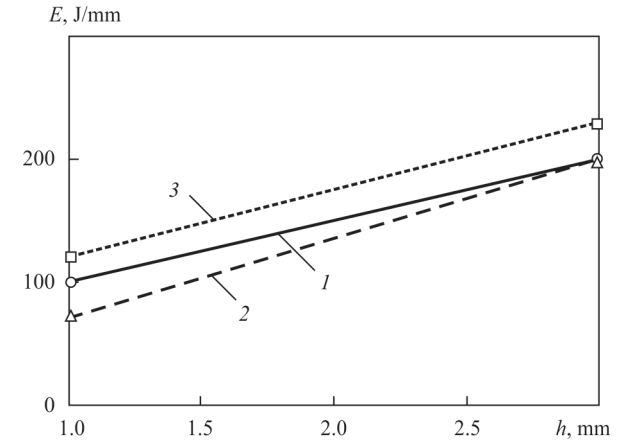
Figure 6. Dependencies of heat input E (J/mm) in laser-microplasma (*1*), laser (*2*) and plasma (*3*) welding on thickness h (mm) of welded sheets of TC4 titanium alloy
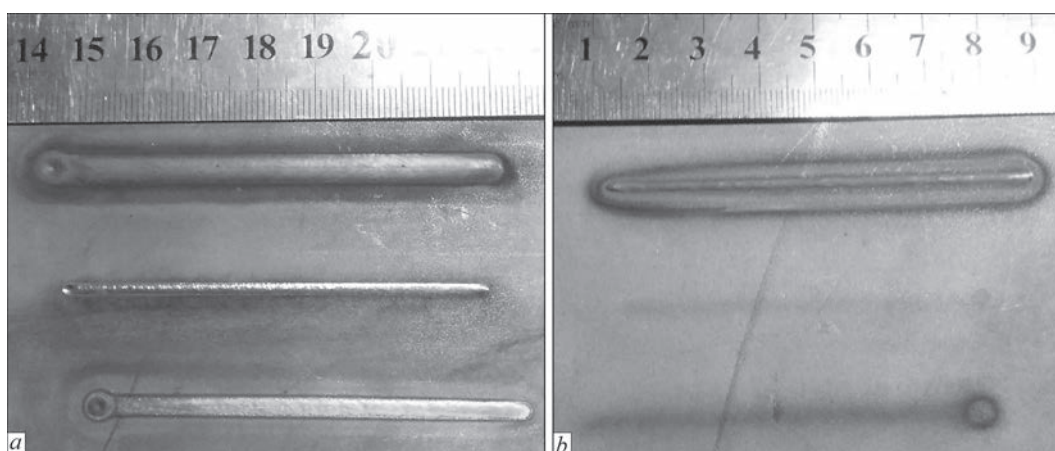
Figure 7. Appearance of face (*a*) and reverse sides (*b*) of the beads in a plate of TC4 alloy of thickness $\delta = 3.0$ mm (from top to bottom): hybrid, laser, microplasma

at $\delta \approx 10$ % for base metal). The given values are acceptable for most of the welding tasks.

During analysis of the conducted technological studies, the process heat input (E, J/mm) was determined as a sum of powers of laser (P, W) and microplasma ($0.8IU$, W) components, related to welding speed (v, mm/s). Calculation results were used to plot the dependencies of the change of heat input of laser-microplasma and laser welding at the same process speeds (Figure 6). Comparison of curves *1*, *2* and *3* showed that the heat inputs of all the considered welding processes are rather close. Note that the energy input of plasma process is the greatest in all the cases, the laser process ensures the lowest energy input in welding sheets 1.0 mm thick, and in case of welding 3.0 mm thick sheets the hybrid and laser processes become close as to the input energy.

The following experiment was performed in order to compare the results of the laser, microplasma and hybrid laser-microplasma welding. Laser-microplasma welding in argon atmosphere was applied to ensure guaranteed penetration of plate from TC4 alloy ($\delta = 3.0$ mm) in the following mode: $P = 1000$ W, $I = 50$ A, $U = 26$ V, $v = 36$ m/h. Then, the same speed with the same mode parameters was used to deposit two beads by the laser and microplasma processes (Figure 7). Here, the sum of heat inputs of the process components corresponded to the heat input of hybrid welding. Examination of transverse sections of these beads showed that the depth of hybrid welding penetration is approximately by 25 to 30 % greater than the sum of penetration depths of laser and microplasma welding. This led to the conclusion about the availability of a pronounced hybrid effect in the case of laser-microplasma welding by the considered process.

## Conclusions

1. In the course of this work, hybrid laser-microplasma welding of sheet titanium alloy TC4 in argon was studied. It was determined that in the case of abutment of the edges to be welded with up to 0.1 mm gap, hybrid welding allows producing sound welded joints without the need for filler wire application, without undercuts or sagging, characteristic for laser welding. Here the speed of the hybrid process is higher than that of the laser one by 30–40 %, and that of the plasma process is higher approximately two times.

2. Analysis of the results of mechanical testing of welded joints of TC4 titanium alloy, made by hybrid laser-microplasma welding, shows that their static tensile strength is equal to approximately 85–90 % of that of the base metal, and relative elongation is higher than 40 %. These values are acceptable for most of the welding tasks.

3. Comparison of heat inputs of the considered welding processes showed that their values are quite close. In all the cases, the energy input is the highest in the plasma process. In welding 1.0 mm thick sheets the lowest energy input is ensured by the laser process, and in case of welding 3.0 mm thick sheets the hybrid and laser processes are comparable in terms of the input energy.

4. Comparative studies of beads deposited on samples of TC4 alloy by laser, microplasma and hybrid processes showed that the penetration depth with the hybrid method is approximately 25–30 % greater than the sum of penetration depths in laser and microplasma welding. Here, the sum of heat inputs of the process components corresponds to the heat input of hybrid welding. This is indicative of the availability of the hybrid effect in the case of application of laser-microplasma welding.

pacity — Building of Innovation — Driven Development for Special Fund Projects of the Programs of the Academy of Sciences of Guangdong Province (PRC) «Investigations of physico-chemical processes at interaction of vapour plasma with metal surface and development of scientific fundamentals of the technology of water-air plasma cutting of sheet steels to produce welded joints».

1. Gurevich, S.M., Zamkov, V.N., Blashchuk, V.E. et al. (1986) *Metallurgy and technology of welding of titanium and its alloys.* 2nd Ed. Kiev, Naukova Dumka [in Russian].

2. Nazarenko, O.K., Kajdalov, A.A., Kovbasenko, S.N. et al. (1987) *Electron beam welding.* Kiev, Naukova Dumka [in Russian].

3. Grigoryants, A.G., Shiganov, I.N. (1988) *Laser technique and technology.* In: 7 books. Book 5: Laser welding of metals. In: Manual for higher education inst. Ed. by A.G. Grigoryants. Moscow, Vysshaya Shkola [in Russian].

4. Krivtsun, I.V., Shelyagin, V.D., Khaskin, V.Yu. et al. (2007) Hybrid laser-plasma welding of aluminium alloys. *The Paton Welding J.*, **5**, 36-40.

5. Krivtsun, I.V., Korzhik, V.N., Khaskin, V.Yu. et al. (2017) Unit of new generation for laser-microplasma welding. In: *Proc. of 8th Int. Conf. on Beam Technologies in Welding and Processing of Materials.* Ed. by I.V. Krivtsun. Kiev, International Association Welding, 2017, 95–100.

INFLUENCE OF LASER POWER AND WELDING VELOCITY ON THE MICROSTRUCTURE OF Zr-BASED BULK METALLIC GLASS WELDED JOINTS[*]

HAIYAN WANG[1], **MA YANYI**[2], **ZHANG YUPENG**[1],
DONG CHUNLIN[1], **YI YAOYONG**[1] and **XI HUAI**[1]

[1]Guangdong Provincial Key Laboratory of Advanced Welding Technology, Guangdong Welding Institute
(China-Ukraine E.O. Paton Institute of Welding), Guangzhou, 510650, China
[2]School of Materials Science and Engineering, Shenyang University of Technology, Shenyang, 110870, China

Laser welding is employed to weld $Zr_{67.8}Cu_{24.7}Al_{3.43}Ni_{4.07}$ bulk metallic glass, and the effects of laser power and welding velocity on the microstructures of bulk metallic glass joints are studied. Owing to the high speed and high-energy density of laser welding, the weld fusion zones remain amorphous structure. Some nano-grains are formed in weld fusion zones and of benefits for the improvement of microhardness. Crystallization happens in heat-affected zone and deteriorates the hardness of materials. The joint welded with laser power of 600 W and velocity of 110 mm/s exhibits the lowest degree of crystallization. Larger laser power or slower welding speed would cause excessive heat accumulation in heat-affected zone. 10 Ref., 1 Table, 3 Figures.

K e y w o r d s : Bulk metallic glass; laser welding; microstructure; crystallization

Zr-based bulk metallic glass (BMG) with specific long-range disordered structure have many promising merits [1], such us high strength, high hardness, and excellent corrosion resistance, etc. These outstanding properties make them promising candidates for potential applications in the field of consumer electronics, medical apparatus, automobile industry and so on. However, as BMGs belong to metastable materials, the relatively weak glass forming ability and the demand for quenching process limits their development of large-scale products. Therefore, to extend the engineering applications, many researches on various welding technologies for BMGs have been carried out, including friction stir welding, explosion welding, and diffusion welding, etc. Among these technologies, laser welding has attracted extensive interests owing to their superiorities of fast welding velocity, deep welding penetration and high energy density [2]. It can fulfill the demands of BMGs' welding for high solidification and thermal quench rate in both weld fusion zone (WFZ) and heat-affected zone (HAZ). Li, Kim and Kawahito et al. utilized laser or pulsed laser welding to realize $Zr_{45}Cu_8Al_7$, $Cu_{54}Ni_6Zr_{22}Ti_{18}$ and $Zr_{55}Al_{10}Ni_5Cu_{30}$ BMGs joints, respectively [3–5]. The reported studies reveal that crystallization easily happens in WFZ and HAZ, so it is critical to control the laser energy input to prevent heat accumulating in welding zone, which depends on the two significant parameters in laser welding, i.e., laser power and welding velocity.

Herein, this work used laser beam to weld $Zr_{67.8}Cu_{24.7}Al_{3.43}Ni_{4.07}$ BMGs. The influences of laser power and welding velocity on the microstructure of welding joints were studied and the optimal parameters were obtained to realized high-quality $Zr_{67.8}Cu_{24.7}Al_{3.43}Ni_{4.07}$ BMG joints.

Experimental. The $Zr_{67.8}Cu_{24.7}Al_{3.43}Ni_{4.07}$ BMGs with sizes of 60 mm×20 mm×1 mm were prepared by arc melting Zr, Cu, Al and Ni metals with a purity above 99.9 %. Before welding, the BMGs were polished by 2000 mesh silicon carbide papers, and cleaned by absolute ethyl alcohol to remove the oxide and residues on welding surface. Then, the BMG plates were welded by TRUMPF TRU DISK10002. The movement of laser beam was controlled by TRUMPF PFO 33, and the diameter of focus spot was about 0.2 mm. Five samples with various laser powers

Welding parameters for $Zr_{67.8}Cu_{24.7}Al_{3.43}Ni_{4.07}$ BMGs

Sample No.	Laser power P (W)	Welding velocity, mm/s
1	600	90
2	600	100
3	600	110
4	570	100
5	630	100

and welding velocities were obtained. Table shows their corresponding parameters in detail.

After welding, the samples were cut along the direction perpendicular to the weld, and inlaid, polished and polished successively. The cross-sectional surfaces were etched by chemical solvent of 3 ml HF, 50 ml HNO_3 and 60 ml H_2O.

The microstructures of BMG welding joints were characterized by optical microscopy (OM, ZEISS Ario Imager.M2m). The Vickers hardness of WFZ and HAZ was evaluated by micro-hardness tester (Buehler VH1202) with load and dwell time of 1 kg and 10 s, respectively. The glassy or crystalline structures were identified by transmission electron microscopy (TEM, FEI Titan G2 300).

Results and discussion. Figures 1, a–e, show the cross-sectional microstructures and morphology of samples 1 to 5, respectively. The three zones of WFZ, HAZ and unaffected base material (BM) can be clearly identified according to the contrasting differences, which are signed in the figures, respectively. As can been observed in Figure 1, b to c, there are some little pores existing in WFZs, which is mainly caused by the key hole formed during laser welding. As for the microstructures of HAZ, the bright spots are corresponding to the crystallization area, and its proportion can be utilized to evaluate the degree of crystallization [4, 6, 7].

Generally, sample 3 which is welded under laser power and velocity of 600 W and 110 mm/s, respectively, shows the weakest degree of crystallization. To study the effect of welding velocity on the crystallization, samples 1, 2 and 3 are compared. It is obvious that as the welding velocity increases from 90 mm/s to 110 mm/s, the crystallization is successively weakened.

This is owing to the relatively larger welding velocity, which is beneficial to promote the heat conduction and thermal quench happening in HAZ [6]. As for the influence of laser power, samples 2, 4 and 5 are taken into considerations. As can be seen from Figure 1, d, when the laser power is 570 W, the bottom of the weld is incompletely fused, indicating that the input energy is too low to weld. As the laser power increases to 600 and 630 W, the BMG joints become completely fused, but the degree of crystallization also gets worse and exhibit the largest crystallization area of sample 5.

To understand the difference of microstructures between glassy WFZ and crystalline HAZ, bright-field TEM (BFTEM) and high-resolution TEM (HRTEM) characterizations are employed. Figure 2, a and c show the typical BFTEM and HRTEM images of HAZs, respectively. Many grains as well as grains boundaries can be observed, and the HRTEM result exhibiting ordered lattice further verifies the crystalline structure of HAZ. Figure 2, b and d are the typical BFTEM and HRTEM results for WFZs, respectively. Different from Figure 2, a, only several nano-grains are identified in Figure 2, b. The HRTEM image shown in Figure 2, d reveals that the microstructure of WFZ is generally amorphous, and the nano-grain is with a size of about 80 nm in circumscribed circle diameter. The formation of such nano-grains is ascribed to the high speed and high-energy density of laser welding [8], which results in the increasing nucleation rate and quickly drop of temperature during welding to retard grain growth. These nano-grains are regarded as the key to improving the mechanical properties of materials [9, 10], including hardness, strength, plasticity, etc.

To evaluate the mechanical properties of as-welded BMG joints, the Vickers hardness of difference zones for samples 1 to 5 is tested by a micro-hardness tester
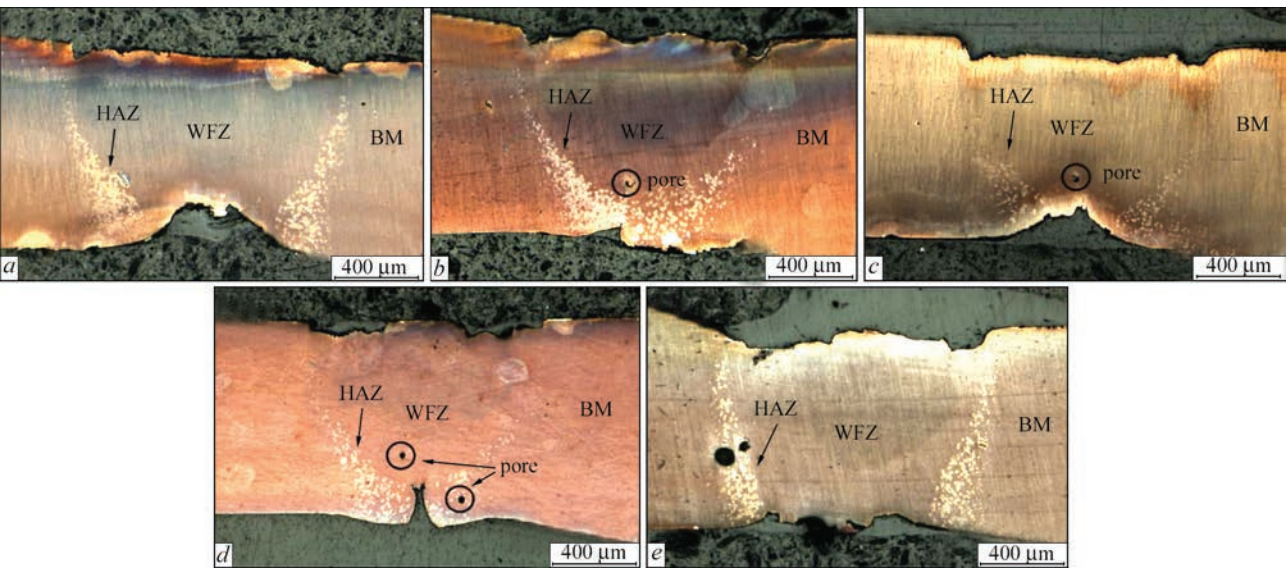
Figure 1. Optical microscopy images for the cross-sections of the welds taken from a–e samples 1–5
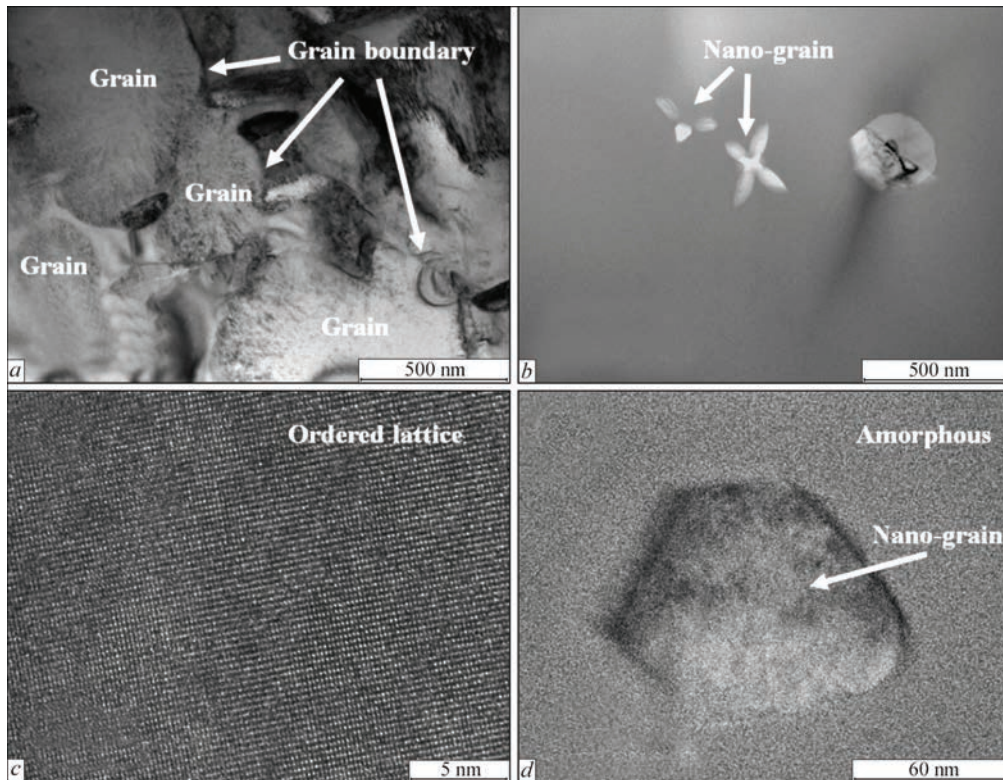
Figure 2. Typical BFTEM images of (*a*) HAZs and (*b*) WFZs, and the corresponding HRTEM images of (*c*) HAZs and (*d*) WFZs for these samples
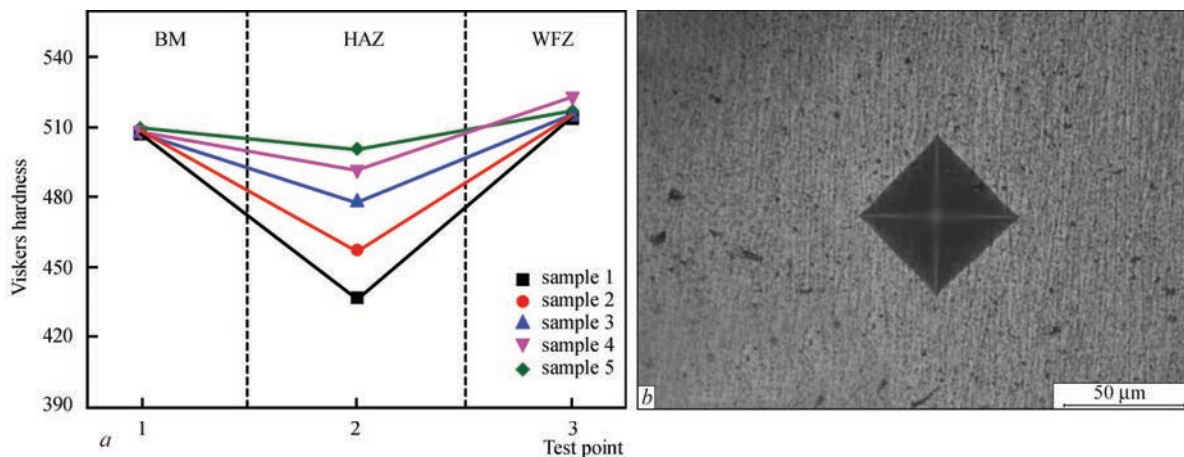
Figure 3. Vickers hardness of different zones for samples 1 to 5, and test point of 1, 2 and 3 are corresponding to BM, HAZ and WFZ, respectively (*a*), the image of typical indentation for each test (*b*)

under the force of 1 kg and dwell time of 10 s, as shown in Figure 3, *a*. Figure 3, *b* displays the typical indentation for each test. According to Figure 3, *a*, the hardness of WFZ as 514~523 *HV* is generally higher than that of BM as 507~509 *HV*, which is attributed to the nano-crystallization happening in WFZ, as revealed in Figure 2, *d*. On the contrary, the hardness of HAZ is greatly decreased to 436, 456.9, 477.4, 491.3 and 500.2 *HV* for samples 1 to 5, respectively. It is considered that the severe thermal crystallization during welding is the main reason for this sharply weakened hardness in HAZ.

Conclusions

In summary, $Zr_{67.8}Cu_{24.7}Al_{3.43}Ni_{4.07}$ BMGs were welded by laser welding, and the effects of laser power and welding velocity on the microstructure, especially the crystallization behavior, of BMG joints were studied. The WFZs' microstructure of all samples remain amorphous generally, but several nano-grains are formed, which is advantageous to improve the Vickers hardness of WFZ. As for HAZ, the joint welded with laser power of 600 W and velocity of 110 mm/s exhibits the lowest degree of crystallization. Larger laser power or slower welding speed would cause

excessive heat accumulation in HAZ, and, therefore, result in severe crystallization reaction and deterioration of the mechanical properties of BMG materials.

1. Williams, E., Lavery, N. (2017) Laser processing of bulk metallic glass: A review. *Journal of Material Processing Technology*, **247**, 73–91.
2. Wang, H.S., Chen, H.G., Jang, J.S.C., Chiou, M.S. (2010) Combination of a Nd:YAG laser and a liquid cooling device to $(Zr_{53}Cu_{30}Ni_9Al_8)Si_{0.5}$ bulk metallic glass welding. *Materials Science & Engineering A*, 528(**1**), 338–341.
3. Kawahito, Y., Terajima, T., Kimura, H. et al. (2008) High-power fiber laser welding and its application to metallic glass $Zr_{55}Al_{10}Ni_5Cu_{30}$. *Materials Science & Engineering B*, 148(**1**), 105–109.
4. Li, B., Li, Z.Y., Xiong, J.G. et al. (2006) Laser welding of $Zr_{45}Cu_{48}Al_7$ bulk glassy alloy. *Journal of Alloys & Compounds*, 413(**1**), 118–121.
5. Kim, J.H., Lee, C., Lee, D.M. et al. (2007) Pulsed Nd:YAG laser welding of $Cu_{54}Ni_6Zr_{22}Ti_{18}$ bulk metallic glass. *Materials Science & Engineering A*, 449(**13**), 872–875.
6. Wang, G., Huang, Y.J., Shagiev, M., Shen, J. (2012) Laser welding of $Ti_{40}Zr_{25}Ni_3Cu_{12}Be_{20}$ bulk metallic glass. *Materials Science and Engineering A*, **541**, 33–37.
7. Wang, H.S., Chen, H.G., Jang, S.C. (2010) Microstructure evolution in Nd:YAG laser-welded $(Zr_{53}Cu_{30}Ni_9Al_8)Si_{0.5}$ bulk metallic glass alloy. *Journal of Alloys & Compounds*, 495(**1**), 224-228.
8. Chen, B., Shi, T.L., Li, M. et al. (2014) Laser welding of annealed $Zr_{55}Cu_{30}Ni_5Al_{10}$ bulk metallic glass. *Intermetallics*, 46(**3**), 111–117.
9. Siegel, R.W. (1993) Nanostructured materials-mind over matter. *Nanostructured Materials*, 3(**1**), 1–18.
10. Karch, J., Birringer, R., Gleiter, H. (1987) Ceramics ductile at low temperature. *Nature*, **330**(6148), 556–558.

EFFECT OF HORIZONTAL MECHANICAL VIBRATION ON SERVICE PROPERTIES OF DEPOSITED METAL

Ch.V. PULKA, M.I. PIDGURSKYI, V.S. SENCHYSHYN, M.V. SHARYK and **V.Ya. GAVRYLYUK**

Ternopil Ivan Puluj National Technical University of MOS of Ukraine
56 Ruska Str., 46001, Ternopil, Ukraine. E-mail: Viktor_Synchyshyn@i.ua

Wear resistance and stability of thickness of the layer of metal deposited by the induction method was studied. It is shown that in surfacing using the powder-like solid alloy PG-S1 by ITES heating system (inductor, thermal and electromagnetic shields) with application of horizontal vibration and energy-saving surfacing mode, the wear resistance is 1.4 times increased, stability of deposited metal layer thickness grows by 10 % and deposited metal quality is improved (transformation from coarse- to fine-grained structure), as compared to the technology without horizontal vibration. 14 Ref., 3 Tables, 5 Figures.

One of the most actual directions in the field of science and technology is the modification of surface of structural and tool steels in order to improve service characteristics of parts of machines and mechanisms operating in the conditions of increased operation and aggressive environments. Today, different methods of surface modification are widely used in machine-building and metalworking industries, such as application of wear-resistant coatings by physical and chemical methods, and different types of thermochemical treatment.

Among the physical methods of forming functional coatings, the method of induction surfacing is the most effective for applying a layer of multicomponent materials. At present, one of the most promising ways to improve the effectiveness of wear-resistant coatings is to introduce additional technological operations in the traditional way of induction surfacing, such as shielding thermal and electromagnetic fields, modes of surfacing with energy savings, exposure of the product to horizontal and vertical mechanical vibration in the process of surfacing, etc., which allow significantly increasing service properties of the deposited metal layer.

Induction surfacing is a process used to restore worn surfaces or to strengthen working surfaces during the manufacture of new parts [1, 2]. This surfacing process has become widely used in agricultural engineering [3]. An important prerequisite for providing a quality surfacing process is correctly selected parameters of surfacing mode, which further affect the quality of layer of deposited metal, and therefore the service life of a deposited part.

In induction surfacing, to insulate those part surfaces which are subjected to unwanted heating, thermal and electromagnetic shields are used. To application of thermal and electromagnetic shields during induction heating a number of works is devoted [4–6]. The shields are used in different technological processes to harden parts, surfacing, etc. They are usually used separately (i.e. only electromagnetic or thermal shield). Moreover, it is very difficult to control temperature in the surfacing zone to produce a high quality layer of deposited metal.

To improve the properties of deposited metal, the authors developed a new surfacing technology using the ITES heating system (inductor, thermal and electromagnetic shields) [7, 8], i.e. a combined simultaneous shielding of thermal and electromagnetic fields, which allows achieving a more stable thickness of layer of deposited metal due to the uniform temperature in the surfacing zone, since the powder-like solid alloy is melted from the surface of base metal during surfacing by heat transfer with a variable specific power over time (energy-saving mode of heating) [9].

It is of interest to study the properties of deposited layer of metal in the case when into the ITES system during the use of energy-saving mode of surfacing, additional technological operation, such as horizontal mechanical vibration of the part to be surfaced, at the moment of melting start of the powder-like solid alloy to its full melting and cooling [10, 11] is introduced, which will greatly improve the service characteristics of the deposited layer of metal.

Procedure of investigations. Measurements of microhardness were performed in the microhardness meter M-400 of Leko Company. The microstructure of the specimens was studied in the microscope NEOPHOT-32 (Germany). The etching of the specimens
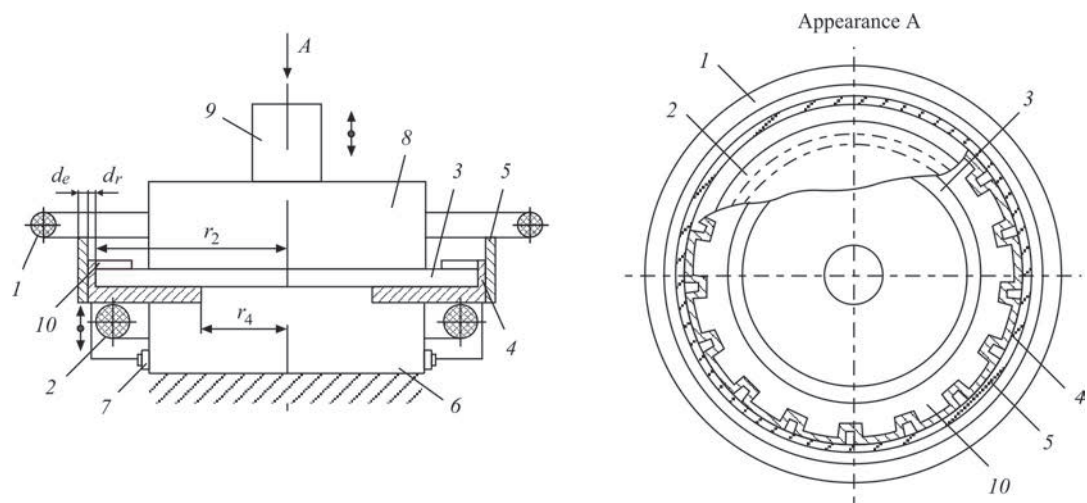
Figure 1. Device for regulating power in the zone of surfacing with thermal and electromagnetic shields rigidly fixed between each other (description *1–10* see in the text)

deposited by the wear-resistant alloy PG-S1 was carried out electrically in a 20 % water solution of chromic anhydride with a voltage of $U = 20$ V, holding time was $\tau = 5$ s.

Analysis of elemental composition of deposited specimens was carried out in the micro-analyzer SX-50 (Camebax) of the Cameca Company. Tests for wear resistance of deposited metal were performed in the machine NK-M [12].

The results of investigations were expressed in terms of relative wear resistance, which is equal to the ratio of reference weight loss to the weight loss of studied specimens.

Surfacing was carried out simultaneously on the entire working surface with the use of a generator of type HFI-63/0.44 by mechanical horizontal vibration on the energy-saving heating mode, which was regulated by the device [13].

Investigation of the process of induction surfacing of thin discs were carried out with the help of a heating system (ITES) (Figure 1) [14], which consists of the upper *8* and lower *6* clamping plates, as well as the drive *9* for lifting the upper plate *8*. The part *3* with the charge *10* of a solid alloy PG-S1, preliminary poured on it, was installed in a two-turn annular inductor, *1* — upper, *2* — lower turn. At the end of the disc and at its lower surface opposite to surfacing, around its perimeter, a thermal shield *4* is located, and also at the end of the disc an electromagnetic shield *5* is installed, which are rigidly interconnected and

fixed to the lower plate. Electromagnetic and thermal shields are manufactured with the possibility of vertical movement relative to the end of the disc *3* and turns of the inductor *1* and *2* by means of the drive *7*, fixed on the lower plate *6*, which allows regulating the temperature field in the surfacing zone, as far as in induction surfacing a powder-like solid alloy is melted from the surface of the base metal.

Investigation of the deposited metal produced by means of the ITES heating system with the use of horizontal vibration was performed on the microstructure, on the thickness of the layer of deposited metal and on wear resistance in order to provide a deposited bead with a width of 10–50 mm and a thickness of respectively 0.8–1.5 mm.

The obtained results were compared with those obtained by the heating system without horizontal vibration.

In this case, discs were used made of 3 mm thick steel St3 and a powder-like solid alloy PG-S1, the chemical composition of which is given in Table 1.
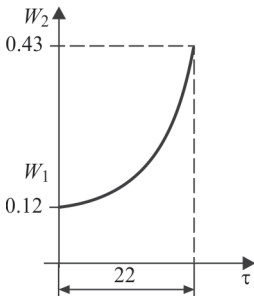
Table 2 presents heating systems and heating parameters in energy-saving mode of surfacing [9].

The process of induction surfacing was carried out simultaneously throughout the entire working surface by using the generator of type HFI-63/0.44 without rotation of the part. The technical characteristics of the generator with horizontal vibration are the same as without vibration, at the initial moment of time they were following: voltage on the circuit was 2.2 kV; volt-

Table 1. Chemical composition (wt.%) of powder-like solid alloy PG-S1

Deposited material / Powder	C	Cr	Si	Ni	Mn	B	Cu	W	Fe	Hardness of deposited metal *HRC*
PG-S1 sormite No.1 (U30Kh28N4S4)	2.5–3.3	27–31	2.8–4.2	3.0–5.0	0.4–1.5	–	–	–	Base	51

Table 2. Heating systems and surfacing modes

Heating systems	Surfacing modes					Type of generator	Nature of change in the specific power on the inductor $W \cdot 10^9$, W/m³
	Circuit voltage, kV	Anode voltage, kV	Mains current of the tube, A	Anode current of the tube, A	Surfacing time, s		
Without and with horizontal vibration	Variables					HFI–63/0.44	
	input numerator (τ = 0 s)			output denominator (τ = 22 s)			
	$\dfrac{2.2}{7.0}$	$\dfrac{8.3}{10.0}$	$\dfrac{3.6}{0.95}$	$\dfrac{1.1}{3.1}$	22		

age on the tube anode was 8.3 kV; current of the tube mains was 3.6 A; current of the tube anode was 1.1 A; surfacing time of the entire working surface of the disc was 22 s. The process was carried out without switching the generator, i.e., the specific power at the inductor was changed by the energy-saving mode, which has the form [9] and is determined by the formula

$$W_{set} = \frac{\lambda_g m^2}{sh(am^2\tau)} T_{set} e^{am^2 t},$$

where T_{set} is the temperature at which the quality surfacing is carried out, which is reached over the time τ; $\lambda_g = ca\gamma$, W/(m·°C); c is the specific heat capacity, a is the temperature conductivity, m²/s; γ is the density, kg/m³; $m^2 = Bi/2h^2$; $Bi = 2ha/\lambda$ is the Bio criterion; λ is the coefficient of thermal conductivity of the disc material, W/(m·°C); α is the coefficient of heat dissipation, W/(m²·°C); t is the running time; τ is the surfacing time.

The final parameters of surfacing mode were respectively 7.0, 10.0, 0.95, 3.1. The specific power without vibration and with vibration, respectively, at the initial moment was $W_1 = 0.12 \cdot 10^9$ W/m³ and at the end of surfacing $W_2 = 0.43 \cdot 10^9$ W/m³ (see Table 2).

Let us consider metallographic examinations of the layer of deposited metal produced with the help of a heating system (ITES) with horizontal vibration and without vibration.

The examinations were conducted in two cases of induction surfacing with and without mechanical vibration. To investigate the structure and wear resistance of deposited metal, from the deposited workpieces the specimens were cut. Etching of the specimens for metallographic examinations was carried out step-by-step, electrolytically in a 20 % solution of chromic acid (voltage was 20 V and holding time was 10 s), the structure of deposited metal was determined by chemical etching in 4 % nitric acid solution.

The microstructure of the base metal represents ferrite and pearlite, and the microstructure of deposited metal of the investigated specimens consists of primary carbides (complex carbides of type $(Fe, Cr)_7C_3$ and $(Fe, Cr)_3C$) in the form of large fan-shaped plates having a hexagonal lattice with a clear boundary interface with the matrix of carbide eutectics and matrix austenitic structure.

The excessive carbides are usually arranged in the form of separate plate precipitations in the central part across the width and thickness of the deposited bead. Rectangular and hexagonal precipitations represent the carbides of different dispersions, a part of which are excessive plate carbides, which are fairly uniformly distributed in the matrix. The microhardness of the carbides varied within HV 0.5–11710–12830 MPa.

The common for the two variants of deposited metal are:

● the presence of hypoeutectic zone in the deposited layer adjacent to the joint line and is characterized by the formation of dendrites of solid solution (alloyed austenite) with the axes of the first and second order, as well as carbide eutectics crystallizing in the interdendritic space. The microhardness of austenite for the specimen without horizontal vibration was (HV 0.5–4550–5140 MPa and HV 0.5–5150–5900 MPa for the specimen with horizontal vibration. In addition, structural heterogeneity along the joint line was detected on the side of PG-S1 sormite, which evidences that hypoeutectic dendritic area has a nonuniform distribution;

● the formation of a limiting white strip of solid solution (alloyed austenite) between the deposited and base metal of variable width of 10–20 μm for the specimen without vibration with microhardness of HV 0.5–3030–3410 MPa, and for the specimen with vibration HV 0.5–4500 MPa;

● on the side of the base metal near the fusion line, a diffusion zone arises, which represents a thin-plate
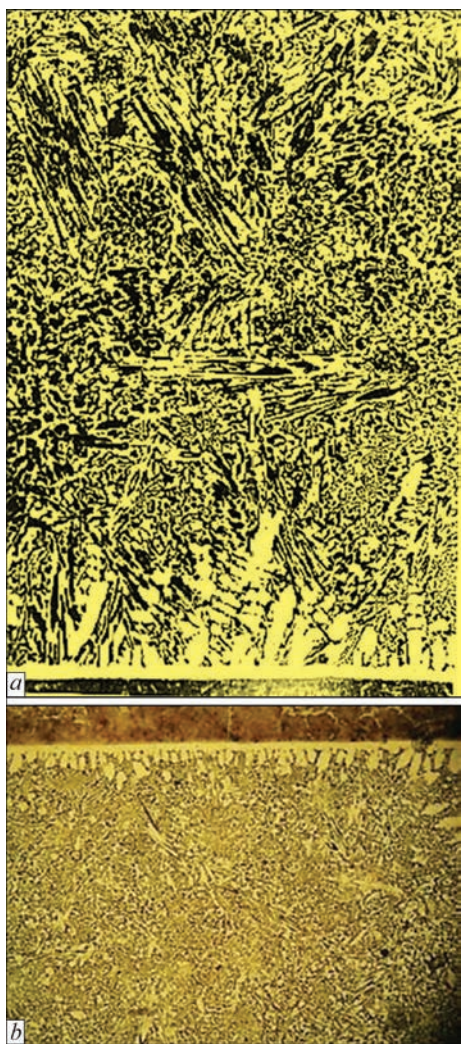
Figure 2. Microstructure (×200) of deposited metal specimens: *a* — without vibration; *b* — with horizontal vibration

Figure 3. Distribution of carbon and chromium across the thickness of deposited metal: *a* — without vibration; *b* — with vibration

pearlite and ferrite along the grain boundaries, sometimes with a Widmannstatten orientation with a microhardness HV 0.5–2440 MPa, which has arisen as a result of diffusion of carbon with sormite into the base metal.

The microstructure of deposited metal is presented in Figure 2.

The characteristics of microhardness of the structural components are given in Table 3.

It is necessary to note differences in the structure of two variants of deposited metal. Horizontal vibration leads to a noticeable refinement of the carbide component (Figure 2, *b*). Carbides having the appearance of hexagons with an average side length of 10–12 μm without vibration (see Figure 2, *a*) are refined to 3.5–5.0 μm with horizontal vibration (Figure 2, *b*).

The maximum depth of the eutectic zone is in the specimen without horizontal vibration (see Figure 2, *a*) and the minimum depth is in the specimen with horizontal vibration (Figure 2, *b*) and it occupies the smallest percentage of austenitic dendrites along the length of surfacing as compared to the first case. During horizontal vibration, the joint line on the side of the sormite represents mainly a white strip with the formation of almost equiaxed grains of austenite (see Figure 2, *b*).

In order to determine the composition of structural components (chromium, carbon) and to establish their influence on properties of deposited metal, micro-X-ray spectral analysis of deposited metal was carried out (Figure 3).

In all cases, the analysis was performed at approximately the centre of the layer of deposited metal perpendicular to the fusion line at a depth of up to 350 μm from the fusion boundary.

It was established that in the metal of the investigated specimens, carbon was bonded into carbides of type $(Fe, Cr)_7C_3$ and $(Fe, Cr)_3C$, a noticeable redistribution of diffusive carbon near the fusion line was not observed.

Figure 4 presents the diagrams of relative wear resistance and hardness of deposited specimens (average for three tests).

As can be seen from Figure 4, for the case when surfacing is performed without vibration, the wear re-

Table 3. Characteristics of microhardness of structural components

Technological operation	Microhardness of structural components, MPa		
	Chromium carbides	Matrix	White strip (transition zone)
Without vibration	11710–12830	4550–5140	3030–3410
With vibration	14300–15440	5150–5900	4500
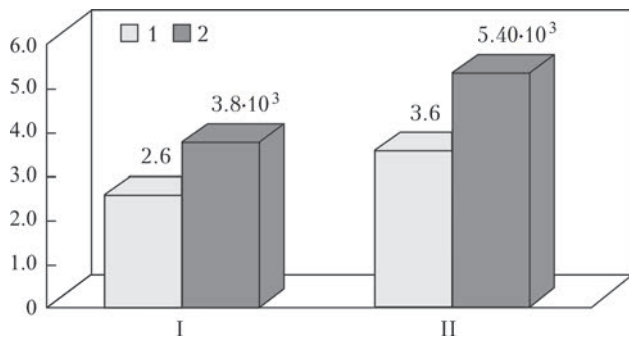
Figure 4. Relative wear resistance and hardness of deposited metal: I — without vibration; II — with vibration; 1 — relative wear resistance; 2 — hardness of deposited metal, MPa

sistance is 2.6 and the hardness is 3800 MPa, and in the case of applying horizontal vibration, the wear resistance is 3.6 and the hardness is 5400 MPa, respectively. This is achieved due to a more favourable distribution of alloying elements in the deposited layer of metal.

Figure 5 shows the curves of a normal distribution of thickness of the layer of deposited metal. The uniform thickness of the layer of deposited metal as compared to surfacing without horizontal vibration is increased by 10 % (see Figure 5), which provides a uniform distribution of liquid metal in the surfacing area.

Conclusions

The studies of induction surfacing of parts showed that with the use of horizontal vibration, combined shielding of thermal and electromagnetic fields and energy-saving surfacing mode, the wear resistance is increased by 1.4 times, the thickness of the deposited metal layer is increased respectively by 10 % and the quality of deposited metal is improved as compared to the technology without application of horizontal vibration.

Figure 5. Curves of normal distribution of thickness of layer of deposited metal (h, mm) at simultaneous surfacing using the energy-saving mode (n is the number of points in the preset interval during measurement of thickness): a — without vibration; b — with horizontal vibration

1. Ryabtsev, I.A. (2004) *Surfacing of machine and mechanism parts*. Kiev, Ekotekhnologiya [in Russian].
2. Tkachev, V.N. (1971) *Wear and improvement of service life of parts of agricultural machines*. Moscow, Mashinostroenie [in Russian].
3. Pulka, Ch.V. (2006) *Technological and energy effectiveness of induction surfacing of thin steel discs*: Syn. of Thesis for Dr. of Techn. Sci. Degree. Kyiv [in Ukrainian].
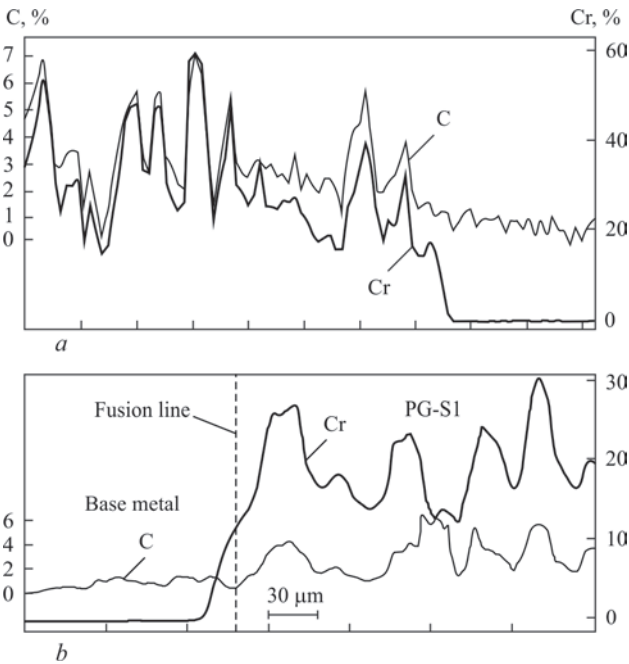4. Lozinsky, M.G. (1958) *Industrial application of induction heating*. Moscow, AN SSSR [in Russian].
5. Babat, G.I. (1965) *Induction heating of metals and its industrial application*. Moscow, Energiya [in Russian].
6. Slukhotsky, A.E., Ryskin, S.E. (1974) *Inductors for induction heating*. Leningrad, Energiya [in Russian].
7. Brezinova, J., Guzanova, A., Draganovska, D. et al. (2016) Study of selected properties of thermally sprayed coatings containing WC and WB hard particles. *Acta Mech. Autom.*, **10**, 296–299. Doi:10.1515/ama-2016-0046.
8. Pulka, Ch.V., Gavrilyuk, V.Ya., Senchishin, V.S. (2013) Improvement of equipment and technology of induction surfacing. *Svarochn. Proizvodstvo*, **4**, 27–30 [in Russian].
9. Shably, O.N., Pulka, Ch.V., Budzan, B.P. (1988) Ways of energy saving in induction surfacing of thin-wall discs. *Avtomatich. Svarka*, **12**, 56–58 [in Russian].
10. Pulka, Ch.V., Shablii, O.M., Gavrylyuk, V.Ya., Senchyshyn, V.S, Sharyk, M.V. (2012) *Method of surfacing of steel discs*. Pat. on utility 72129 UA, Int. Cl. B23K 13/00. Ternop. NTU [in Ukrainian].
11. Pulka, Ch.V., Shablii, O.M., Gavrylyuk, V.Ya., Senchyshyn, V.S, Sharyk, M.V. (2012) *Method of surfacing of steel discs*. Pat. on utility 73032 UA, Int. Cl. B23K 13/00. Ternop. NTU [in Ukrainian].
12. Yuzvenko, Yu.A., Gavrish, V.A., Marienko, V.A. (1979) *Laboratory units for evaluation of wear resistance of deposited metal. Theoretical and technological principles of surfacing. Properties and tests of deposited metal*. Kiev, PWI, 23–27 [in Russian].
13. Pulka, Ch.V. (1998) Programming of heating mode in induction surfacing of thin steel discs. *Avtomatich. Svarka*, **1**, 48–50 [in Russian].
14. Shablii, O.M., Pulka, Ch.V., Pysmennyi, O.S. (2004) *Device for control of power in surfacing zone*. Declar. Pat. UA 68940A, Int. Cl. 7B23K 13/00 [in Ukrainian].

DIFFUSION HEAT-RESISTANT COATINGS FOR STAINLESS AND CARBON STEELS

A.L. BORISOVA[1], **N.I. KAPORIK**[1], **T.V. TSYMBALISTA**[1] and **M.A. VASILKOVSKAYA**[2]

[1]E.O. Paton Electric Welding Institute of the NAS of Ukraine
11 Kazymyr Malevych Str., 03150, Kyiv, Ukraine. E-mail: borisov@pwi.ru.kiev.ua
[2]I. M. Frantsevich Institute of Problems of Materials Science
3 Krzhyzhanovskogo Str., 03680, Kyiv, Ukraine. E-mail: kiparis-gpk@ukr.net

The paper presents the results of investigation of heat-resistant diffusion coatings on steel 08Cr7Ti and steel 45, produced by aluminizing and chromoaluminizing methods in powder mixtures at a temperature of 900–950 °C during 2–5 h. On the kinetic dependencies of oxidation of the specimens with coatings in the temperature interval of 800–1000 °C, the parametric diagrams of thermal shock resistance were plotted. They allow evaluating endurance of protective coatings at any temperatures up to 1000 °C. 8 Ref., 3 Tables, 7 Figures.

K e y w o r d s : aluminizing, chromoaluminizing, heat-resistant coatings, microstructure, phase composition, oxidation kinetics, thermal shock resistance parameter

All types of protective coatings, including heat-resistant ones, can be divided into two main groups by the nature of their formation: diffusion and layered coatings [1].

I — diffusion-type coatings, the composition of which is the product of interaction of the saturating medium with the base metal. They are produced by saturating the surface of protected metal by one or more elements to form a protective layer.

II — layered-type coatings deposited on the surface of protected metal of a heat-resistant material, for example, applying the methods of thermal spraying.

The coatings of diffusion type are the most widely used. Their advantage is a good bond strength with the base and a relatively simple technology of deposition, the disadvantage is a high temperature of formation and rather active diffusion interaction with the base.

Layered-type coatings are as a rule deposited on cold or slightly preheated base, but they have weaker bond strength with the base than diffusion coatings and require the use of more complex equipment.

Combining the methods of forming protective coatings, obviously, will significantly reduce disadvantages of both groups.

During fulfillment of the project of the Program *«Resurs-2»* P5.1.2 *«Improving life time and effectiveness of recuperative heat exchangers by deposition of heat-resistant radiating coatings to protect heating surfaces, operating in combustion flows, and modernization of inner secondary emitters»*, heat-resistant coatings of two types were developed. The results of investigations of the coatings produced by the methods of thermal spraying using composite powder FeAlCr with the addition of 2 wt.% CeO$_2$, were pub-

lished in [2]. This paper is devoted to the solution of the same problem by using diffusion-type coatings.

The most promising diffusion methods for producing heat-resistant coatings on steels include aluminizing and chromoaluminizing processes [3–6]. Moreover, in addition to thermal shock resistance, diffusion saturation of the surface of metals and alloys with aluminum and simultaneous or consequent saturation with aluminum and chrome leads to increase in corrosion and erosion resistance. Among numerous methods of aluminizing and chromoaluminizing, the method of saturation in powder mixtures obtained the most widespread and industrial application.

It is known that structure, phase composition, protective properties and endurance of coatings depend on such factors as composition of powder mixture, temperature and time of diffusion saturation, content of alloying elements, and many other factors, in connection with which the solution of the problem of increasing endurance and efficiency of specific parts requires additional investigations.

In the present work, the processes of aluminizing and chromoaluminizing of steel 08Cr17Ti (used for outer secondary radiators of recuperators) and steel 45 (to investigate the possible replacement of alloy steel with carbon steel) were investigated.

Methods and materials. The processes of aluminizing and chromoaluminizing were carried out in special containers with a seal at a temperature of 900–950 °C during 2–5 h. The main components of the powder mixtures were:

● powder of aluminum parting dust (source of aluminum during aluminizing), a mixture of powders of chrome and aluminum (during chromoaluminizing);
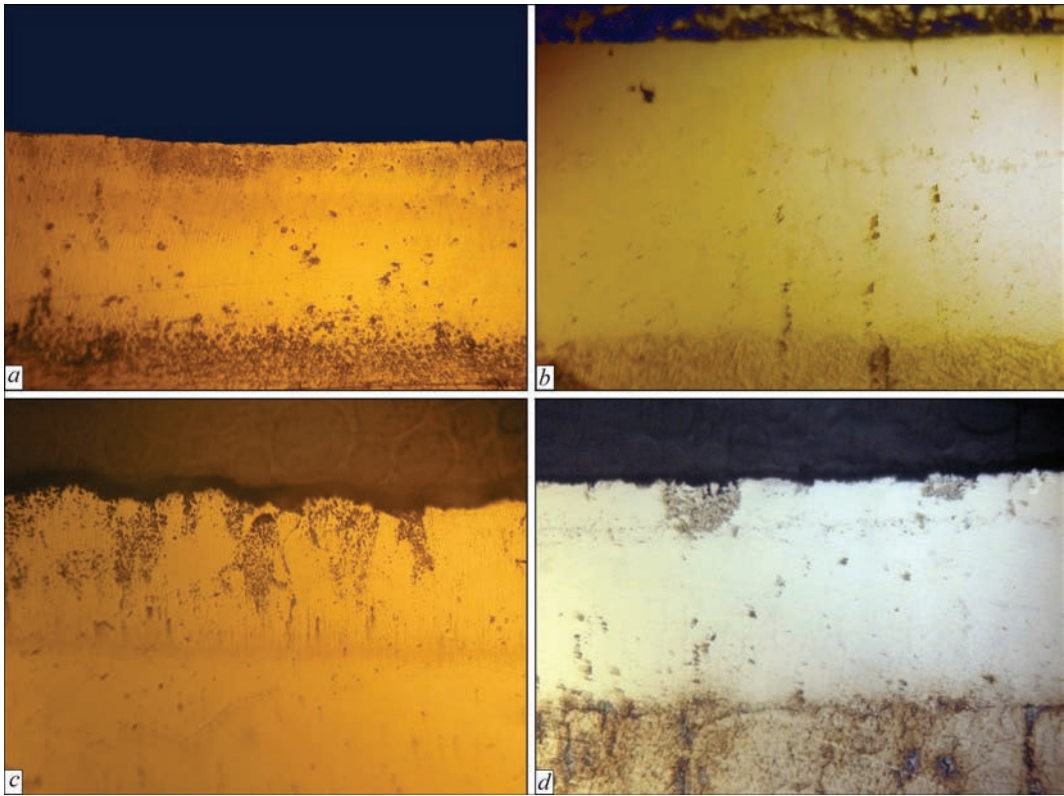
Figure 1. Microstructure (×400) of aluminized (*a*, *b*) and chromoaluminized (*c*, *d*) steel 08Cr17Ti and steel 45
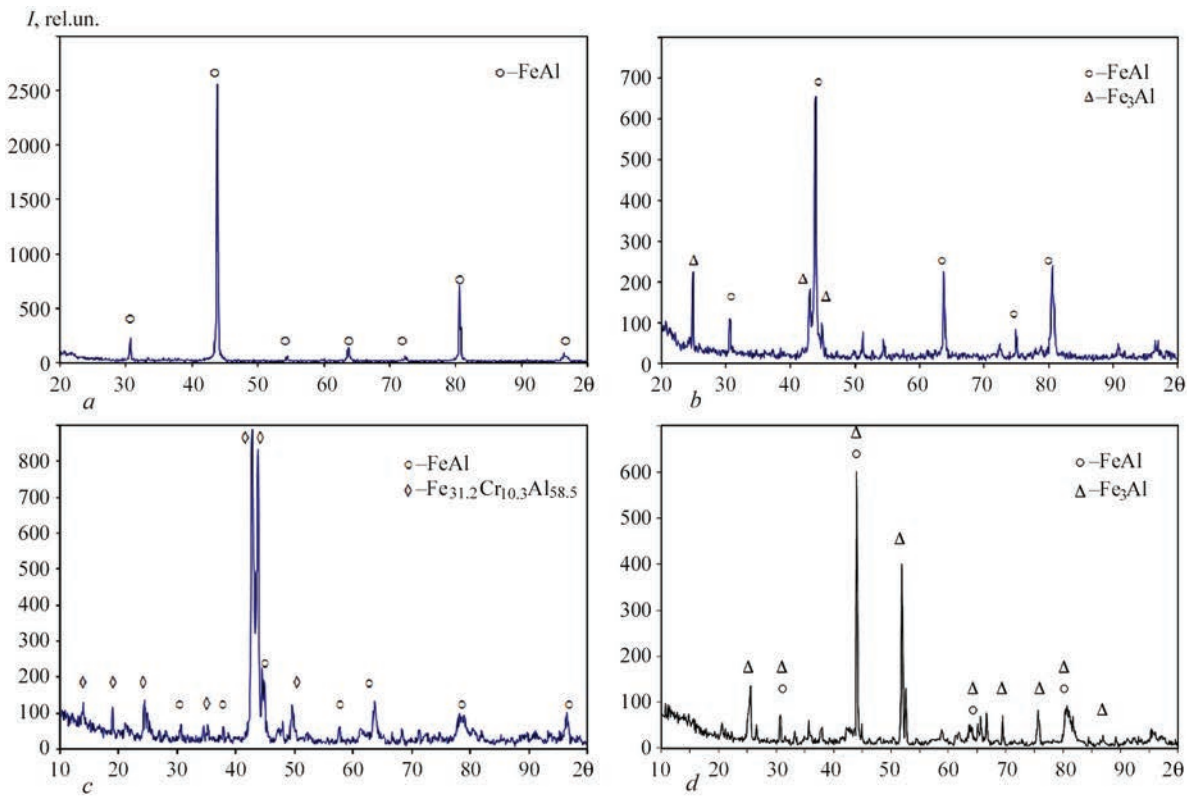
Figure 2. X-ray patterns of diffusion coatings on steel 08Cr17Ti (*a*, *c*) and steel 45 (*b*, *d*) produced by the methods of aluminizing (*a*, *b*) and chromoaluminizing (*c*, *d*)

Table 1. Characteristics of heat-resistant coatings

Coating	Characteristics of coating					
	Thickness, μm		Microhardness, MPa		Phase composition	
	08Cr17Ti	Steel 45	08Cr17Ti	Steel 45	08Cr17Ti	Steel 45
Aluminized	160±15	230±20	3240±450	2560±490	FeAl	FeAl, Fe$_3$Al
Chromoaluminized	200±10	205±10	3340±630	2800±690	FeAl, Fe$_{31.2}$Cr$_{10.3}$Al$_{58.5}$	FeAl, Fe$_3$Al

● aluminum fluoride powder AlF$_3$ (process activator);

● aluminum oxide powder (inert additive that prevents sintering of aluminum powder particles and a mixture of aluminum with chrome);

● titanium hydride powder (to remove oxygen remainders from powder mixture).

X-ray structural analysis (XRD) was performed by applying the X-ray diffraction meter DRON-3 in CuK_α-radiation with a graphite monochromator. The phases were decoded using the ASTM hardware components.

Cutting of specimens with coatings was performed in the machine-tool Isomet 1000. The cut specimens were filled with protacryl of grade M, grinding was performed using an abrasive paper with a grain size from 600 to 1200, and polishing was performed using diamond discs from 80–40 to 20–14 in the machine-tool Row Rathenow Metasines. The final polishing was performed in a felt disc using a chrome oxide suspension. To reveal the microstructure, etching of the specimens was carried out in an alcohol solution NHO$_3$ for steel 45 and HF for steel 08Cr17Ti. Metallographic examinations were performed with the use of the microscope Neophot 32 equipped with a digital photo camera. Microhardness was measured by using of the microhardness tester PMT-3 at a load of 50 g. The number of measurements was at least 50.

Results and discussion. Figure 1 presents the microstructure. Figure 2 shows X-ray patterns of diffu-
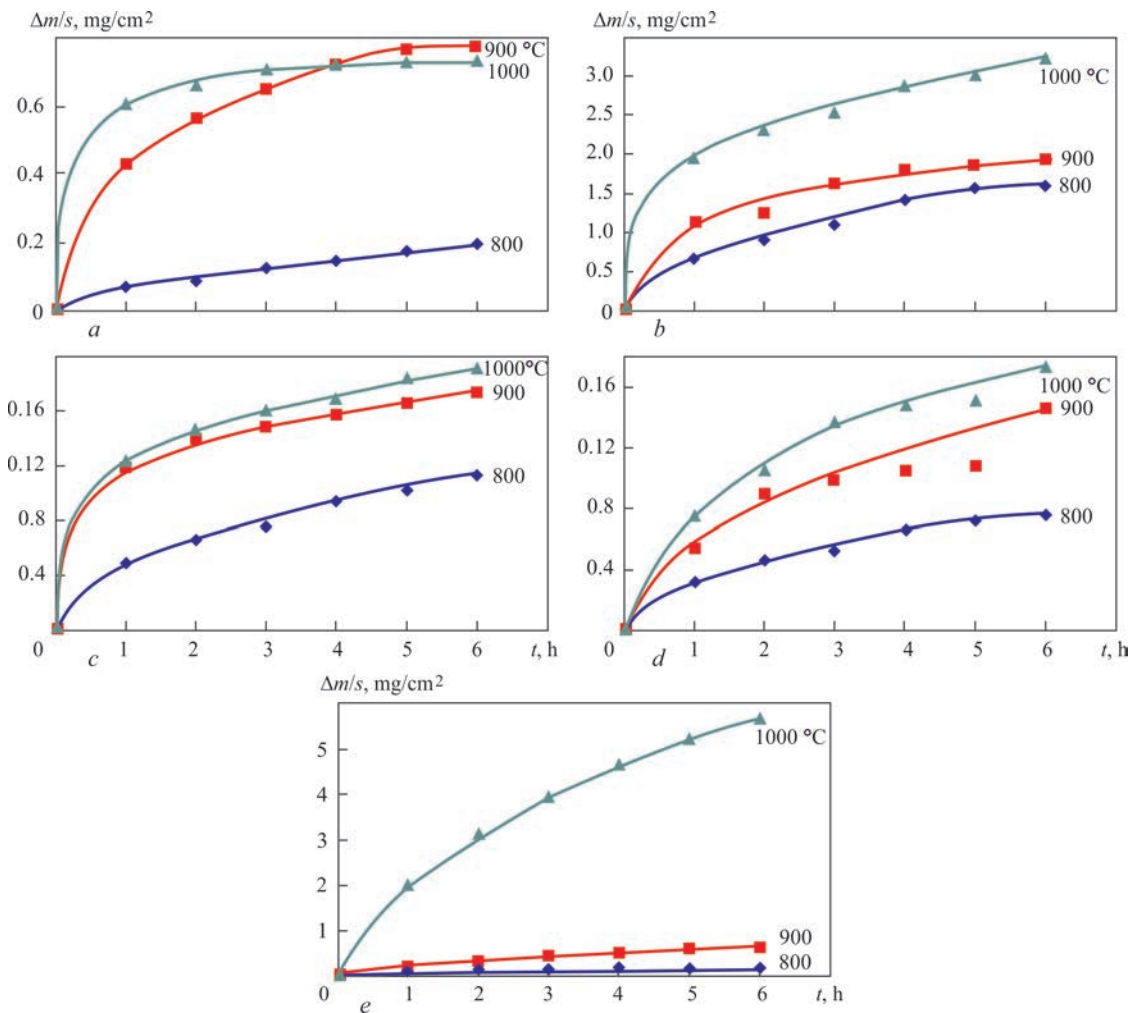
Figure 3. Kinetic dependencies of oxidation of aluminized (*a*, *b*) and chromoaluminized (*c*, *d*) steel 08Cr17Ti (*a*, *c*) and steel 45 (*b*, *d*) and also unprotected steel 08Cr17Ti (*e*)

Figure 4. Microstructure (×200) of aluminized (*a*, *b*) and chromoaluminized (*c*, *d*) steel 08Cr17Ti (*a*, *c*) and steel 45 (*b*, *d*) after tests on thermal shock resistance at a temperature of 1000 °C during 5 h

sion coatings on steel 08Cr17Ti and steel 45, and in Table 1 their characteristics are given.

As follows from the presented data, at diffusion saturation of steels with aluminum, on their surface layers of iron intermetallide are formed, which differ in thickness and hardness. As is known, chrome inhibits the diffusion of aluminum into iron, which results in a smaller thickness of aluminized layer on steel 08Cr17Ti as compared to that of steel 45, while its hardness increases due to the presence of chrome. It should be noted, that beyond the region of intermetallide FeAl, the region of solid solution of aluminum in iron is located, spreading to the depth up to 400 μm (for steel 08Cr17Ti) and to 600 μm (for steel 45). Its microhardness is smoothly decreased in the direction to the core (from 2000 to 1500 MPa).

During chromoaluminizing of steel 08Cr17Ti in the surface layer of the coating, two intermetallides were revealed: FeAl alloyed with chrome, and $Fe_{31.2}Cr_{10.3}Al_{58.5}$ (a phase close to Fe_3CrAl_6 as to its composition), and on steel 45 — FeAl and Fe_3Al al-

loyed with chrome. The microhardness of these coatings is slightly higher than that of the aluminized layers on the same steels.

Typical kinetic dependences of oxidation of diffusion coatings and unprotected steel 08Cr17Ti are shown in Figure 3, *a* and Figures 4 and 5 demonstrate microstructure and X-ray diffraction patterns of coatings after tests on thermal shock resistance at a temperature of 1000 °C.

As follows from the presented data (Figure 3), the mechanism of oxidation of diffusion coatings submits to the parabolic temporal law in the entire studied temperature range of 800–1000 °C. Judging by the results of X-ray diffraction analysis (Figure 5, Table 2), the main changes in phase composition during oxidation of diffusion coatings are the formation of aluminum oxide Al_2O_3 in the surface layers, behind which there is a region of intermetallides FeAl or Fe_3Al (in case of aluminizing) or intermetallides FeAl and Fe_3Al alloyed with chrome (in case of chromoaluminizing), gradually passing into solid solutions. Judging by the

Table 2. Characteristics of coatings after tests on thermal shock resistance at a temperature of 1000 °C during 5 h

Coating	Characteristics of coating					
	Thickness, μm		Microhardness, MPa		Phase composition	
	08Cr17Ti	Steel 45	08Cr17Ti	Steel 45	08Cr17Ti	Steel 45
Aluminized	320±15	320±20	2780±560	2370±400	FeAl, Al_2O_3	FeAl, Al_2O_3
Chromoaluminized	290±5	300±10	3260±520	2230±320	$(F, Cr)_3Al$, Al_2O_3	$(Fe_2Cr)Al$, Al_2O_3
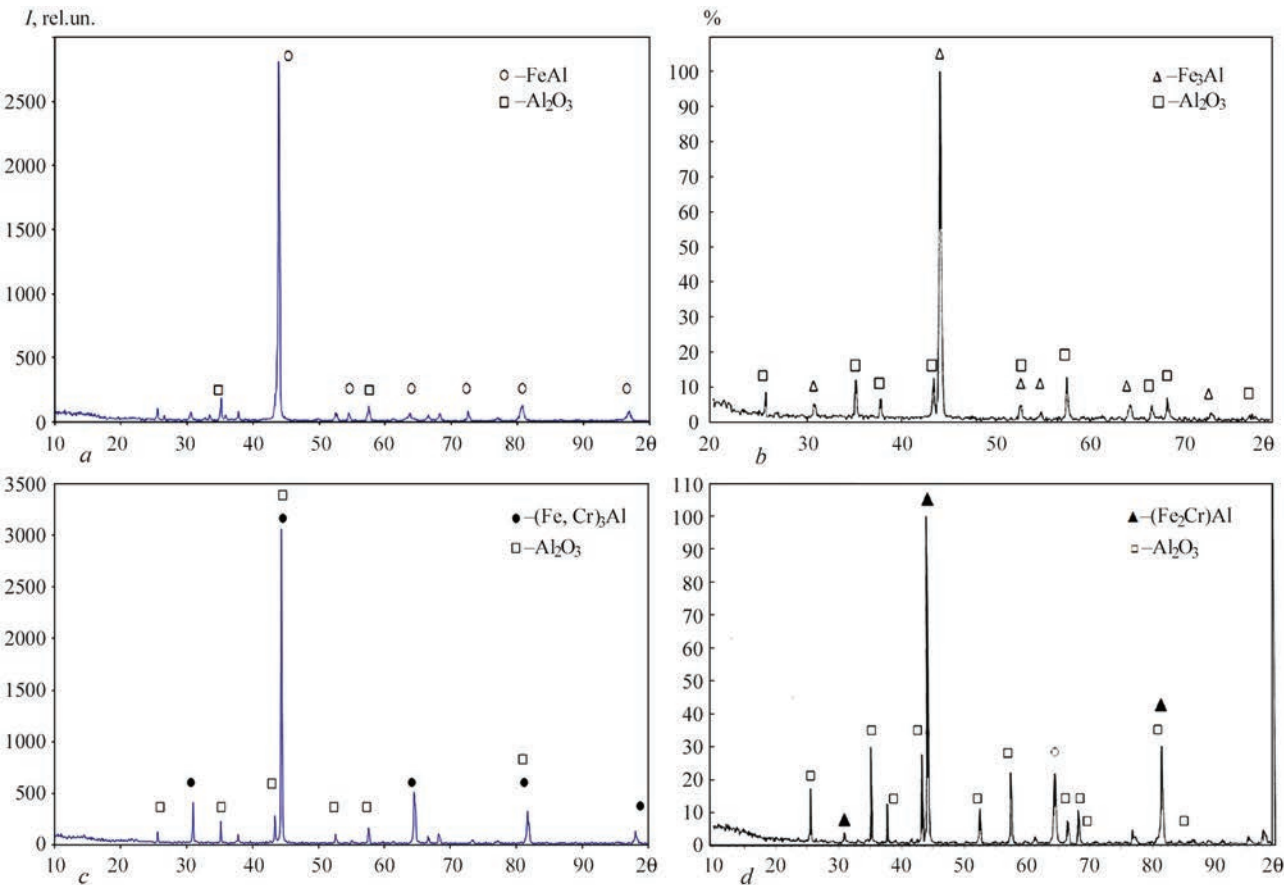
Figure 5. X-ray patterns of aluminized (*a*, *b*) and chromoaluminized (*c*, *d*) steel 08Cr17Ti (*a*, *c*) and steel 45 (*b*, *d*) after tests on thermal shock resistance at a temperature of 1000 °C during 5 h

results of X-ray spectral microanalysis, the content of aluminum in the coating decreases both as a result of the formation of an oxide film, as well as due to its resorption in the base. Thus, for example, on the surface of chromoaluminized steel 08Cr17Ti in the initial state (Figure 6, *a*), the content of aluminum is about 31 wt.%, which corresponds to the composition of intermetallide FeAl, gradually decreasing at a depth of about 150 μm to 15 % (approximate content of Al in Fe$_3$Al), and then to 2 % at a depth of 600 μm. Af-

ter oxidation at a temperature of 1000 °C during 6 h, these values amount approximately to about 20 %, respectively, and in the surface layer to about 15 wt.% at a depth of about 200 μm (Figure 6, *b*).

Comparing the microstructure of diffusion coatings in the initial state (Figure 1) and after oxidation at a maximum temperature of 1000 °C (Figure 4), the presence of longitudinal (in depth) cracks on steel 08Cr17Ti and their practical absence on steel 45 can be noted.
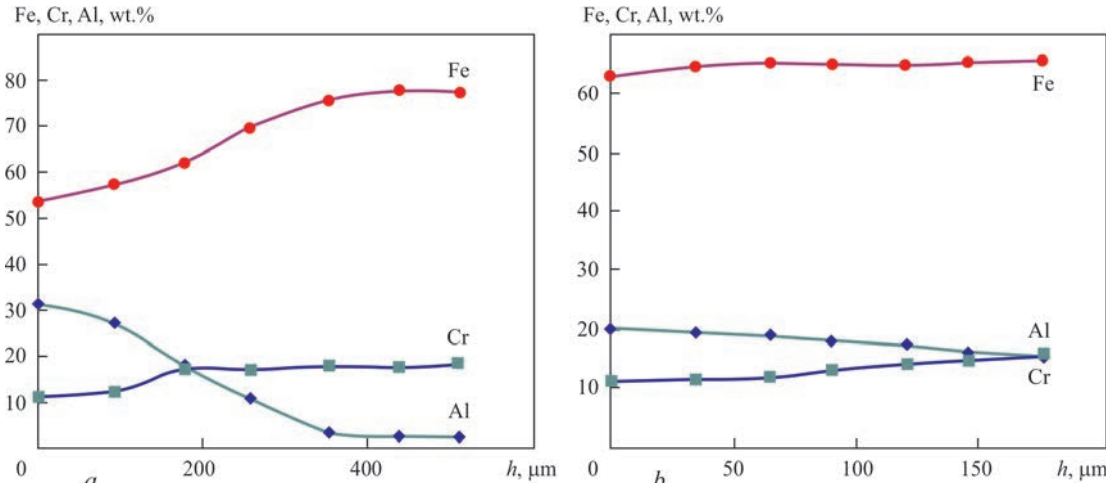
Figure 6. Distribution of elements in depth of diffusion layers of chromoaluminized steel 08Cr17Ti in the initial state (*a*) and after oxidation in air at a temperature of 1000 °C during 5 h (*b*)
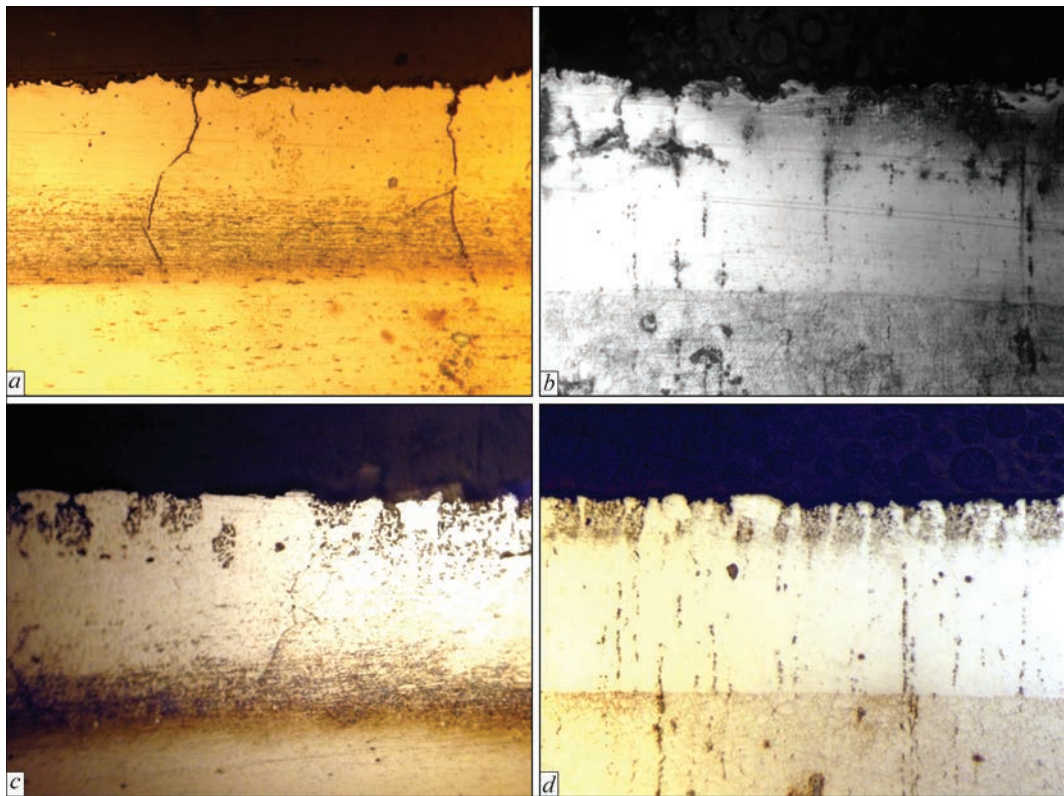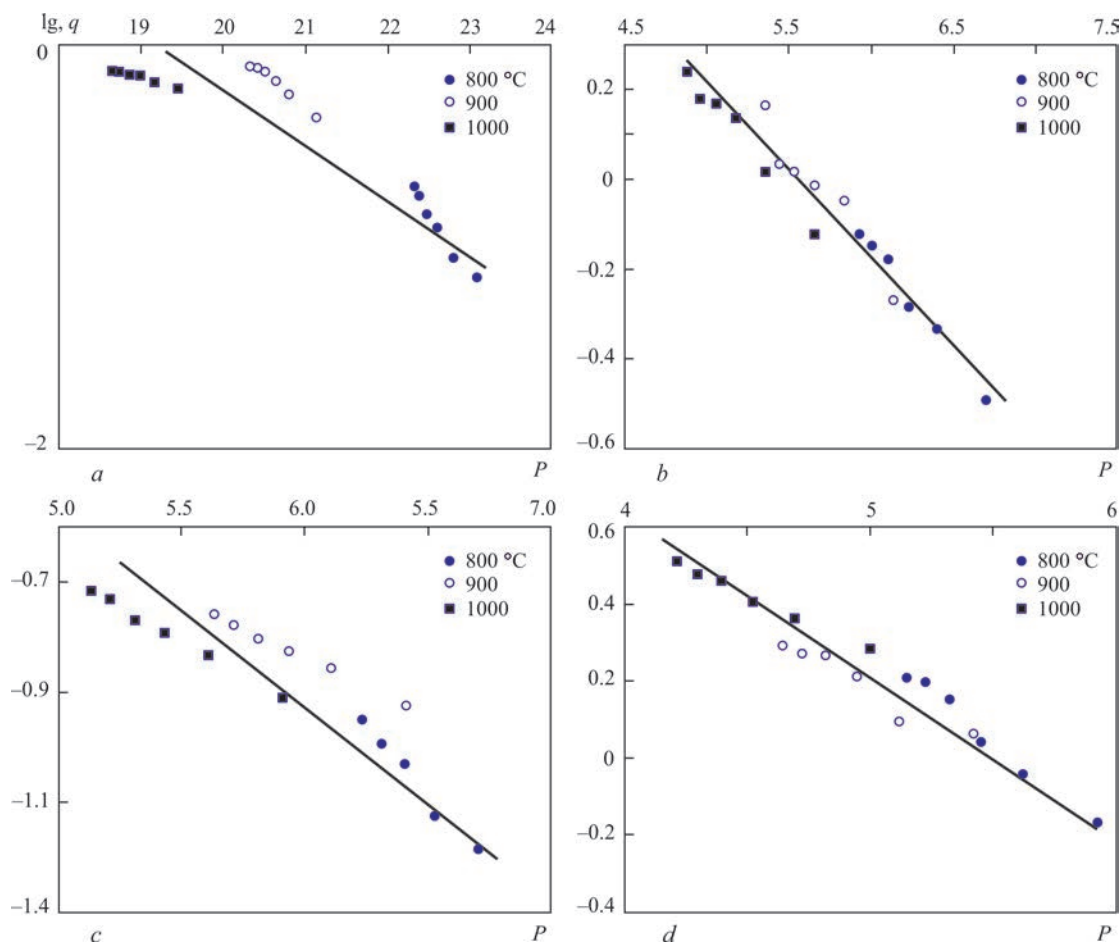
Figure 7. Parametric diagrams of thermal shock resistance for aluminized (*a*, *b*) and chromoaluminized (*c*, *d*) steel 08Cr17Ti (*a*, *c*) and steel 45 (*b*, *d*) according to the results of tests on thermal shock resistance at a temperature of 1000 °C during 5 h

Defects in diffusion coatings of this kind arise in connection with occurrence of residual stresses, the value and sign of which depend on chemical and phase composition of diffusion layer, which in this case is significantly different (see Figure 2, Table 1).

As for the effect of such kind of cracks on thermal shock resistance of protective coatings, it is far from unique. The fact is that to provide endurance of coatings operating at high temperatures, thermal shock resistance is an equally important characteristic, on

Table 3. Results of calculation of parameters of thermal shock resistance of chromoaluminized steel 45

Temperature, K	$10^3/T$	Oxidation time, h	lg t	Specific increment of mass, mg/cm²	lg q	$\dfrac{Q \lg e}{RT}$	Parameter of thermal shock resistance P
1073	0.932	1	0	0.32	−0.49	6.71	6.709746
		2	0.301	0.467	−0.33		6.408746
		3	0.477	0.52	−0.28		6.232746
		4	0.602	0.66	−0.176		6.107746
		5	0.699	0.72	−0.143		6.010746
		6	0.778	0.75	−0.12		5.931746
1173	0.852	1	0	0.54	−0.267	6.138	6.137731
		2	0.301	0.9	−0.046		5.836731
		3	0.477	0.97	−0.012		5.660731
		4	0.602	1.04	0.018		5.535731
		5	0.699	1.08	0.03		5.438731
		6	0.778	1.457	0.16		5.359731
1273	0.785	1	0	0.75	−0.122	5.65	5.655584
		2	0.301	1.04	0.0185		5.354584
		3	0.477	1.36	0.136		5.178584
		4	0.602	1.47	0.168		5.053584
		5	0.699	1.51	0.179		4.956584
		6	0.778	1.727	0.237		4.877584
$Q = 33025.5$							

which preservation or delamination of protective layer in the process of tests depends. One of the ways to increase thermal shock resistance is to reduce the effective elasticity modulus of the protective layer by creating deformation structure [7]. This can be achieved due to preservation of a significant residual porosity or creation of microcracks in an artificial way, oriented perpendicularly to the surface of a coating interface with the base [8]. As was shown by the investigations, in this work the presence of cracks in coatings did not impact the nature of their oxidation, which is evidenced by kinetic dependencies of oxidation of diffusion coatings, presented in Figure 3.

The carried out investigations allowed evaluating endurance of protective parts for any temperatures up to 1000 °C by plotting parametric diagrams of thermal shock resistance (Figure 7).

The methodology of plotting parametric diagrams of thermal shock resistance is described in detail in [4], and in Table 3 as an example, the results of calculating parameter of thermal shock resistance of chromoaluminized steel 45 are presented according to the results of this work.

Conclusions

As a result of carried out investigations, it was found that aluminizing increases thermal shock resistance of steel 45 by 2 times, steel 08Cr17Ti — by more than 7 times, and chromoaluminizing of steel 45 — by 3.5 times. The highest thermal shock resistance in the range of 800–1000 °C belongs to the chromoaluminized steel 08Cr17Ti, which exceeds the resistance of unprotected steel at 1000 °C by more than 25 times. Comparison of results of this work with previous investigations [1] showed that diffusion coatings (aluminizing and chromoaluminizing) are able to protect steel 08Cr17Ti and steel 45 from oxidation to higher temperatures (up to 1000 °C) as compared to AM- and EM-coatings produced of a composite powder FeAlCr — CeO_2 (up to 800 °C). However, it should be borne in mind that as compared with diffusion methods, the methods of thermal spraying are characterized by such advantages as ability to protect large-sized parts and producing large thicknesses of a protective layer.

At present time, prototype specimens of inner secondary emitters of recuperators of steel 08Cr17Ti and steel 45 with diffusion and thermal sprayed coatings were made for long-term tests by using the main workbench of the Gas Institute of the NASU during 2019–2020.

1. Borisov, Yu.S., Borisova, A.L., Tsymbalista, T.V. et al. (2019) Heat-resistant thermal coatings based on intermetallics with CeO$_2$ additives. *The Paton Welding J.*, **9**, 23–29.
2. Appen, A.A. (1976) *Temperature-resistant inorganic coatings*. 2nd ed. Leningrad, Khimiya [in Russian].
3. Borisenyuk, G.V., Vasiliev, L.A., Voroshnin, L.G. et al. (1981) *Chemical and heat treatment of metals and alloys*: Refer. Book. Moscow, Metallurgiya [in Russian].
4. Lygdenov, B.D., Guriev, A.M., Mosorov, V.I., Butukharov, V.A. (2015) Perspective diffusion coatings. *Int. J. of Experimental Education*, 12(**4**), 1, 572–573.
5. Muboyadzhyan, S.A., Galoyan, A.G. (2012) Diffusion aluminium coatings for protection of surface of inner sealing band of turbine blades. *Metally*, **5**, 4–13 [in Russian].
6. Burnyshev, I.N., Poryvaev, D.A. (2015) Aluminizing of steels in dynamic saturation medium. *Khimicheskaya Fizika i Mezoskopiya*, 17(**3**), 364–371 [in Russian].
7. Grot, A.S., Mortin, I.K. (1981) Behavior of plasma-sprayed ceramic thermal-barrier coating for gas turbine applications. *Amer. Ceram. Soc. Bull.*, **60**, 807–811.
8. Borisova, A.L., Adeeva, L.I., Tunik, A.Yu. (1994) Influence of characteristics of initial material and conditions of spraying on structure and properties of thermal coatings. Kyiv, PWI [in Russian].

To the 70th anniversary of the creation of electroslag welding

ELECTROSLAG WELDING PROCESS. ANALYSIS OF THE STATE AND TENDENCIES OF DEVELOPMENT (Review)

B.E. PATON, K.A. YUSHCHENKO, S.M. KOZULIN and **I.I. LYCHKO**

E.O. Paton Electric Welding Institute of the NAS of Ukraine
11 Kazymyr Malevych Str., 03150, Kyiv, Ukraine. E-mail: office@paton.kiev.ua

The paper presents the results of analytical review of investigations and commercial application of electroslag welding and surfacing in Ukraine, as well as foreign countries from the beginning of the XXI century. Analysis showed that the volume of application of electroslag welding of thick metal (more than 100 mm) in different branches of industry has noticeably decreased. However, stable growth of its application in the recent years has been noted in construction of bridges and high-rise buildings, ship building, as well as repair of large parts of machines on-site. The developed steels having low sensitivity to grain growth in the heat-affected zone, allowed expanding the range of products made by electroslag welding. There is a considerable increase of the volume of application of electroslag surfacing with strip electrode for anticorrosion coatings in pressure vessels, separators, steam generators, compressors and other equipment, being operated in oil and gas, power, metallurgical, paper-and-pulp and chemical industries. 51 Ref., 5 Figures.

K e y w o r d s : *electroslag welding, electroslag surfacing, welding equipment, technology, wire electrode, consumable nozzle, strip electrode, specific energy input, heat input, steel, heat-affected zone, impact toughness*

Electroslag welding process in Ukraine. Seventy years ago [1], a new method of electric fusion welding, named electroslag welding (ESW), was developed and successfully implemented at the E.O. Paton Electric Welding Institute (Kyiv) for welding vertical butt joints of blast furnace casings. This method featured a whole range of technical and technological advantages compared to the available industrial methods of fusion welding [2].

The phenomenon of emergence, development and subsequent application of the methods of ESW and electroslag surfacing (ESS) in industrialized countries is attributable to the high potential of the process [3, 4] for development of the economy.

Its successful application was promoted by cooperation with leading industrial enterprises of the USSR, CMEA, as well as many other foreign companies [2, 5].

On the threshold of the XXI century, the high scientific and technical level of the currently available methods, welding equipment, fixtures and technologies of ESW and ESS in welding production of various industries of mechanical engineering and construction allowed successfully solving the important tasks. For instance, development of the technique and technology of consumable nozzle ESW of structures from stainless steels of 18-8 type; investigation and development of the technology and technique of ESW of steels for elements of superconducting magnetic systems of ITER thermonuclear reactor; development of the technology and technique of ESW of position butt joints in titanium ring blanks of 1000 mm diameter with 100 mm wall

thickness; welding of copper to chromium-zirconium bronze by large cross-section electrode in manufacture of powerful current conduits of the power system of Tokamak fusion reactor, etc. [3, 4, 6].

Tendencies in ESW development over 10–15 years, starting from 1990 and analysis of information (about 3000 titles from 37 countries) [3] allowed determination and systemizing the main directions:

● development of low-alloyed steels with good weldability, the welded joints of which at up to 200 mm thicknesses have the required properties without subsequent heat treatment;

● improvement and development of new filler materials for welding;

● application of new low-alloyed steels (up to 30 to 40 % of the total material volume), used in structures made by ESW;

● development of requirements to the quality of metal and thick initial billets (up to 3000 mm) from higher strength alloyed steels;

● improvement of the technique and technology of ESW of circular butt joints predominantly for large billets of more than 2500 mm diameter;

● investigation and development of new types of welded joints at lowering of specific unit costs;

● development of the techniques and methods of producing permanent joints of a compact cross-section with application of the electroslag process and liquid filler metal.

Forecast estimates of future welding production envisaged, first of all, development and application of new generation welding equipment with program
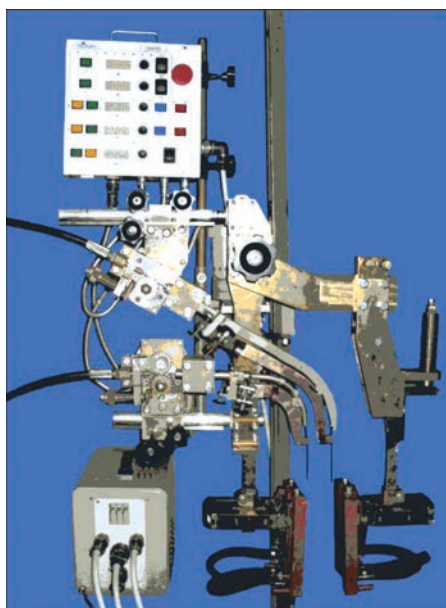
Figure 1. Two-electrode AD-381Sh machine for ESW of 30–100 mm thick metal

control of ESW technological process. Here, at introduction of new welding equipment, it is rational to provide the maximum possible level of mechanization and automation of assembly and auxiliary operations, as they take up to 50–70 % of the time of total cycle of welded metal structure fabrication [3].

In order to realize the technologies of ESW and ESS of large nontransportable metal structures in site, mobile groups were set up, fitted with the required set of equipment, including local heat treatment means.

The following two processes became the most widely accepted in welding production in mechanical engineering sectors and construction: electroslag welding with wire electrode (ESW WE) and with consumable nozzle (ESW CN). They are used to make the main types of the joints (butt, fillet, tee) and types of welds (straight, circular, variable profile). For these

Figure 2. Two-electrode ASh 115M2 machine for ESW of position circular and curvilinear butts joint of 40–200 mm thickness

processes, PWI developed a whole range of welding machines, including batch-produced machines of A-535, A-1304 and A-820K type [2, 3].

In 1990 a new machine was developed for ESW with wire electrodes for metal of up to 450 mm thickness (instead of A-535), which was designated ASh-112 [3]. For ESW of butt joints of low-alloyed steels of 09G2S type 30–100 mm thick, new generation assembly welding machine of AD-381Sh type was designed (Figure 1) [7].

In 2004-2006 a two-electrode machine ASh 115 M was developed for ESW of position circular welds of large metal structures of 14000 mm and larger diameter, which has no analogs in the world practice of welding production (Figure 2) [8].

In order to perform ESW CN, machines of ASh-110, ASh-113 and AShP113 M2 types (Figure 3) were developed, which ensure duplication during welding of practically all the elements of the welding circuit (mechanical and electrical) [3, 9, 10]. New generation machines of modular type are fitted with systems of welding process control, and enable continuous monitoring and certification of the mode parameters [11].

ESW development in Ukraine and in the world practice is going on, both as regards investigations of welding process proper and its industrial application.

An important direction in development of the electroslag process is regulation of input and distribution of thermal energy in the welded joint zone to ensure thermal cycles, not lowering the strength characteristics of the HAZ metal without subsequent high-temperature treatment [12].

Application of higher-strength structural materials opens up the possibilities for increasing the scopes of ESW application [13]. These steels have low sensitivity to overheating in the HAZ [2, 14–16].

Studies of electrode and base metal melting in the welding zone [17–19] showed that electrode surface melting in interelectrode gap of the slag pool is accompanied by formation of higher temperature energy nugget. Dimensions (volume) of the nugget vary cyclically due to electrode metal inflow to it. Nugget contact with the metal pool surface is accompanied by electrodynamic shock, as a result of which the metal pool, absorbing the thermal energy of the nugget, shifts towards the edges being welded, and performs their partial melting. It is shown that the dimensions of the energy nugget, welding current values and metal pool shapes have common regularity of a cyclic nature. Each cycle is completed by formation of a «discharge» into the metal pool. Welding current oscillogram at the moment of such a «discharge» shows peak increase of current 3 to 5 times [17, 18]. If this is confirmed by further studies, it will be possible to determine the optimum conditions of energy nugget existence and improve process control system.

The high level of service properties of welded joint metal is achieved under the condition of reducing the heat input. Specific energy input E_w of the electroslag welding process is in the range of 104–208 kJ/cm^2 for most of the cases of ESW of low-alloy steel metal [2].

At ESW with wire electrode, E_w lowering is limited by the conditions of preservation of the stability of running of the process proper and satisfactory weld formation.

It is shown that:

● at E_w < 45.0 kJ/cm^2 sound welds (without solidification cracks) are produced for metal of 30–60 mm thickness using one electrode (V_w = 3.0–5.0 m/h, V_e up to 600 m/h);

● in the range of V_w = 1.0–3.0 m/h E_w lowering from 90 to 55 kJ/cm^2 is observed, respectively. Here, even V_w increase up to 7–8 m/h does not allow lowering E_w below 45 kJ/cm^2;

● ESW in forced modes (V_w > 4.0 m/h) can be performed with new generation machines at complete automation of the process;

● it is recommended to perform ESW in forced modes in a narrow gap (24–18 mm) with flux-cored wire of 2.6–1.8 mm diameter, as well as solid wire of 2.0–1.6 mm diameter;

● metal of the welded joint produced at values E_w (75–45 kJ/cm^2) of ESW is characterized by higher quality.

Lowering of the specific energy input E_w (by 23 %) in ESW of titanium into a narrow gap (22 mm) leads to reduction of the HAZ width and lowers the probability of running of undesirable structural transformations in the base metal.

Noteworthy is the work aimed at further development and improvement of the technique and technology of repair of large metal structures directly on site. Processes have been developed for restoration of defects (predominantly, through-thickness cracks), arising in service of large-sized nontransportable metal structures by the method of multipass ESW with consumable nozzle [20, 21].

Technologies and technique have been developed for refurbishment of working elements of rapidly wearing machine parts using ESW, such as large gear teeth, heavy hammers of coal mills, steel and cast iron hot rolling rolls. Welding equipment was designed and practical recommendations on their application were issued [22, 23].

A method was proposed for ESW or ESS by corrosion-resistant stationary consumable sectioned electrodes of a large cross-section in a narrow gap for rectilinear and curvilinear butt joints of thick metal [24]. Large cross-section electrode and wire electrode, powered from different sources, are used in the welding zone. Such a scheme of welding process running allows an effective application of the advantages
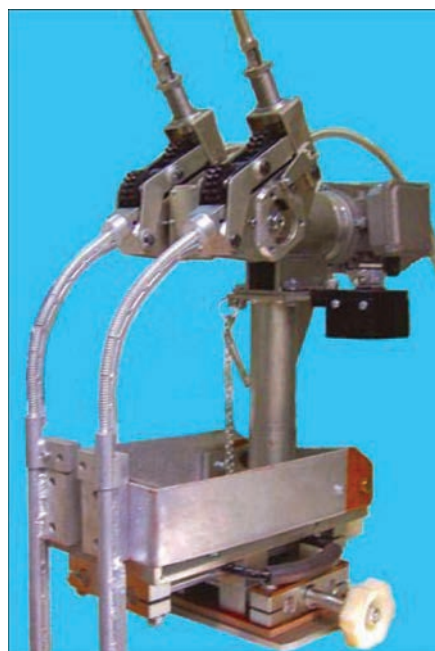
Figure 3. Portable two-electrode AShP 113M machine for ESW with consumable nozzle of 40–120 mm thick metal

and eliminating the disadvantages of the above welding processes [2]. The gap between the edges being welded and stationary sectioned electrode is equal to 1.5–3.0 mm and it should be filled with a ceramic type dielectric. The optimum material of the insulators are fluxes of AN-9U or AN-45 type, applied on the surface of electrodes in the form of powders, flux paper or flux board with binder additives (3–8 % of liquid glass). Investigations of ESW conditions showed that at a narrow gap and large cross-section of the stationary electrode, the area of existence of the stable process becomes narrower and shifts towards lower stresses in the slag pool (for the canonic method U_w = 52–40 V; for this method U_w = 40–25 V). The effectiveness of using the new method will be ensured by applying for stationary electrodes the power sources with program control of the main parameters of the welding mode (U_w, I_w, P_w) within the specified limits, both in the manual and in the automatic cycle. This ensures reduction of the amount of deposited metal; satisfactory conditions for weld formation at smaller E_w. There is a change in the distribution of thermal energy across the thickness of the edges being welded, in the technological capabilities of producing the welded joints, including those from dissimilar materials, in repair operations on restoration in large-sized parts in heavy engineering.

ESW by wire electrodes and consumable nozzle is widely applied for joining metals of 30–100 mm thickness [25, 26]. PJSC NKMZ together with PWI created a unique installation for ESW CN (Figure 4) of metal, the welded cross-section of which can reach the dimensions of 4000×6000 mm [9]. The machine was brought into operation in 2002. The production section, where

Figure 4. Appearance of an installation for ESW with consumable nozzle for joining metal, the cross-section of which can reach the dimensions of 4000×6000 mm. (G.Z. Voloshkevich Section of ESW of thick metal at PJSC «NKMZ», Kramatorsk)

the machine operates, was named after G.Z. Voloshkevich, who made the most significant contribution into ESW creation, development and introduction. Over the last almost twenty years the installation welded unique metal structures [27] of rolling mill bed plates, and other heavy engineering equipment (Figure 5).

Electroslag welding process abroad. In major Russian enterprises the scope of ESW application for manufacture of traditional products has markedly decreased by now. Increase of this process application for repair purposes, as well as for joining oversized parts of a large thickness in site is noted. The range of products, restored using electroslag surfacing (ESS) has changed [28]. Known are examples of revival of ESW sections in mechanical engineering plants. For instance, in 2016, the market demand for drums for modular power boilers and pressure vessels (cylinders) increased. In 2017, an installation based on A-535 machine for ESW of circular welds of drums was restored at LLC «Sibenergomash-BKZ» [29].

Figure 5. Welded billet of the hydraulic press beam. Billet weight is 150 t, cross-section of a weld (shown by an arrow) made by ESW with consumable nozzle, is 2490×3860 mm

It allows making welds of up to 2000 mm diameter with up to 150 mm wall thickness. ESW of the drum of BKZ-160-100 GM boiler of the capacity of 160 t of steam per hour was performed, and work on manufacture of the drum for E-550-13.8-560 KT boiler and pressure vessels (cylinders of hydraulic type BG-10000/32) is conducted. Technology of ESW of vessels is successfully applied instead of multilayer automatic submerged-arc welding.

In 2016 ESW was applied to manufacture an oxygen converter of the capacity of 320 t of liquid metal for JSC «EVRAZ-ZSMK» for the first time in Russia and in the South-Ural Machine Building Plant [30]. Advanced technology of ESW of thick metal was mastered. A-535 machines are used to make rectilinear butt joints of 40–160 mm thickness, and curvilinear position welds of 40–160 mm thickness are made using ASh-115M2 machines, developed at PWI [8].

JSC «Atommash» uses the technology of electroslag surfacing by strip electrode, allowing a significant reduction of the time for surfacing operations. Welds of up to 10000 mm length and up to 300 mm thickness are made in ESW installation, including those for manufacturing thick-walled spherical bottoms. Investigations are performed in order to improve the quality of NPP products from pure 10GN2MFA and 15Kh2NMFA steels with application of ESW [31].

JSC «Tyazhmash», OJSC «Uralmash» and OJSC «Penzkhimmash» operate installations, using A-535 machines for ESW of circular and rectilinear butt joints of up to 350 mm thickness. At OJSC «Tyazhmekhpress» the bed tables of hot stamping presses with nominal force of 153 MN of 240 t weight are made from cast parts using ESW CN of up to 400 mm thicknesses [32]. At OJSC «Uralkhimmash» ESW with strip electrode of 60 mm width was mastered and applied for the first time in manufacture of the bottom and casing shells of the equipment. Application of this method allowed significantly reducing the labour intensity due to the fact that surfacing was performed without the transition zone in one layer. Application of this process allowed reducing welding material consumption and improving the processed surface quality. OJSC «Baltiysky Zavod», as a result of joint work with PWI, mastered ESW of panels of 4000×9000 mm up to 7000×9000 mm size from 08Kh18N10T steel of 40–50 mm thickness, using AD-381Sh machine in construction of tanks for metal-water protection. At OJSC «Volgotsemmash» three ESW shop sections, based on A-645, A-535 and A-433R machines are in operation, where welding of jaw crusher frames, cement kiln bands, band shells, mill covers, etc. of 45 to 1200 mm thickness is performed [33]. LLC «Pneumatic conveying equipment Plant», together with LLC «Remax» use precision ESW of bands of rotary cement kilns and metallurgical furnaces directly at customer enterprise. Longitudinal butt joints of met-

al shells of 60 to 120 mm thickness are made, as well as repair of service cracks by multipass ESW in cement kiln bands without their dismantling [34].

The mechanical-repair plants of Bratsk TIC, OJSC «Severvostokzoloto» and OJSC «Yakutskugol», together with PWI, set up reconditioning sections with application of ESS of worn helical gears of Swedish debarking drums, combs of lugs of Komatsu caterpillar tractors and platform swing drive gear of Japanese excavators Marion-204. Setting up the repair sections allowed reducing import purchases of wearing parts.

Portal «naplavit.rf» demonstrates electroslag surfacing (ESS) in the current-conducting sectioned mold of stamps, punches, working ends of mandrels of a piercing mill and other products of up to 100 mm diameter. The installation for ESS of flat surfaces of products in the horizontal position allows forming a thin (from 3 mm) and wide (up to 55 mm) layer of deposited metal at minimum (from 1 mm) and uniform penetration depth [35].

A stable growth of the scope of ESW and ESS investigations and application in different industries is observed in Western countries.

In the USA the method of narrow-gap consumable nozzle ESW was used to make twenty welds in the support tower of San-Francisco-Oakland bridge under construction [36]. The length of each single-pass weld was 10 m, butt thickness was 100 and 60 mm. Five types of edge preparation were used. ESW technology (equipment and training) was provided by Electroslag Systems (EST & D), Portland, Oregon within the framework of cooperation with the University of Portland and American Bridge Company. Welding was followed by ultrasonic and X-ray inspection of welded joints. The total time of welding all the butt joints was two months. ESW application allowed a significant reduction of the time and labour intensity of welding operations, as proceeding from preliminary calculations, the total time of welding the butt joints with the arc method was six months. Ultrasonic testing of quality of 200 m of welds was repeated in 2013.

According to the materials of a review paper [37], the latest modification of narrow-gap ESW (ESW-NG) has currently being recognized by AASHTO in the USA to be suitable for welding regular types of bridge steels and was included into the bridge welding code (AWS D1.5: 2010 c). Work is in progress on inclusion of ESW-NG welding into AWS D1.8 Structural Welding Code — Seismic Supplement. It is shown that the process of narrow-gap ESW is stable both at direct and at square sine wave alternating current. Linde Union Carbide Division and Hobart Brothers Company patented two designs of the consumable nozzles and method of ESW with oscillating consumable nozzle. Flat plates of the consumable nozzles, having a channel for welding wire passage,

which replaced the round cross-section nozzles, allowed reducing the gap from 32 to 19 mm. ESW-NG method is designed for application during mounting at the site of construction of the steel structure. It is particularly acceptable for welding W-shaped extended heavy flanges, with 45 to 50 deg. deviation from the vertical. Welding a heavy column with application of submerged-arc welding takes 30 h or more. For comparison, it takes about 30 min. to weld both the flanges of any thickness, using ESW-NG. Thus, the authors of review [37] summarize the following. ESW is no longer considered as the only variant for joining thick plates in the shop. It can be used and be cost-effective in site, in welding stiffeners and support plates to steel section flanges, as well as in joining the diaphragms to inner walls of box-type columns. Modern achievements in ESW field, implemented in ESW-NG, are used in the construction sites of large high-rise buildings and in bridge construction. ESW-NG has established itself as the most cost-effective method for many joints, including large thickness welds in steel bridges and buildings.

Arcmatic Welding Systems Company (USA) specializes in modular systems with computer program control of the welding process, specially developed for ESW of thick plates [38]. Portable systems are proposed for consumable nozzle ESW with manual control of the console, which carries the ducts for electrode wire feeding, power cables and hoses for cooling water supply. Installations based on a two-position manipulator are also used, providing its fast (5 min) readjustment from the arc welding method to ESW of metal of up to 300 mm thickness. The above equipment is proposed for fabrication of wind towers, off-shore platforms, heavy pressure vessels, beams and columns from structural steel, bridge beams and other structures. These installations are becoming the most widely accepted in ESW CN of construction column diaphragms.

Transportation Research Board (TRB) of the National Academy of Sciences of the USA conducted studies on welding the railway rails using ESW. Comparison and analysis with ESW showed that thermit welding of rails is a less capital intensive, less expensive, more portable process, but the weld quality is poor. Average cost of making thermit welds is 350 USD for each butt joint. Joints produced by other welding processes are more costly, of the order of 500 USD each. Flash-butt welding is highly capital intensive and, therefore, costly, requires application of trains for transportation of rail-welding machines. It is anticipated that ESW will take a position between the two above-mentioned processes, and will be comparable with them as to quality and cost (about 250 USD).

Typical areas of application of electroslag welding in Japan in the XX century, included the following objects: joining large castings, stiffeners of the upper deck

of ships, longitudinal welds in cylindrical pressure vessels, housings of blast and oxygen furnaces. However, the low impact toughness of metal of the weld HAZ was the greatest obstacle to wider introduction of ESW in Japan. Studies were performed to increase the impact toughness of HAZ metal [39, 40] due to application of steel, insensitive to grain growth in the HAZ, with the purpose of expanding the range of products manufactured using ESW, [15, 16]. In order to increase the scope of application of ESW of steels with ultimate tensile strength of 490–590 MPa, Nippon Steel Corporation developed a new technology of improving the impact toughness of HAZ metal, which is called Super High HAZ Toughness Technology with fine microstructure (HTUFF®). With this technology, thermally stable oxides and sulphides, containing Mg and Ca, are dispersed in the steel in the form of fine particles, and growth of γ-grains in the HAZ metal near the welded joint line is significantly delayed by the fine particles, which results in manifestation of the effect of grain refinement and in achieving ≥ 70 J Charpy impact toughness in the HAZ metal at 0 °C. In keeping with the developed technology, metal of 60 and 80 mm thickness, is widely used in fabrication of shelf structures, pipes, buildings and in civil engineering, with ESW application. Total mass of steel used for ESW was about 280 000 t [16]. From the beginning of the XXI century, production of large sea container ships, in which the loading hatches had to be made from steel sheets of 70 to 100 mm thickness, has markedly increased in Japanese shipbuilding [41]. TMCP technology of steel production was developed, which includes controlled rolling and heat treatment in A_{c1}–A_{c3} temperature range, in order to perform single-pass welding of steel of such thickness using welding processes with a high heat input (arc welding with forced formation and ESW). This technology allows markedly increasing the strength and impact toughness by grain refining with formation of bainite or martensite with addition of microalloying elements, such as titanium and niobium. High-strength steels with the yield point of 390 and 460 N/mm^2 have been developed, in ESW of which formation of a coarse structure in the HAZ metal is excluded. Steels developed with application of TMCP and HTUFF technologies are applied in production of tankers, cargo ships, ships for liquefied petroleum and natural gas transportation that allowed lowering the ship weight and increasing the transportation effectiveness.

Over the recent years the process of ESW of aluminium busbars was developed [42] in Canada. CANMEC Company (Quebec Province) purchased Linde Company developments on application of ESW technology for welding 50 mm aluminium. For welding busbars of 275 mm thickness, CANMEC Company together with CQRDA (Quebec Center for Research and Development of Aluminium) and National Research Council of Canada (NRC) developed new machines, capable of feeding three- … five-electrode wires and ESW technology. New technology was applied in construction of an aluminium plant (346 000 t/y) in Iceland. Aluminium busbars were welded by ESW 4 times faster, compared to the traditional welding method (arc method of «chequered plate»). The welds ensured the high quality of the welded joints, electric conductivity of busbars in the weld zone was increased at least by 20 %. Electric losses were lowered due to complete penetration of the edges.

Chinese companies offer machines and units of console and gantry types for ESW with wire electrodes and consumable nozzle, as well as HJ431 flux [43]. The above equipment is designed for ESW of housing covers of construction beams and transverse partitions of columns. Thickness of welded butts is mainly equal to 16–65 mm. Research group of the Academy of Construction of the Hunan Province performed extensive analysis of weldability of high-strength R-bars HRB400, both theoretically and experimentally. ESW of R-bars from strengthened steel of 20MnSiV grade is applied [44]. Kingarc Autopweld Company, Taiwan demonstrates a simplified machine for consumable tubular nozzle ESW of construction column diaphragms.

In Turkey the paper on «Electroslag Welding Process and Its Application» was published, where the history of ESW creation and development in industrialized countries was described [45]. Turkish experience of ESW application and prospects for its application in the future are also described there. ESW is currently used for welding of circular butt joints of presses, furnaces, engine housings, wheels for asphalt machines. Butt joints of ship plates and castings of parts of 13 – 400 mm thickness are welded in chemical, petroleum, marine and power plants. Examples of application of ESW of low-alloyed carbon steels are given, namely, pressure vessels, tank cars, boilers, compressors, bridges, tankers with double-hull. In Turkey ESW is used as the welding process, providing more effective results, compared to the traditional methods. The most often used electrode wire diameters are 2.4 and 3.2 mm. In addition, wires of 1.6 up to 4.0 mm diameter are also successfully applied. Electrode wire reels of two types are used: small ones for winding 27 kg and large ones for 270 kg of wire. It is planned to apply ESW for manufacturing nuclear reactors, construction of industrial buildings, double-wall fuel tanks and other structures.

In Italy ESW by three wire electrodes is used for joining low-carbon steel plates of 25 to 300 mm thickness in the vertical or close to vertical position [46].

Voestalpine Boehler Welding Company, Austria, proposes equipment, technology and welding consumables for electroslag cladding (ESSC) with strip electrode 15–120 mm wide [47]. Advantages of this process are shown, compared with submerged-arc cladding with strip electrode for instance, ESS depo-

sition rate is up to 23 kg/h, and that of electric arc cladding is not more than 14 kg/h. Deposited metal dilution by base metal does not exceed 7 %. In electric arc cladding it reaches 18 %. It is noted that an ideally smooth outer surface of the deposited metal and sound overlapping of the layers are ensured owing to electromagnetic control of the process of deposited metal formation, in ESS with strip. Examples of ESS with strip electrode of unalloyed, low-alloyed, martensitic, and stainless steels, nickel alloys, as well as cobalt and copper alloys, are given. In the oil and gas industry ESS with strip electrode is applied for deposition of anticorrosion coatings of a large area in such equipment as pressure vessels, separator vessels and high pressure separators. Electroslag facing is also widely used for cladding the inner surface of pipes, and valves for oil and gas transportation. In chemical and pulp and paper industry this process has found application in equipment, exposed to corrosive media, high pressures and temperatures. This process is the most efficiently applied for anticorrosion cladding of vessels, tanks, valves, pumps, compressors, drums for production of paper, mixers, etc. In power industry, ESS with strip electrode is applied for facing the internal surfaces of reactor vessels, steam generators, etc. In Belgium, Germany [48], India [49] and Poland [50] the process of ESS with strip electrode became accepted in similar industries instead of flame surfacing and submerged-arc strip cladding. ESAB (Sweden) applies ESS with strip electrode (60–90 mm width, 0.5 mm thickness) for anticorrosion cladding of carbon steel with 316L or 347 steels [51]. ESS of stainless and nickel layers is applied for repair of corroded equipment and improvement of corrosion properties of the new structures. In Norway ESS with strip electrode is applied for facing the inner surfaces of CLAD metallurgical pipes of up to 254 mm diameter and up to 12.5 m length. Typical dimensions of strip electrodes from Inconel 625, 825, 316 alloys, are 15/20/30×0.5 mm. Surfacing deposition rate is 12 to 24 kg/h, depending on the strip size.

In Estonia, a section for reconditioning worn teeth of large-modular gear shafts of the drive of rotation of the platform of stepping excavators ESh 15/90 and ESh 10/70, using ESS, was set up on the base of «Estonslanets» Concern, as a result of joint work with PWI. Gear shafts reconditioned without subsequent machining of involute profile, are successfully operating in Narvsky and Aidu open-pit mines.

Conclusions

1. Over the past period from the beginning of XXI century, the scope of ESW application in manufacture and repair of products of greater than 100 mm thickness has markedly decreased both in Ukraine and abroad. Nonetheless, a stable growth of the scope of its application for joining 30 to 100 mm thick metal is noted over the recent years.

2. A range of new welding equipment was designed, featuring a high reliability of ESW performance, and ensuring continuous monitoring and certification of the main mode parameters. New technologies have been developed, which allowed widening the range of products, manufactured with ESW and ESS application. Recently, the methods of ESW with tubular consumable nozzle (diaphragms, stiffeners, reinforcement and other elements of construction columns, bridges) became the most widely accepted, as well as methods of ESS with electrode strip and consumable nozzle (deposition of protective coatings, reconditioning worn parts of machines, etc.).

3. The following is expected in the next 5 to 10 years: widening of the scopes of ESW with wire electrode, as well as with tubular consumable nozzle in a narrow gap in fabrication of large-sized structures (primarily, construction) from metal with lower sensitivity to HAZ overheating in the shop and site conditions; producing large cast-welded, rolled-welded and forge-welded billets for heavy engineering with up to 4000×6000 mm cross-sectional dimensions, which can be realized by the technology of consumable nozzle ESW, applied with success at PJSC «NKMZ»; expansion of the fields of application of the process of ESS with strip electrode for deposition of anticorrosion coatings of a large area for pressure vessels and separators, tanks, valves, pumps, compressors, steam generators, pipes, operated in oil, gas, power, chemical and other industries; increase of the scope of application of the technologies of reconditioning repair of metal structures and rapidly wearing parts of machines, based on application of ESW with wire electrodes, multipass ESW and new methods of ESS.

1. Voloshkevich, G.Z. (1956) *Method of electric fusion welding*. USSR author's cert. 104248, Int. Cl. 21 B 29/13 [in Russian].
2. (1980) *Electroslag welding and surfacing*. Ed. by B.E. Paton. Moscow, Mashinostroenie [in Russian].
3. Sushchuk-Slyusarenko, I.I., Lychko, I.I. (1990) *Technology and equipment for electroslag welding*. Kiev, PWI [in Russian].
4. Paton, B.E., Dudko, D.A., Yushchenko, K.A. et al. (1997) Electroslag welding: Main results and prospects of development. *Automatich. Svarka*, **5**, 32–42 [in Russian].
5. Medovar, B.I., Tsykulenko, A.K., Bogachenko, A.G., Litvinchuk, V.M. (1982) *Electroslag technology abroad*. Kiev, Naukova Dumka [in Russian].
6. Lychko, I.I., Sushchuk-Slyusarenko, I.I., Yushchenko, K.A., Blinov, V.A. (1999) Peculiarities of ESW of thick-wall extended butt joints from steel of 18-8 type. *Automatich. Svarka*, **9**, 61–65 [in Russian].
7. Lankin, Yu.N., Moskalenko, A.A., Tyukalov, V.G. et al. (2008) Experience of application of electroslag welding in mounting of metallurgical equipment. *Svarochn. Proizvodstvo*, **6**, 32–36 [in Russian].
8. Zhuk, G.V., Semenenko, A.V., Lychko, I.I. et al. (2016) Ash115M2 machine for electroslag welding of vertical, in-

clined and curvilinear butt joints. *The Paton Welding J.*, **10**, 44–45.

9. Nevidomsky, V.A., Krasilnikov, S.G., Panin, A.D. et al. (2002) New machine for electroslag welding of large parts at JSC «NKMBF». *Ibid.*, **2**, 49–51.

10. Yushchenko, K.A., Lychko, I.I., Kozulin, S.M. et al. (2012) Portable apparatus for consumable-nozzle electroslag welding. *Ibid.*, **8**, 45–46.

11. Lankin, Yu.N. (2007) Computer system of monitoring the technological parameters of ESW. *Ibid.*, **5**, 48–50.

12. Paton, B.E., Dudko, D.A., Palti, A.M. et al. (1999) Electroslag welding (Prospects of development). *Avtomatich. Svarka*, **9**, 4–6 [in Russian].

13. Egorova, S.V., Sterenbogen, Yu.A., Yurchishin, A.V. et al. (1980) New structural steels not requiring normalizing after electroslag welding. *Ibid.*, **6**, 44–47 [in Russian].

14. Sineok, A.G., Demchenko, Yu.V., Proskudin, V.N. et al. (2015) Substantiation of economic efficiency for application of different methods of welding and steels for repair of blast-furnace jacket No. 4 of PJSC «Azovstal Iron and Steel Works». *Svarshchik*, **4**, 18, 21 [in Russian].

15. *Akihiko* Kojima, Akihito Kiyose, Ryuji Uemori et al. (2004) Super high HAZ toughness technology with fine microstructure imparted by fine particles. *Nippon Steel Technical Report,* No. 90, July 1–6.

16. Kojima, Ken-Ichi Yoshii, Tomohiko Hada (2014) Development of high HAZ toughness steel plates for box columns with high heat input welding. *Nippon Steel Technical Report*, No. 90, July 39–49.

17. Paton, B.E., Lychko, I.I., Yushchenko, K.A. et al. (2013) Melting of electrode and base metal in electroslag welding. *The Paton Welding J.*, **7**, 31–38.

18. Lychko, I.I., Yushchenko, K.A., Suprun, S.A., Kozulin, S.M. (2019) Peculiarities of electrode and base metal melting in electroslag welding. *Ibid.*, **3**, 6–10.

19. Lankin, Yu.N., Sushy, L.F. (2009) Electrical conductivity of slag pool in electroslag welding with wire electrode. *Ibid.*, **12**, 37–38.

20. Lankin, Yu.N., Tyukalov, V.G., Moskalenko, A.A. et al. (2004) Application of electroslag welding in repair of blast furnace body at OJSC «KGMK Krivorozhstal». *Ibid.*, **5**, 26–28.

21. Yushchenko, K.A., Kozulin, S.M., Lychko, I.I., Kozulin, M.G. (2014) Joining of thick metal by multipass electroslag welding. *Ibid.*, **9**, 30–33.

22. Kozulin, S.M., Lychko, I.I., Podyma, G.S. (2008) Electroslag surfacing of rotating kiln gear shaft teeth. *Ibid.*, **5**, 31–34.

23. Kuskov, Yu.M. (1999) Surfacing in current-conducting mould — perspective direction for development of electroslag technology. *Avtomatich. Svarka*, **9**, 76–80 [in Russian].

24. Paton, B.E., Yushchenko, K.A., Lychko, I.I. (2003) *Method of electroslag welding or surfacing*. Ukraine Pat. 68576A [in Ukrainian].

25. Lankin, Yu.N., Demchenko, Yu.V., Moskalenko, A.A. et al. (2019) Electroslag welding of billet of body of traction electric motor at PJSC NPO «Dnepropress». *Svarshchik*, **3**, 28–29 [in Russian].

26. Yushchenko, K.A., Lychko, I.I., Kozulin, S.M. et al. (2018) Application of welding in construction. *The Paton Welding J.*, **9**, 23–27.

27. Shapovalov, K.P., Belinsky, V.A., Merzlyakov, A.E. et al. (2016) Electroslag welding of large-sized press frame. *Ibid.*, **8**, 36–39.

28. Zorin, I.V., Sokolov, G.N., Tsurikhin, S.N. et al. (2005) Restoration of working surfaces of parts and assembly-welding tooling by electroslag method using composite heat-resistant materials. *Sborka v Mashinostroenii, Priborostroenii*, **5**, 17–20 [in Russian].

29. (2017) *Made in USSR: Electroslag welding of thick-wall vessels is renewed at Sibenergomash-BKZ. TEK Community*. http://www.energyland.info/analitic-show-165713

30. (2016) 24ri.ru/down/open/tehnologicheskij-proryv-v-proizvodstve-konverterov-na-juzhuralmashe.html

31. Podrezov, N.N. *Development of technological bases of electroslag welding of pure vessel steels for NPP*: Syn. of Thesis for Cand. of Techn. Sci. Degree [in Russian].

32. Merabishvili, M.O. (2013) LLC «Tyazhmekhpress» is a leader in manufacturing of press-forging equipment. *Zagotovitelnye Proizvodstva v Mashinostroenii*, **10**, 15–18 [in Russian].

33. Kozulin, M.G. (1999) ESW in cement engineering. *Avtomatich. Svarka*, **9**, 55–60 [in Russian].

34. http://www.zpto-tlt.ru/service

35. http://naplavka34.ru

36. Turpin, B. et al. (2012) Narrow gap electroslag is process of choice for welding San-Francisco-Oakland Bay Bridge. *Welding J.*, 91(**5**), 24–31.

37. Janice, J., Chambers, Brett R. Manning (2016) Electroslag welding: From shop to field. *Structure Magazine*, February, 20–23.

38. https://www.arcmatic.com/index.php?option=com_content&view=featured&Itemid=124

39. Kitani, Y., Ikeda, R., Ono, M. et al. (2013) Improvement of weld metal toughness in high heat input electro-slag welding of low carbon steel. *Welding in the World*, February.

40. *Takahiko* Suzuki, Takumi Ishii (2017) Guidebook for preventing brittle fractures of inner diaphragm electroslag welds. *Steel Construction Today and Tomorrow*, **52**, 9–12.

41. *Ryuji* Uemori, Nasaaki Fujioka, Takehiro Inoue, Masanori Minagawa et al. (2012) Steels for marine transportation and construction. *Nippon Steel Technical Report*, No. 101, November, 37–46.

42. Leroux, B. (2015*) Electroslag welding (ESW): A new option for smelters to weld aluminum bus bars*. Ed. by M. Hyland. The Minerals, Metals & Materials Society, Canada. bleroux@canmec.com

43. www.hwayuan.com

44. Xu, C., Chen, Y., Liu, Y. (2003) Study and application of high-strength reinforcing bar. In: *Proc. of Vanitec Symp. (China, Hangzhou, October 2003)*, 106–109.

45. Kaluc, E., Taban, E., Dhooge, A. (2006) Electroslag welding process and industrial applications. *Metal Dunyasi*, 152(**13**), 100–104.

46. www.steelmecsald.it>eng>products

47. www.voestalpine.com/welding

48. https://www.haane.de/

49. *Takare Niraj S.*, Ram Yadav (2014) Electroslag strip cladding process. Mechanical Engineering/SSJCET College, India. *International OPEN ACCESS Journal of Modern Engineering Research (IJMER)*.

50. www.oerlikon-welding.com

51. https://www.offshore-mag.com

PECULIARITIES OF HYBRID LASER-ARC WELDING OF STAINLESS STEEL*

E. TURYK, M. BANASIK, S. STANO and **M. URBANCHYK**

Lukasevich Research Network — Institute of Welding

16–18 Bl. Czeslava Blvd., Gliwice, 44-100, Poland

The use of hybrid laser-arc welding laser + MAG for joining elements of large structures of stainless steel is a relatively new problem. The paper discusses the issues of technology of hybrid welding of austenitic steel X2CrNi18-9 and austenitic-ferritic steel X2CrNiMoN21-5-1 using a disc laser of 12 kW capacity. The technological conditions of hybrid welding with a full penetration of butt joints of steel with a thickness of 8, 12 and 20 mm, as well as T-joints with a butt weld with a partial penetration were determined. The typical defects in welds of high-alloy stainless steels, produced by hybrid welding, were indicated. 5 Ref., 20 Figures.

Keywords: hybrid welding, laser+arc, active gas, stainless steels, arc and beam parameters, location of sources, typical welding defects

Hybrid laser-arc welding is a process which has been intensively studied, developed and implemented during recent years [1–5]. The application of hybrid laser-arc welding using consumable electrode (HLAWCE) laser + welding with solid wire in inert and active gases (ISO 4063: 521 + 135 process) for joining parts of large structures of stainless steel is a relatively new problem. The method of hybrid welding is technologically complex – it is necessary to select the parameters of welding arc and laser beam, a suitable mixture of shielding gas and a spatial arrangement of both used energy sources (end of electrode wire and spot of beam focusing) with respect to each other and to the line of edge butt for each type of joint.

This paper discusses the technology of hybrid laser + MAG welding of austenitic steel X2CrNi18-9 and ferritic-austenitic steel X2CrNiMoN21-5-1 with the use of a disc laser of 12 kW power and a special hybrid head.

Results of experiments. Technological tests for selection of shielding gas for hybrid welding of steel X2CrNi18-9 with electrode wire G 19 9 L Si and welding of steel X2CrNiMoN21-5-1 with electrode wire G 22 9 3 N L showed that the stability of hybrid process, the required shape of welds and minimal spattering are provided by a gas mixture of 97.5 % Ar + 2.5 % CO_2.

The penetration depth and width of the butt joint were measured for the four values of diameter of the used light guide (200, 300, 400 and 600 μm) and two directions of moving the hybrid head: with a laser as the leading heating source (designation $L — A$) and an electric arc as a leading heating source (designation $A — L$). The measurements confirmed that regardless

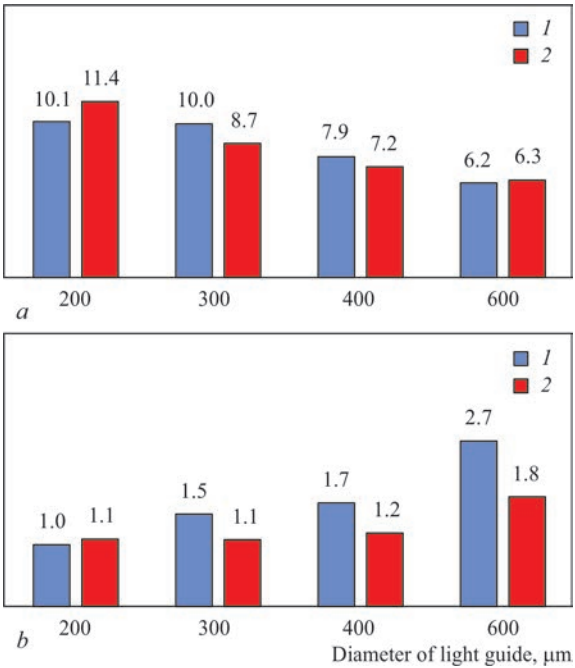**Figure 1.** Change in penetration depth (*a*) and width of the lower part (*b*) of the weld for different values of diameter of the used light guide and the direction of moving the hybrid head. For *a*: *1* — penetration depth $L — A$, mm; *2* — penetration depth $A — L$, mm; for *b*: *1* — width of the lower part of the weld $L — A$, mm; *2* — width of the lower part of the weld $A — L$, mm
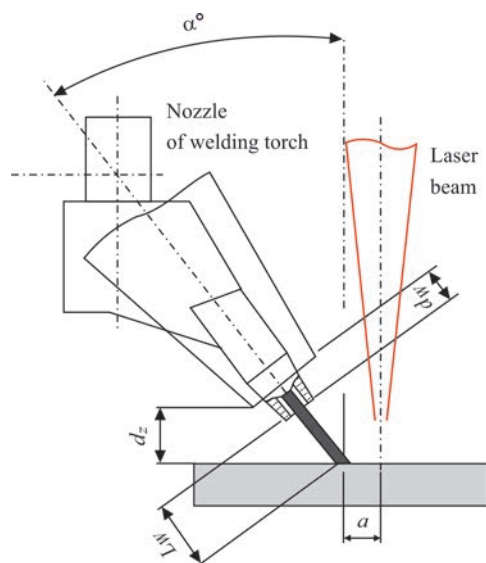

Figure 2. Spatial position of the system «laser beam – welding head MAG – element to be welded», laser beam perpendicular to the material: *a* is the distance from the end of the wire to the zone of laser beam focusing, α is the inclination angle of welding torch MAG relative to the laser beam axis; L_w is the electrode stickout; d_z is the distance from gas nozzle to element, d_w is moving forward of contact end from gas nozzle

Figure 4. Location of laser beam focus relative to the surface of the specimen ($f = 0$ — position of the focus on the sheet surface)

diameter of 400 μm and with the direction of welding *A — L* was used.

An important group of parameters is a mutual spatial position of the system «laser beam – MAG welding torch – element to be welded» (Figure 2).

The most advantageous for automatic MIG/MAG welding is setting of a holder perpendicular to the material being welded (angle α = 0°). In the process of hybrid welding, laser beam is responsible for the obtained penetration depth to a much greater extent than welding arc and therefore it is set perpendicular to the material being welded.

For the technological head used in the study, the inclination angle of the torch holder MAG was selected as α = 25° and the distance from the end of the wire to the focusing zone of laser beam was selected as $a \leq 2$ mm, providing a safe (without collisions with laser beam) welding process. Increasing the distance α to about 4 mm does not have a significant effect on the process. The produced weld shape is comparable (Figure 3, *a*, *b*). A further increase in the distance causes a decrease in the volume of the weld (Figure 3, *c*) and, in extreme case, a noticeable decrease in the penetration depth (Figure 3, *d*).

of direction of welding, penetration depth is comparable for individual diameters of applied light guides, and with an increase in diameter of the light guide, penetration depth decreases and the width in the lower part of the weld increases (Figure 1).

From the point of view of maximizing penetration depth, the most suitable solution seems to be the use of a light guide with the smallest diameter. However, due to the stability of HLAWCE welding process (stability of the gas-dynamic channel formed as a result of a laser beam effect) and to provide the width of the weld in the region of its lower part at a level of more than 1 mm, it is recommended to choose a light guide with a larger diameter. Further, a light guide with a
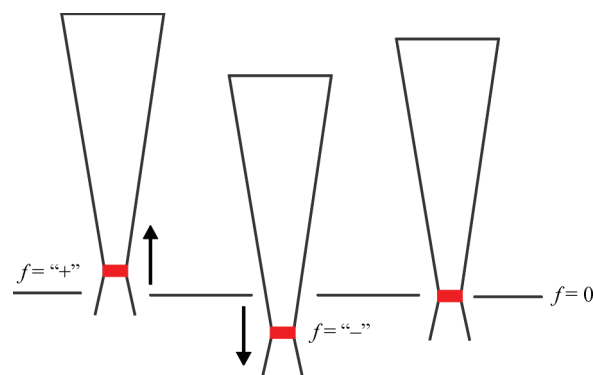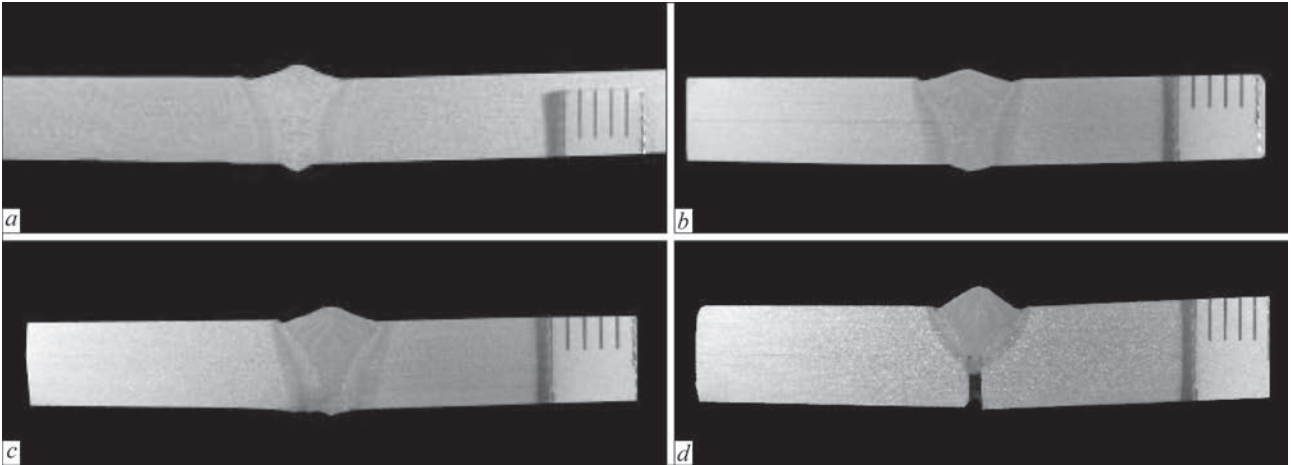

Figure 3. Patterns of macrostructure of the weld produced at different distance of wire end from the zone of laser beam effect: *a — a =* = 2; *b* — 4; *c* — 6; *d* — 8 mm
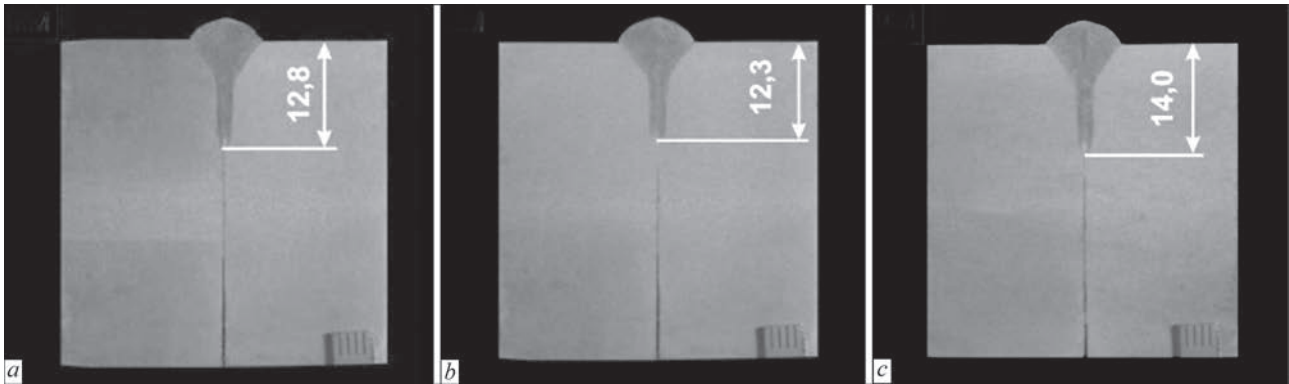
Figure 5. Macrostructure of butt joints of specimens of 40 mm thickness produced at different arrangement of laser beam focus relative to the surface of material to be welded (power of laser radiation P_l = 11 kW, welding speed v_w = 0.7 m/min, wire feed rate v_{wf} = = 11 m/min): a — f = 0; b — –5; c — –10 mm

A separate issue is arrangement of the laser beam focus relative to the material being welded (Figure 4). Technological tests of HLAWCE were carried out on specimens of 40 mm thickness with different setting of the position of the laser beam focal point: f = 0; –5 and –10 mm (Figure 4).

The penetration depth did not change significantly, it ranged from 12.3 to 14 mm (Figure 5). Based on the latter, in future it is recommended to set the position of focusing laser beam on the surface of the material being welded.

Then, the dependence of the penetration depth and geometric dimensions of welds on the power of laser beam in the HLAWCE process was studied. Depending on the power of laser beam in the range of 6–12 kW, the penetration depth was 12.5–18.5 mm. A significant effect on the penetration depth is also exerted by the gap of elements being joined, which was confirmed by tests at a gap of 0 and 0.8 mm (Figure 6).

Technological tests of welding butt joints with a thickness of 8, 12 and 20 mm after laser cutting (roughness of surface was respectively ≤ 11.3; ≤ 14.2 and ≤ 70.0 µm) showed that the roughness of surface of welded edges up to R_z = 70.0 µm does not cause violation of stability of the HLAWCE process. In the case of plasma-arc cutting in the installation
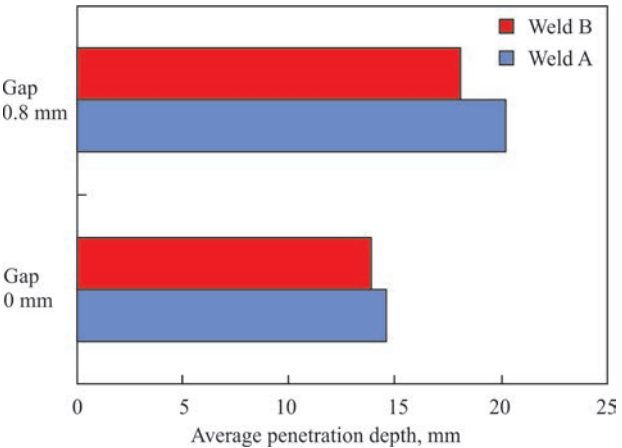
Figure 6. Average values of penetration depth of butt joints of specimens of 40 mm thickness, produced at different gap value g (double-sided welding, first weld — A, second — B)

YUN-3000M, applying the mixture Ar–H$_2$ as a plasma-forming gas, the roughness is lower than 70.0 µm and the surface is also suitable for HLAWCE welding.

The bevel of edges, characteristic for plasma cutting can cause axial displacement of individual welds in a double joint. The bevel of edges in the specimens with a thickness of 25 mm and a length of 600 mm was measured after industrial plasma cutting at an industrial partner. The measurement results showed that the bevel of edges is relatively large and at an unfavourable combination of sheets for welding, when the
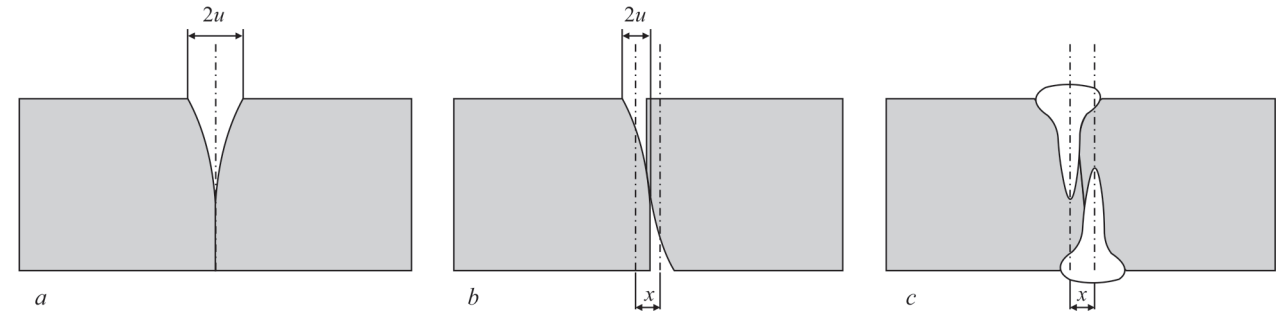
Figure 7. Different methods of combining parts, prepared for welding, after plasma cutting: a — summing of bevel at one side of a butt; b — displacement of x axis of separate welds in a double joint; c — visualization of absence of penetration, arising as a result of combination of parts with the bevel
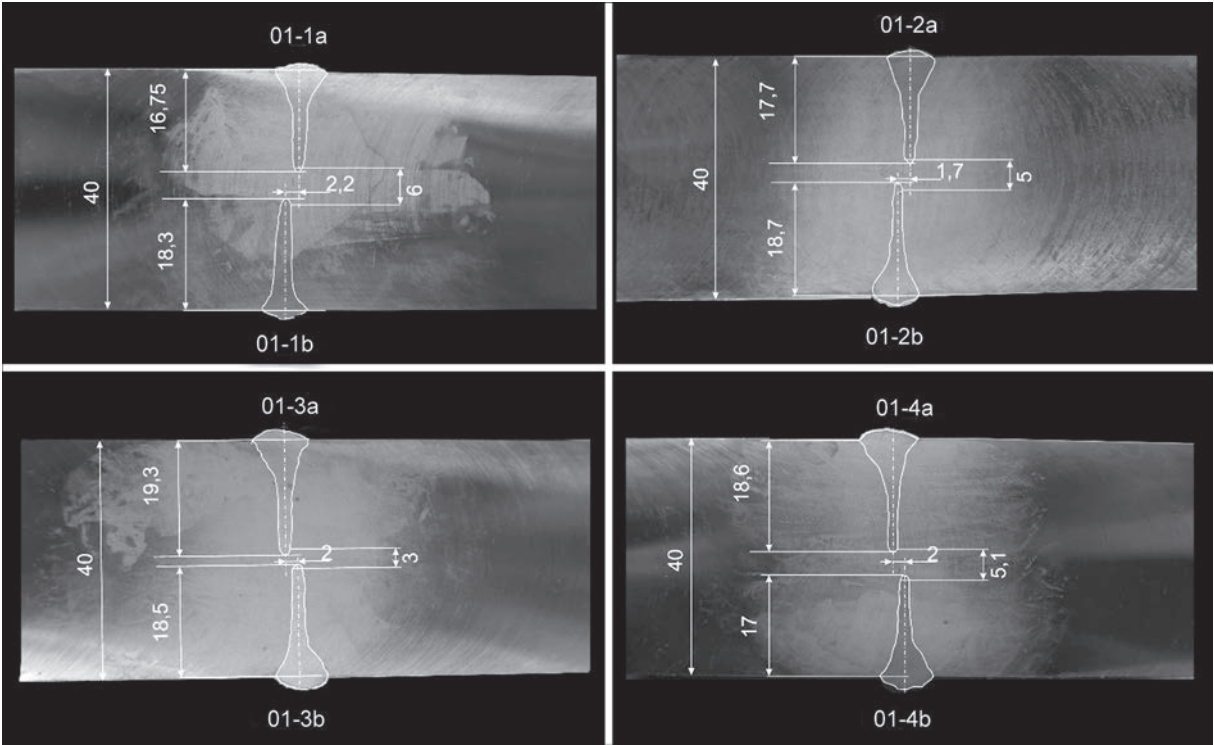
Figure 8. Arrangement and dimensions of welds of double-sided hybrid joint of sheets of 40 mm thickness with edge preparation after industrial plasma cutting and grinding

bevel is folded, on the surface of the sheets a gap of more than 2 mm width is formed. As the thickness of a sheet increases, the bevel becomes larger.

The appeared bevel leads to the fact that combination of parts in the butt joint can be obtained in two ways (Figure 7). In the first case, the bevel is summed on a one side of a butt of the parts, causing an increase in the gap. In the second case, the bevels are located on the opposite sides, and that allows mating parts at a smaller gap. However, a risk of axial displacement of individual welds in a double-sided weld exists. In this case, insufficient penetration in the central part of the joint is probable, despite providing the appropriate penetration depth of individual welds (Figure 7, c).
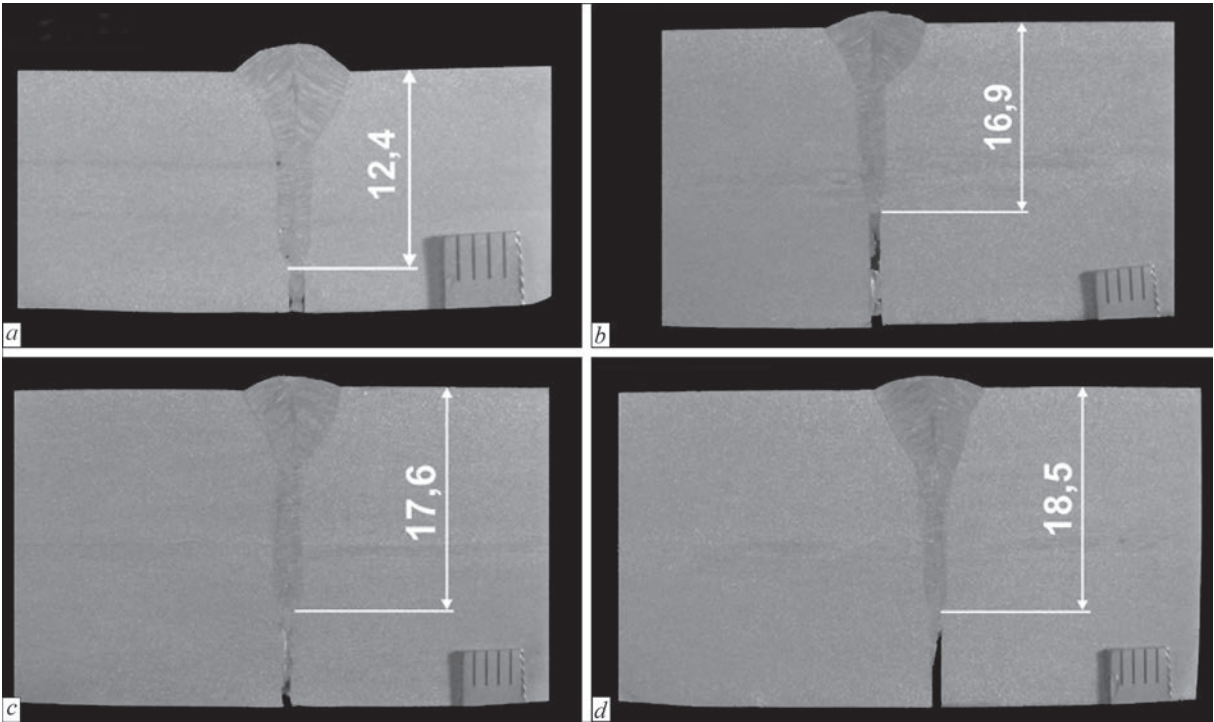
Figure 9. Macrostructure of welds produced by laser beam hybrid welding with a power of 6–12 kW: a — P = 6; b — 8; c — 10; d — 12 kW

Figure 10. Dependence of penetration depth *t* on the power of laser beam P_l in HLAWCE

Figure 12. Macrostructure of double-sided welded joint of 8 mm thickness (P_l = 5.0 kW, v_w = 1.2 m/min, v_{wf} = 8.4 m/min, arc current I_a = 225 A, arc voltage U_a = 21 V, welding input energy Q = 3.9 kJ/cm)

The considerations mentioned above confirm the results of HLAWCE of sheets of 40 mm thickness after industrial plasma cutting on the specimens provided by an industrial partner. Due to the fact that during mating of sheets in accordance with Figure 7, *a*, the gap 2*u* was more than 3 mm, an attempt was made to mate sheets for welding in accordance with the second m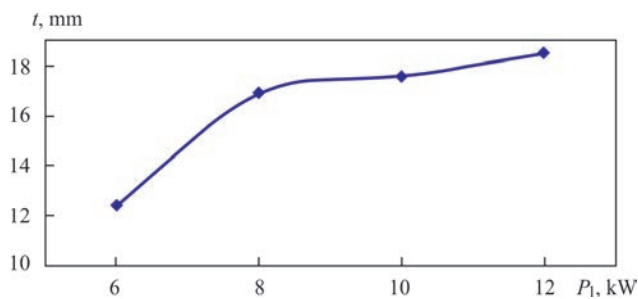ethod (Figure 7, *b*) in order to obtain the smallest possible gap. After welding, metallographic specimens in four selected locations along the length of the welded joint were manufactured. Macrosections of the produced joints are shown in Figure 8.

The average penetration depth was about 18 mm, which did not allow producing a double-sided welded joint of 40 mm thickness with a full penetration. On metallographic sections, displacement of axes of individual beads was observed as a result of using plasma cutting as a method of butt joint preparation. Due to

the need in maintaining coaxial alignment of individual weld beads in a double-sided weld, it is necessary to provide a method of edge preparation which will guarantee a side edge, perpendicular to the sheet surface. For materials of up to 15 mm thick, laser cutting is sufficient. For thicker materials edge machining may be required.

To determine the effect of laser beam power in the HLAWCE process on the penetration depth and the shape of welds, welding of sheets of 40 mm thick was carried out with the edge surface after milling, with a gap of 0.8–1.0 mm, varying the power of laser radiation from 6 to 12 kW (Figures 9–11).
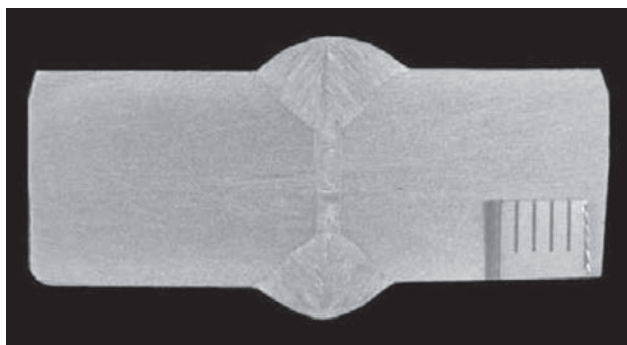
Figure 13. Macrostructure of welded joint of 12 mm thickness (P_l = 5.5 kW, v_w = 1.2 m/min, v_{wf} = 8.6 m/min, arc current I_a = 250 A, arc voltage U_a = 28 V, Q = 6.3 kJ/cm)
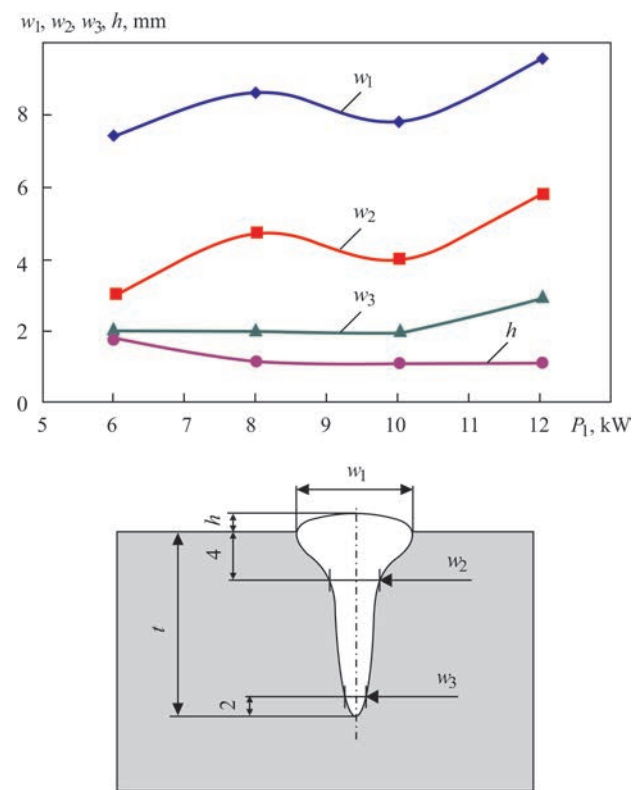

Figure 11. Dependence of weld dimensions on laser beam power in HLAWCE
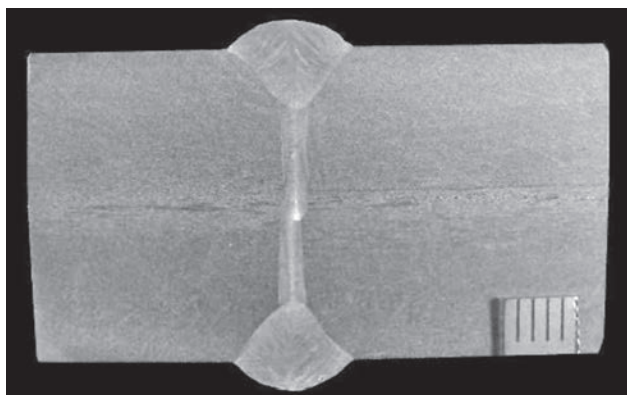
Figure 14. Macrostructure of welded joint of 20 mm thickness (P_l = 6.5 kW, v_w = 1.0 m/min, v_{wf} = 8.5 m/min, arc current I_a = 235 A, arc voltage U_a = 27 V, Q = 7.7 kJ/cm)
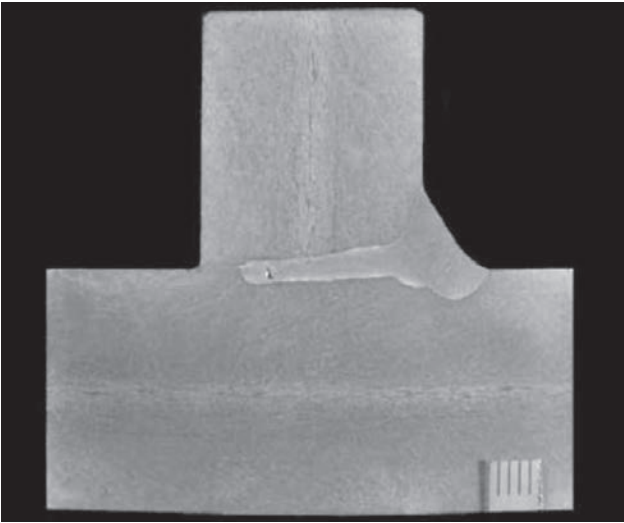
Figure 15. Macrostructure of one-sided T-joint of 20 mm thickness with partial penetration (P_1 = 10.0 kW, v_w = 0.7 m/min, v_{wf} = 8.5 m/min, I_a = 227 A, U_a = 29 V, Q = 14.2 kJ/cm)
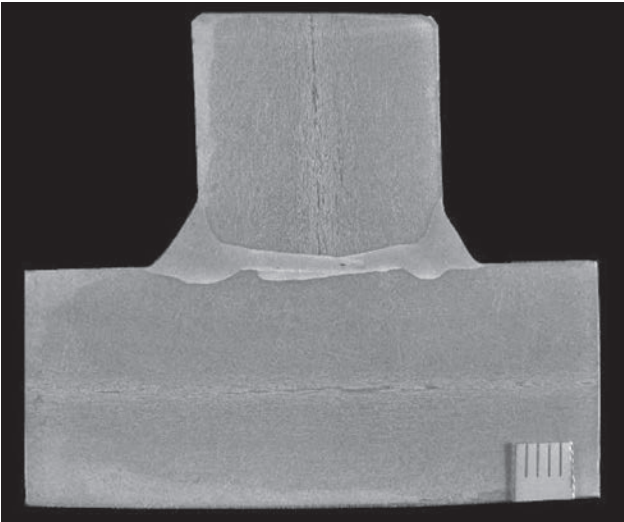
Figure 16. Macrostructure of double-sided T-joint of 20 mm thickness (P_1 = 10.0 kW, v_w = 1.3 m/min, v_{wf} = 8.5 m/min, I_a = 241 A, U_a = 28 V, Q = 7.7 kJ/cm)

Figure 17. Back side of T-joint of sheets of 20 mm thickness — humps

Figure 18. Longitudinal section of butt joint of 8 mm thickness – humps and porosity
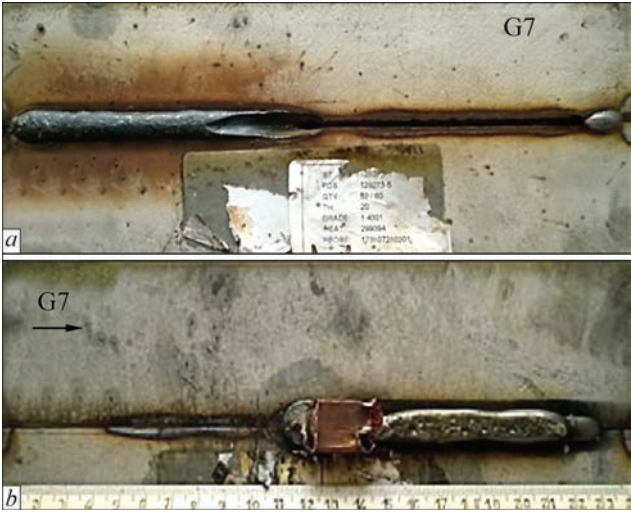
Figure 19. Appearance of one-sided welded joint with a thickness of 20 mm (P_1 = 11.0 kW, v_w = 0.4 m/min, v_{wf} = 8.5 m/min, I_a = 222 A, U_a = 31 V, Q = 21.5 kJ/cm): *a* — face side — unfilled groove and burn-through after about 110 mm; *b* — root side — lack of penetration, excess melting and penetration of copper pipe for forming gas supply

With an increase in the power of laser beam, penetration depth increases, however, not according to linear dependence. A change in the power of laser beam from 6 to 8 kW leads to an increase in the penetration depth by about 4.5 mm (Figure 10). With a further increase in the power by 2 kW, the penetration is higher by 0.7 mm. At a power of laser beam being 12 kW, the penetration depth was 18.5 mm. With an increase in the laser beam power by 50 %, from 8 to 12 kW, the penetration depth is increased by 1.6 mm, i.e., only by 9 %.

Based on these results, the modes of laser + MAG hybrid welding of double-sided butt joints of steels X2CrNi18-9 and X2CrNiMoN21-5-1 with a thickness of 8, 12 and 20 mm (Figures 12–14) in flat position, butt joints of these sheets with backing welding using MAG and HLAWCE method, as well as one-sided and double-sided T-joints were determined (Figures 15, 16).
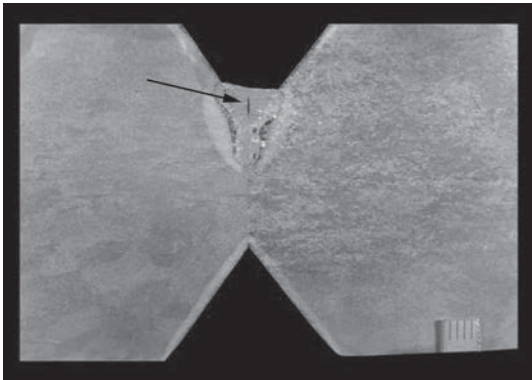
Figure 20. Macrostructure of root weld of butt joint of steel X6Cr13 with a crack (indicated by an arrow)

Non-destructive and destructive tests of a double-sided butt joint of plates of steel X2CrNi18-9 with a thickness of 12 + 12 mm (see Figure 13) showed that they meet the requirements of the standard ISO 15614-14 for certification of hybrid welding procedure.

Defects in welds of HLAWCE. Specific defects of one-sided welds made by hybrid welding include unstable formation of back side (root) of welds and porosity (Figures 17, 18).

In one-sided welding of hybrid butt joints, typical defects are lack of penetration at the weld root and excess of penetration. At the beginning there is a region of the weld without a full penetration, then, a short region with a full penetration goes, followed by a burnout and leakage of liquid metal of weld pool (Figure 19).

Defects of welds of high-alloy steels, made by hybrid welding, include also hot cracks. The susceptibility to hot cracks formation was observed in case of producing a root weld of a butt joint of steel X6Cr13 of 50 mm thickness with root face of 15 mm (Figure 20).

Conclusions

1. Hybrid laser + MAG welding allows producing double-sided butt joints of steel X2CrNi18-9 and X2CrNiMoN21-5-1 with a thickness of 8, 12 (one-sided) and 20 mm (double-sided), as well as butt joints with backing welding by the MAG and HLAWCE method with a full penetration in flat position.

2. Hybrid welding allows producing T-joints of sheets susceptibility of 8, 12 and 20 mm thickness with a butt weld with a partial penetration, often replacing T-joints with a fillet weld, as well as T-joints of sheets of up to 20 mm thickness with a butt weld in flat position.

3. Specific defects of welds of high-alloy stainless steels made by hybrid welding include: unstable formation of the root of welds, porosity and hot cracks.

1. Atabaki Mazar, M., Ma, J., Yang, G., Kovacevic, R. (2014) Hybrid laser/arc welding of advanced high strength steel in different butt joint configurations. *Materials and Design*, **64**, December, 573–587.

2. Brian, M. Victor (2011) Hybrid laser arc welding. *Edison Welding Institute, ASM Handbook, 6A, Welding Fundamentals and Processes*, 321–328

3. Krivtsun, I.V., Krikent, I.V., Demchenko, V.F. et al. (2015) Interaction of CO_2-laser radiation beam with electric arc plasma in hybrid (laser + TIG) welding. *The Paton Welding Journal*, **3–4**, 6–15.

4. Lembeck, H. (2010) Laser hybrid welding of thick sheet metals with disk lasers in shipbuilding industry. *Int. Laser Technology Congress AKL*.

5. Turichin, G., Velichko, O., Kuznetsov, A. et al. (2014) Mobile hybrid system for pipeline welding on the base of 20 kW fiber laser. In: *Proc. of 8th Int. Conf. on Photonic Technologies LANE*, 1–4.

VACUUM DIFFUSION WELDING OF γ-TiAl INTERMETALLIC WITH HIGH-TEMPERATURE NICKEL ALLOY WITH APPLICATION OF INTERMEDIATE Al/Ni NANOLAYERS

Iu.V. FALCHENKO, L.V. PETRUSHYNETS, T.V. MELNICHENKO, A.I. USTINOV and **V.E. FEDORCHUK**

E.O. Paton Electric Welding Institute of the NAS of Ukraine
11 Kazymyr Malevych Str., 03150, Kyiv, Ukraine. E-mail: office@paton.kiev.ua

Effect of structural characteristics and chemical composition of nanolayered interlayers based on Al–Ni system on formation of joints of γ-TiAl-based alloy and high-temperature nickel alloy in vacuum diffusion welding was studied. It is shown that application of nanolayered clad interlayers ensures formation of a diffusion zone with monotonic change of the content of components, where the phase composition and micromechanical characteristics are determined by the interlayer chemical composition, as well as lowers the probability of brittle phase appearance in the butt joint. 18 Ref., 6 Tables, 7 Figures.

Keywords: vacuum diffusion welding, intermetallics, nanolayered interlayers

Titanium aluminides are a promising materials for manufacturing parts of aircraft engines, sheathing and honeycomb structures of supersonic flying vehicles [1]. Casing seals, air filters, nozzle parts, compressor blades, combustion chamber structure elements, car engine valves, etc. are manufactured from cast titanium aluminides [2].

With progress of aerospace technologies and development of new structural high-temperature alloys, the need arises for joining pairs of dissimilar materials, for instance, γ-TiAl intermetallic alloys and nickel-based high-temperature alloys. Combination of dissimilar high-temperature materials in the structure widens the possibilities of its functional application.

The currently available technologies of fusion welding of these materials do not allow obtaining high-quality welded joints, because of liquation phenomena, structural and phase transformations in the weld metal and HAZ, that leads to hot cracking in the joint [3, 4]. Vacuum diffusion welding (VDW) is the most promising method of joining γ-TiAl-based alloys to nickel-based high-temperature alloys [5–7]. However, with this welding method, joint formation is accompanied by appearance of a diffusion zone of a complex phase composition, including brittle phases, which can have a negative effect on the joint mechanical properties. On the other hand, such low ductility of γ-TiAl makes it more difficult to establish physical contact in VDW. Ductile interlayers are usually used for activation of the surfaces being joined in diffusion welding of dissimilar materials and intensification of diffusion processes [8]. However, application of interlayers, produced by rolling and having 50–300 μm thickness, leads to formation of a diffusion zone with chemical composition and mechanical properties, markedly different from those of the materials being welded [9]. At application of such an approach, preliminary hydrogenation of the interlayers is used for intensification of diffusion processes in the joint zone. However, to prevent hydrogen evolution at the heating stage, welding is performed with application of high-intensity heat sources, capable of ensuring the rate of temperature rise of up to 1200 °C/min [6].

In order to activate the diffusion processes at formation of the joint, it is promising to apply coatings or intermediate foils with nano- and submicrocrystalline structure, characterized by superplasticity that allows localizing plastic deformation of the surfaces being welded directly in the butt. So, the authors of [6] conducted laser modification of titanium aluminide surface that in combination with deposition of TiAl layer on the nickel alloy surface ensured producing a sound joint. The authors of [7, 10, 11] showed that application of nanolayered interlayers in the form of foil or coatings in VDW of dissimilar and difficult-to-deform materials, allows activation of the surfaces being welded, increasing the intensity of the diffusion processes and reducing the thermomechanical impact on the materials being welded. From this viewpoint, it is promising to apply an interlayer in the form of nanolayered reactive foil, produced by EBPVD method, which is characterized by intensive running of phase transformations and low-temperature plastic deformation at thermomechanical loading [12, 13]. Selection of chemical composition and structural characteristics of the interlayer is determined by chemical composition of the materials being welded and product operating temperature.

Table 1. Alloy chemical composition

Alloy	Chemical composition, wt.%							
	Al	Si	Ti	Cr	Mn	Fe	Ni	Nb
Ni-alloy EI437B	0.92	0.46	2.65	21.01	0.25	0.83	73.88	–
γ-TiAl alloy	32.65	–	59.24	3.9	–	–	–	4.21

The objective of this work is studying the features of formation of joints of γ-TiAl-based alloy and high-temperature nickel alloy with chromium content > 20 wt.% and with volume fraction of γ′-phase < 10 vol.% by VDW method through nanolayered interlayers.

Experimental procedure. Chemical composition of γ-TiAl-based alloy and high-temperature nickel alloy is given in Table 1.

γ-TiAl-based alloy was produced by the method of electron beam remelting with subsequent isostatic pressing under pressure of 120–150 MPa at the temperature of 1260 °C for 4 h that ensured heating of casting defects. The produced material was subjected to homogenizing annealing at 1100 °C for 6–8 h, low-speed rolling at the temperature of 1200 °C and homogenizing heat treatment at 1100 °C for 6–8 h. Produced alloy based on γ-TiAl intermetallic is characterized by lamellar two-phase structure of γ/α₂.

High-temperature nickel alloy with < 10 vol.% volume fraction of γ′-phase belongs to the group of satisfactorily weldable alloys and is characterized by high heat resistance, low heat conductivity, high susceptibility to mechanical hardening (work hardening) during mechanical treatment [14].

Sample preparation for welding consisted in their cutting in electroerosion machine, surface grinding and degreasing. Samples were butt welded in U-394M unit. Diffusion welding of γ-TiAl intermetallic alloy with high-temperature nickel alloy was conducted in vacuum $V_w = 1.33 \cdot 10^{-3}$ Pa at temperature $T_w = 1050$ °C, pressure $P_w = 20$ MPa, and welding time $t_w = 20$ min.

Interlayers based on Al–Ni system in the form of nanolayered foil with uniform distribution of components and clad by metal layers 20–35 μm thick, with layer alternation period of 60–200 nm (Figure 1, *a*, *b*),
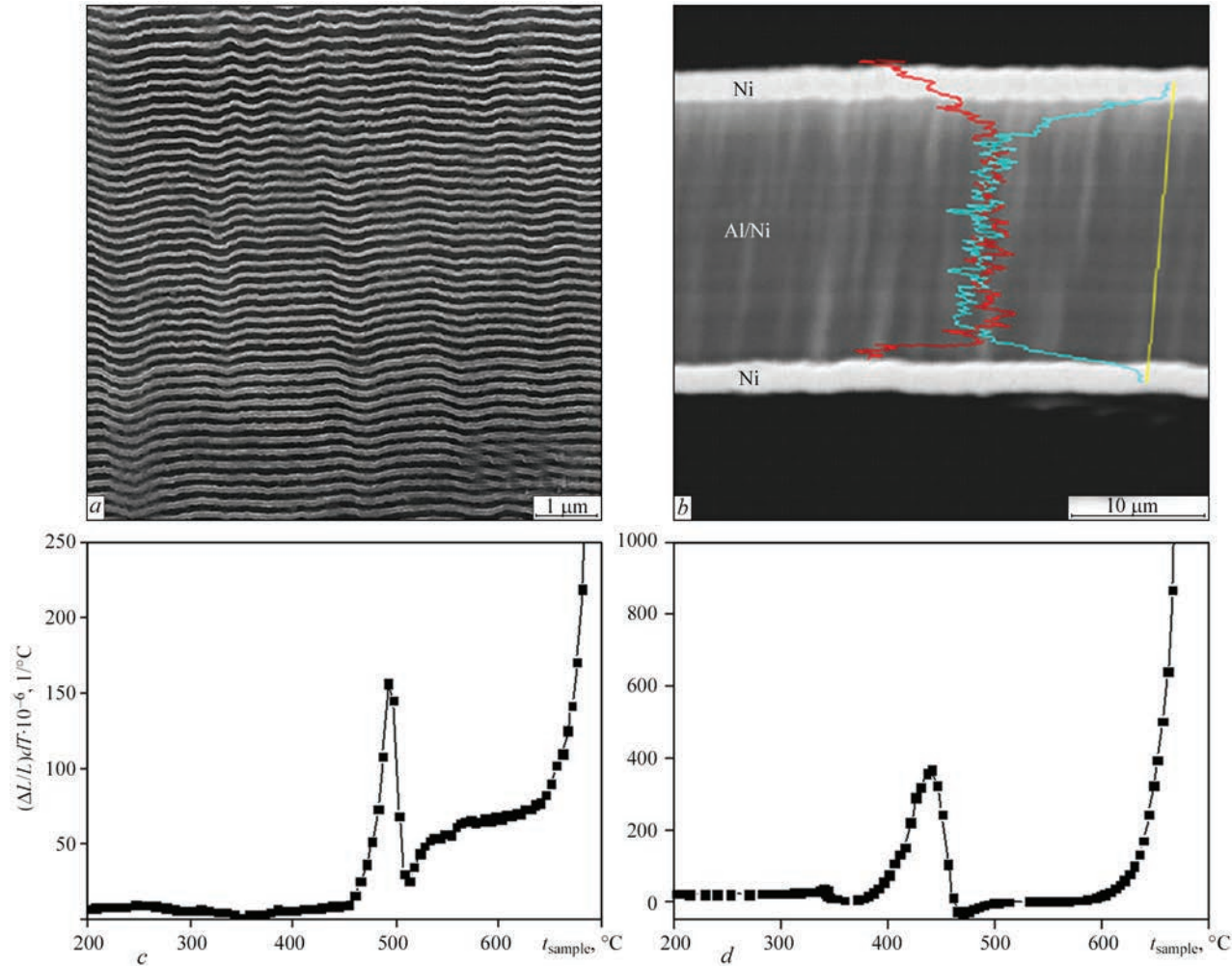

Figure 1. Microstructure and strain rate at heating under uniaxial tension of nanolayered foil with uniform distribution of the components (*a*, *b*) and of clad foil (*b*, *d*), respectively

Table 2. Interlayer characteristics

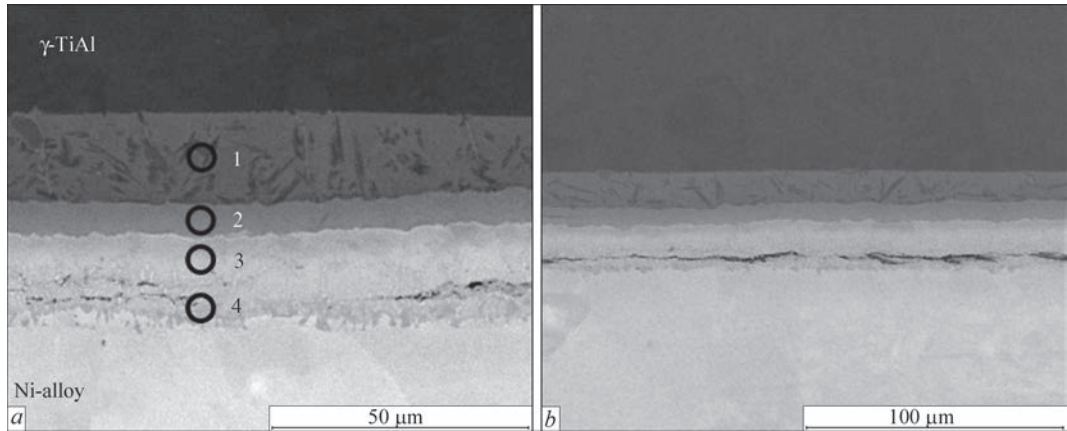| Interlayer	Chemical composition of Al/Ni reactive interlayer, wt.%		Thickness of reactive and cladding interlayers, μm		
	Al	Ni	Reactive interlayer	Cu	Ni
Al/Ni (AlNi)	34.82	65.18	30	–	–
Al/Ni (AlNi$_3$)	13.32	86.68	34	–	–
Ni–Al/Ni–Ni	32.56	67.44	17	–	3+3
Cu–Al/Ni–Ni	12.03	87.97	22	2	1

Figure 2. Microstructure of the joint of γ-TiAl — nickel alloy, produced by diffusion welding without an interlayer (*1–4* —analysis region)

were produced by the method of layer-by-layer electron beam deposition of vapour phases of aluminium and nickel, described in detail in [15]. Structure and chemical composition of interlayers are shown in Table 2. At heating of multilayer foil under the conditions of uniaxial tension, it undergoes low-temperature intensive plastic deformation, similar to superplastic deformation, that is due to phase and structural transformations, occurring in it at heating [13] (Figure 1, *c*, *d*).

Analysis of microstructure of welded joints and nanolayered foils was conducted using scanning electron microscope CamScan-4, fitted with a system of energy-dispersive analysis EDX INCA 200 for determination of chemical composition of material on flat samples. Samples for investigations in the form of transverse sections of the foils and welded joints were prepared by a standard procedure, using grinding-polishing equipment of Struers Company.

Evaluation of microhardness and coefficient of ductility of welded joints was performed by determination of micromechanical characteristics in Mi-

Table 3. Chemical composition of sections in the joint zone, shown in Figure 2, *a*

Analysis region	Chemical composition of analysis zones, wt.%						Phase
	Al	Ti	Cr	Fe	Ni	Nb	
1	22.92	65.48	4.3	–	3.78	3.52	–
2	24.45	39.41	4.4	0.48	28.15	3.11	τ$_3$
3	12.77	13.36	7.06	–	66.8	–	τ$_4$
4	7.7	5.83	35.66	–	50.82	–	–

cron-gamma unit by the method of automatic indentation, using Berkovich diamond pyramid (α = 65°) at 0.4 N load [16].

Investigation results. *Welding of γ-TiAl intermetallic alloy with high-temperature nickel alloy.* In VDW of titanium aluminide with EI437B alloy without interlayers the joint forms a diffusion zone approximately 35 μm thick, made up by intermetallic layers based on Ti–Ni–Al system of different composition (Figure 2, Table 3), predominantly consisting of τ$_3$-Al$_3$NiTi$_2$ and τ$_4$-AlNi$_2$Ti phases [17]. Formation of intermetallic layers leads to an increase of diffusion zone microhardness up to 14 GPa.

Formation of intermetallics with mechanical characteristics, markedly different from those of the alloys being welded, is due to stresses arising in the joint, leading to cracking at cooling (Figure 2) in the zones, adjacent to the nickel alloy, in which chromium diffusion results in formation of CrNi$_2$ brittle phase (Figure 2, *b*).

It can be assumed that the ductile nanolayered interlayer will not only ensure physical contact of the surfaces being welded, but will also have an effect on the nature of diffusion processes in the joint and formation of the diffusion zone phase composition. In order to assess such an effect, we studied the role of nanolayered interlayers based on Al–Ni system, having chemical composition, corresponding to the stoichiometry of AlNi and AlNi$_3$ intermetallics and of clad interlayers on their base, namely Ni–Al/Ni(AlNi)–Ni, Cu–Al/Ni(AlNi$_3$)–Ni in formation of γ-TiAl joints with the high-temperature nickel alloy.

Table 4. Chemical composition of sections in the joint zone, shown in Figure 4, *a*

Analysis region	Chemical composition of joint zones, wt.%					Phase
	Al	Ti	Cr	Ni	Nb	
1	22.94	59.72	1.76	11.62	3.97	–
2	13.69	24.27	–	60.64	1.4	τ_4
3	12.25	5.59	–	82.16	–	–
4	12.83	0.31	1.35	85.51	–	–

Investigation of the effect of Al/Ni interlayer on formation of the joint of intermetallic γ-TiAl alloy and nickel alloy.

1. Interlayer of AlNi composition.

Use of nanolayered foil of AlNi composition as an interlayer does not lead to joint formation (Figure 3), that, apparently, is the consequence of high reactivity of the foil and formation of a brittle intermetallic layer based on AlNi compound in the joint, the presence of which promotes cracking in the butt joint at cooling.

2. Interlayer of AlNi$_3$ composition.

Diffusion welding of γ-TiAl alloys and high-temperature nickel alloy was conducted using nanolayered foil of Al–Ni system as an interlayer, the composition of which corresponds to AlNi$_3$ intermetallics. As one can see from analysis of the joint microstructure (Figure 4, *a*), use of such an interlayer ensures activation of interdiffusion of the components of foil and alloys with formation of a sound joint. Considering the fact that the reactivity of nanolayered foil of AlNi$_3$ composition is by an order of magnitude lower [18] than of that of AlNi composition, it can be assumed that the nature of phase transformations at nanolayered interlayer heating has an effect on the diffusion processes in the joint. Interdiffusion of the components results in formation of a diffusion zone approximately 50 μm wide with a monotonic change of the component concentration in it (Figure 4, *b*, Table 4). Reaction diffusion of the alloys and interlayer
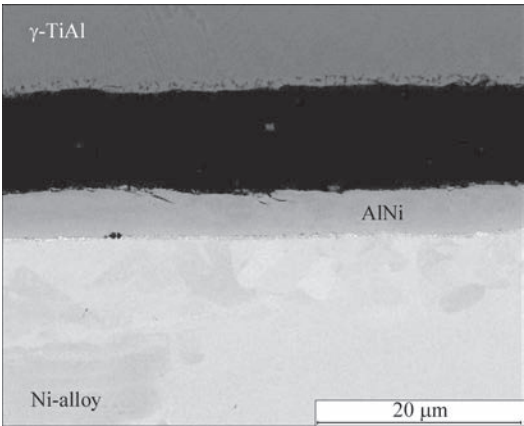

Figure 3. Microstructure of the joint of γ-TiAl — nickel alloy, produced using AlNi interlayer

components from the side of γ-TiAl results in formation of a ternary intermetallic phase τ_4 in the joint, leading to increase of the material microhardness in the butt joint area (Figure 4, *c*).

Effect of the clad interlayer based on Al-Ni system on formation of the joint of intermetallic alloy γ-TiAl and nickel alloy.

1. Ni–Al/Ni–Ni interlayer.

Absence of the joint formation when using an interlayer of the composition, corresponding to AlNi stoichiometry, gave grounds to assume that the presence of cladding interlayers of nickel on the nanolayered foil surfaces allows improving the physical contact of the surfaces being welded due to chemical affinity of nickel interlayers to γ-TiAl and nickel alloy [12].

Diffusion welding of γ-TiAl and nickel alloy was conducted through a clad Ni–Al/Ni–Ni interlayer, which consists of nanolayered foil of Al–Ni composition, corresponding to AlNi stoichiometry, and nickel cladding layers (Table 2). As shown by metallographic studies of welded joints, the butt joint does not have any pores or cracks (Figure 5).

Application of clad nanolayered foil in welding provides joint formation and promotes activation of
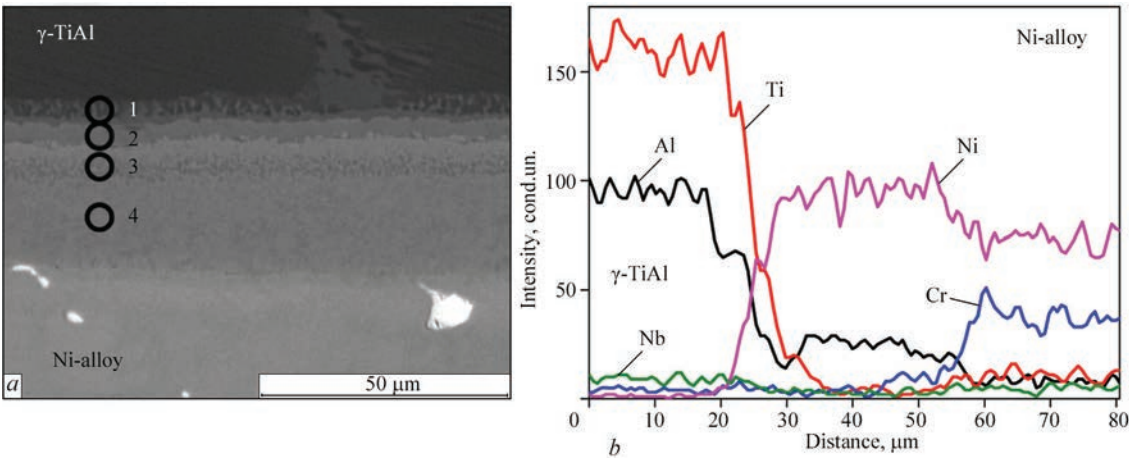

Figure 4. Microstructure (*a*) and component distribution (*b*) in the joint of γ-TiAl — nickel alloy produced using a nanolayered interlayer of AlNi$_3$ composition
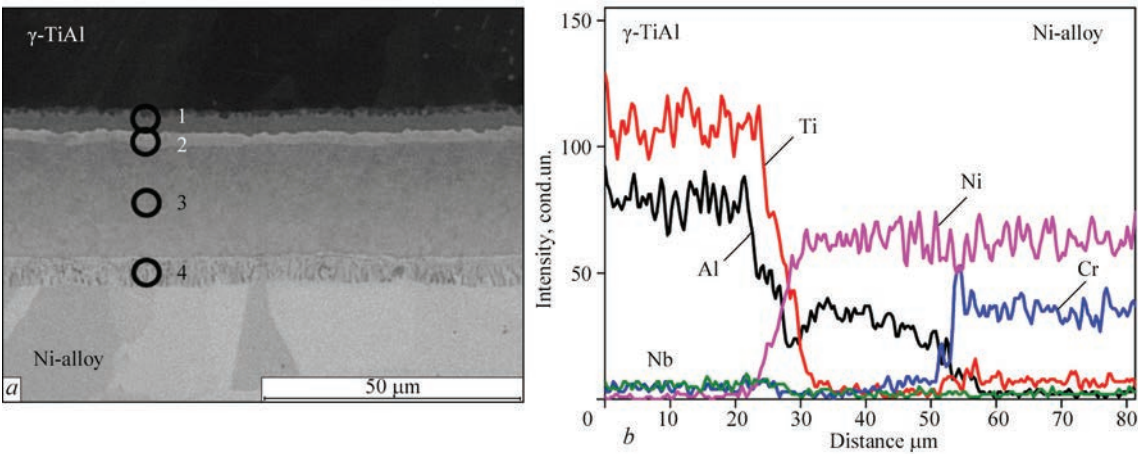
Figure 5. Microstructure (*a*) and component distribution (*b*) in the joint of γ-TiAl — nickel alloy, produced using clad Ni/Al–Ni/Ni interlayer

Table 5. Chemical composition of sections in the joint zone, shown in Figure 5, *a*

Analysis region	Chemical composition of the joint zones, wt.%				
	Al	Ti	Cr	Ni	Nb
1	24.94	40.39	3.52	28.05	3.11
2	13.77	24.07	0.40	60.67	1.10
3	21.78	0.75	1.06	76.41	–
4	6.20	3.01	24.56	66.23	–

the diffusion processes in the interlayer. Interdiffusion of the alloy and foil components leads to formation in the butt of a diffusion zone 45 μm wide with a monotonic change of component concentration (Figure 5, *b*) and laminated structure. Layers of intermetallic phases based on Ti–Ni–Al with different component ratios form from γ-TiAl side (Table 5). Presence of nickel layers on the intermediate foil surface, on the one hand, promotes reduction of chromium diffusion from the nickel alloy, that is indicated by a low chromium content in the diffusion zone, and on the other hand, ensures formation of an intermetallic enriched in nickel (Al_3Ni_5) in the central part of the diffusion

zone (Table 5, analysis region 3), that promotes lowering of material microhardness to 6.8 GPa.

2. Cu–Al/Ni–Ni interlayer.

Diffusion welding of γ-TiAl and nickel alloy was conducted through a clad Cu–Al/Ni–Ni interlayer, consisting of nanolayered foil of Al–Ni system, corresponding to stoichiometry of $AlNi_3$ and cladding layers of copper and nickel (Table 2). The interlayer was placed so that the copper layer contacted γ-TiAl, and the nickel layer was in contact with the nickel alloy. Such a placement of the interlayer is predetermined by the chemical affinity of the components of the cladding layers and the alloys.

The joint microstructure is shown in Figure 6, *a*. Diffusion mixing of the alloy components ensures formation of the diffusion zone, consisting of layers with different phase composition (Figure 6, *b*, Table 6), where copper is concentrated in the area close to titanium intermetallic, that is the consequence of chemical affinity of titanium and copper and, probably, formation of a low-temperature eutectic component, that improves the physical contact of the surfaces being welded.
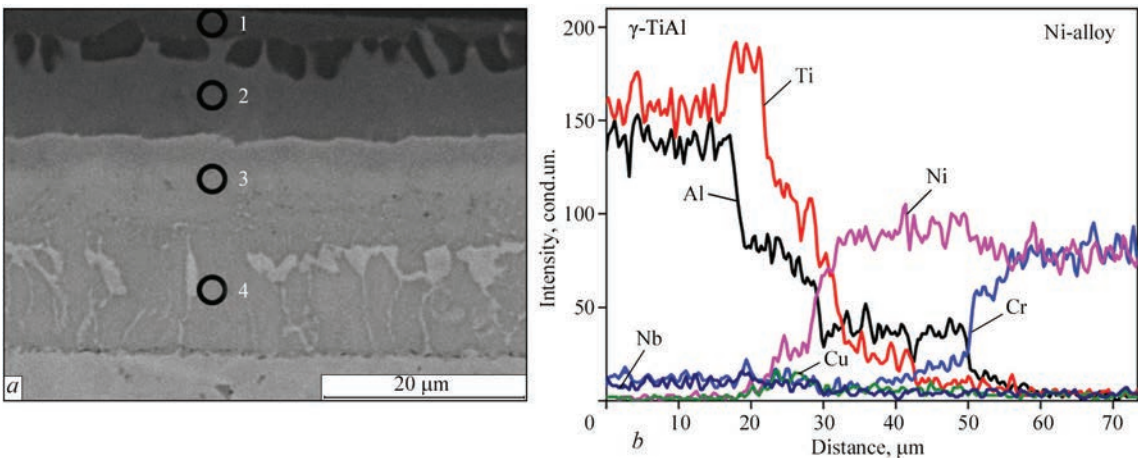

Figure 6. Microstructure (*a*) and component distribution (*b*) in the joint of γ-TiAl — nickel alloy, produced with application of clad Cu/Al–Ni/Ni interlayer

Table 6. Chemical composition of sections in the joint zone shown in Figure 6, *a*

Analysis region	Chemical composition of the joint zones, shown in Figure 6, *a*						
	Al	Ti	Cr	Fe	Ni	Cu	Nb
1	22.74	62.65	6.24	–	1.63	3.07	3.66
2	25.38	39.19	4.70	–	16.48	11.32	2.94
3	15.34	10.45	2.37	0.92	67.40	3.51	–
4	16.14	4.69	4.92	1.96	72.30	–	–

Figure 7 gives the values of microhardness and coefficient of ductility of the alloys being welded and the diffusion zone of the joints, produced by VDW without an interlayer and with a clad interlayer of different composition. One can see that application of a clad nanolayered interlayer allows lowering the material microhardness in the diffusion zone more than two times, compared to the joints produced without an interlayer at preservation of the coefficient of ductility on the level of that of the base materials.

Conclusions

1. Defects in the form of extended cracking sections appear in the joint from the nickel alloy side in diffusion welding of γ-TiAl alloy and high-temperature nickel alloy, that is the consequence of formation of brittle intermetallic phases with high microhardness (up to 14 GPa) and of $CrNi_2$ phase.

2. Application of a clad nanolayered interlayer based on Al–Ni system in diffusion welding of γ-AlNi alloy with the high-temperature alloy ensures producing sound joints due to formation of a diffusion zone with the monotonic nature of component distribution and lowering of its microhardness.

Figure 7. Microhardness and coefficient of ductility of γ-TiAl based alloy and nickel alloy, as well as their joints, produced by diffusion welding without the interlayer (1), with Ni–Al/Ni–Ni (2) and Cu–Al/Ni–Ni (3) interlayers

1. Bannykh, O.A., Povarova, K.B., Braslavskaya, G.S. et al. (1996) Mechanical properties of cast alloys γ-TiAl. *Metallovedenie i Termich. Obrab. Metallov*, **1**, 11–14 [in Russian].

2. Polkin, I.S., Kolachev, B.A., Iliin, A.A. (1997) Titanium aluminides and alloys on their base. *Tekhnologiya Lyogkikh Splavov*, **3**, 32–39 [in Russian].

3. Shorshorov, M.Kh., Erokhin, A.A., Chernyshova, T.A. (1973) *Hot cracks in welding of high-temperature alloys*. Moscow, Mashinostroenie [in Russian].

4. Zamkov, V.N., Velikoivanenko, E.A., Sabokar, V.K., Vrzhizhevsky, E.L. (2001) Selection of temperature of preheating of γ-titanium aluminide in electron beam welding. *The Paton Welding J.*, **11**, 17–20.

5. *Peng* He, Jun Wanga, Tiesong Lin, Haixin Li (2014) Effect of hydrogen on diffusion bonding of TiAl based intermetallics and Ni-based superalloy using hydrogenated Ti_6Al_4V interlayer. *Int. J. Hydrog. Energy*, **39**, 1882–1887.

6. Li, Z.F., Wu, G.Q., Huang, Z., Ruan, Z.J. (2004) Diffusion bonding of laser surface modified TiAl alloy/Ni alloy. *Materials Letters*, **58**, 3470–3473.
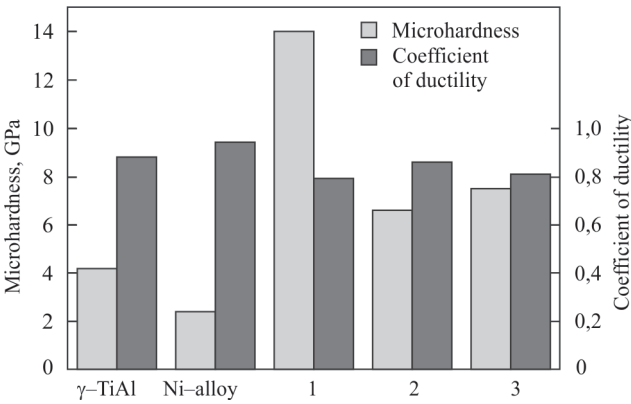
7. Ramos, A.S., Vieira, M.T., Simoes, S., Viana, F., Vieira, M.F. (2009) Joining of superalloys to intermetallics using nanolayers. *Advanced Materials Research*, **59**, 225–229.

8. Lyushinsky, A.V. (2001) Criteria of selection of intermediate layers in vacuum diffusion welding of dissimilar materials. *Svarochn. Proizvodstvo*, **5**, 40–43 [in Russian].

9. Yushtin, A.N., Zamkov, V.N., Sabokar, V.K. et al. (2001) Pressure welding of intermetallic alloy γ-TiAl. *The Paton Welding J.*, **1**, 33–37.

10. Ramos, A.S., Vieira, M.T., Simoes, S., Viana, F., Vieira, M.F. (2010) Reaction-assisted diffusion bonding of advanced materials. *Defect and Diffusion Forum*, **297–301**, 972–977.

11. Ustinov, A.I., Falchenko, Yu.V., Ishchenko, A.Ya. et al. (2008) Diffusion welding of γ-TiAl based alloys through nano-layered foil of Ti/Al system. *Intermetallics*, **8**, 1043–1045.

12. Ustinov, A., Olikhovska, L., Melnichenko, T., Shyshkin, A. (2008) Effect of overall composition on thermally induced solid-state transformations in thick EB PVD Al/Ni multilayers. *Surface and Coatings Technology*, **16**, 3832–3838.

13. Ustinov, A.I., Melnichenko, T.V., Shishkin, A.E. (2013) Deformational behavior of multilayer Ti/Al foils at heating under the conditions of continuously applied loads. *Sovrem. Elektrometallurgiya*, **4**, 27–33 [in Russian].

14. Anikeev, A.I., Vereshchaka, A.A., Vereshchaka, A.S., Bublikov, Yu.I. (2015) Superdispersed hard alloys as a tool material for milling of hard-to-machine materials. *Izv. Vuzov. Povolzhsky Region*, **3**, 152–162 [in Russian].

15. Ustinov, A.I., Olikhovskaya, L.A., Melnichenko, T.V. et al. (2008) Solid-phase reactions in heating of multilayer Al/Ti foils produced by electron beam deposition method. *Advances in Electrometallurgy*, **2**, 19–26 [in Russian].

16. Firstov, S.A., Gorban, V.F., Pechkovsky, E.P., Mameka, N.A. (2007) Equation of indentation. *Dopovidi Nats. Akademii Nauk Ukrainy*, **12**, 100–106 [in Russian].

17. Zeng, K., Schmid-Fetzer, R., Huneau, B. et al. (1999) The ternary system Al–Ni–Ti. Pt II: Thermodynamic assessment and experimental investigation of polythermal phase equilibria. *Intermetallics*, **12**, 1347–1359.

18. Dyer, T.S., Munir, Z.A. (1995) The synthesis of nickel aluminides by multilayer self-propagating combustion. *Metallurgical and Materials Transact. B*, 26(**3**), 603–610.
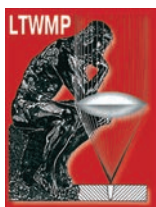
INTERNATIONAL CONFERENCE «BEAM TECHNOLOGIES IN WELDING AND MATERIALS PROCESSING»

In the period **from September 9 to 13, 2019**, IX International Conference «Beam Technologies in Welding and Materials Processing» (LTWMP-2019) was held in Odessa at «Arkadia» hotel. The Conference was organized by the E.O. Paton Electric Welding Institute of the NAS of Ukraine, NTUU «Igor Sikorsky Kyiv Polytechnic Institute» and International Association «Welding».

More than 60 scientists and specialists from Ukraine, Slovakia, Germany, Belarus and China took part in the Conference. It was organized in the form of plenary and poster sessions; conference working languages were Russian, Ukrainian and English (synchronous translation of the papers was provided). 37 presentations were made during the plenary and poster sessions.

The Conference was opened by Academician I.V. Krivtsun, Deputy Director of PWI, Chairman of Conference Program Committee. In his address he noted that papers on laser subjects, hybrid and 3D technologies were submitted for presentation at the conference, as well as papers on electron beam technologies in welding and special electrometallurgy. Academician I.V. Krivtsun also noted the role of the vapour-gas channel in beam technologies at forma-

tion of welded joints and role of the synergic effect in hybrid technologies.

Let us mention some of the papers which give an idea about the issues raised at the conference:

● «Features of formation of metal structure of products from titanium alloys, produced by 3D printing with application of profiled electron beam by xBeam 3D Metal Printing Technology», *Kovalchuk D.V.*, PJSC «NVO «Chervona Hvilya», Kyiv;

● «Contribution to the welding of hot-rolled aluminium-lithium alloys by electron beam», *Drimal Daniel*, PRVA ZVARACSKA a. s., Bratislava, Slovak Republic;

● «Specialized technological electron beam equipment for realization of additive process of layer-by-layer manufacturing of metal products with application of powdered materials», *Nesterenkov V.M.*, PWI, Kyiv;

● «Electron beam melting of high-temperature titanium alloys of Ti–Si–Al–Zn–Sn system», *Severin A.Yu.*, SC «SPC Titan» of PWI, Kyiv;

● «Optimization of technological parameters of layer-by-layer formation of products from VT6 titanium alloy using EBW based on mathematical modeling», *Kandala S.M.,* PWI, Kyiv;

Academician I.V. Krivtsun addressing the Conference at the opening

Participants of LTWMP-2019 Conference

● «Optimization of technological operations of laser welding and laser surfacing of elements of small-sized nozzle blocks of liquid rocket engines», *Shelyagin V.D.,* PWI, Kyiv;

● «Modeling of temperature fields in electron beam sintering», *Semenov O.*, PWI, Kyiv;

● «Electron beam technology as a method of producing thermal barrier coatings of ZrO_2–Y_2O_3 system with good functional characteristics on different types of metal bond coats», *Kurenkova V.V.,* LLC «Paton Turbine Technologies», Kyiv;

● «Formation of consumable electrodes from sponge titanium by the method of electron beam surface melting», *Pikulin A.N.*, SPC «Titan» of PWI, Kyiv;

● «Microstructure of VT20 titanium alloys produced by the method of layer-by-layer electron beam surfacing with application of local powdered materials», *Matviichuk V.A.*, PWI, Kyiv;

● «Hybrid laser-microplasma welding of stainless steels», *Khaskin V.Yu.,* Chinese-Ukrainian Paton Institute of Welding, Guangzhou, PRC;

● «Adaptive control of the process of laser welding and surfacing of parts of a complex shape, while ensuring the geometrical accuracy of trajectory movements», *Kombarov V.V.,* SPC «KHAI-Engineering». Kharkiv;

● «Regularities of the effect of the parameters of selective laser melting (SLM) on formation of a single layer from high-temperature nickel alloy INCONEL 718», *Adzhamskyi S.V.,* LLC «Laser additive technologies of Ukraine», Dnipro;

● «Structure and properties of the joints of AA7056 T351 aluminium alloy, made by electron beam welding», *Berdnikova E.N.,* PWI, Kyiv*;*

● «Modeling of the stress-strain state of steam turbine blades from titanium alloy at reconditioning repair with application of electron beam surfacing», *Kandala S.M.,* PWI, Kyiv;

● «Investigations of laser-casting process of producing bimetals for different functional purposes», *Salii S.S.*, NTUU «Igor Sikorsky Kyiv Polytechnic Institute», Kyiv;

● «EBW and heat treatment of sparsely doped titanium alloys based on β-phase», *Belous V.Yu.*, PWI, Kyiv;

● «Elimination of humping effect in laser-arc welding of higher strength steels», *Khaskin V.Yu.,* Chinese-Ukrainian Paton Institute of Welding, Guangzhou, PRC;

● «Structure and properties of dissimilar titanium-aluminium welded joints, produced by laser welding», *Sidorets V.N.,* PWI, Kyiv;

● «Hybrid system for electron beam evaporation and ion sputtering», *Kuzmichev A.I.,* NTUU «Igor Sikorsky Kyiv Polytechnic Institute»;

● «Electron beam melting of sparsely doped titanium-based alloys», *Berezos V.A.,* SPC «Titan» of PWI, Kyiv;

● «Investigation of the features of the processes of welded joint formation in laser welding of steels and alloys in different positions», *Bernatskyi A.V.*, PWI, Kyiv;

● «Effect of condensed multilayer protective coatings on cyclic strength of VT-6 alloy», *Mikitchik A.V.*, International Center for Electron Beam Technologies of PWI, Kyiv;

● «Microstrengthening of the boundaries of deposited layers in items produced by electron beam surfacing», *Khokhlova Yu.A.*, PWI, Kyiv.

Presentations on laser application in medicine, for 3D printing of plastics and two presentations on application of non-beam concentrated heat sources were also made:

● «Effect of pulsed-arc welding modes on thermal cycles and geometrical parameters of welds and HAZ of welded joints made by high-alloyed welding consumables», Poznyakov V.D., *PWI*, Kyiv;

● «Melting temperature of metal nanoparticles in plasma», *Dragan G.S.,* SRI of Physics of I.I. Mechnikov Odessa National University.

Outside of conference program, *A.P.Mukhachev*, Director of the Center of Chemical Technologies of the Academy of Engineering Sciences (Kam'yanske) spoke about the directions of the Center activity on restoration of hafnium, zirconium, niobium and molybdenum production in electron beam remelting units in Ukraine.

Polishko A.A. (PWI) made a presentation about YPIC/WRTYS 2020 «Young Professionals International Conference on Welding and Related Technologies», May 19–22, 2020, Kyiv (https://ypic2020.com) and invited the scientists, specialists and business leaders to take part in it as presenters, listeners and sponsors. Representatives of a number of Ukrainian industrial enterprises from Kyiv, Dnipro, Zaporizhzhia, Kharkiv, Kryvyi Rih, Kam'yanske, using laser and beam technologies in the production cycle, also participated in the conference without making presentations.

The Conference was completed by a Round Table on «New developments in the field of 3D beam technologies». During the round table urgent problems of development of beam welding technologies were discussed in relation to manufacturing 3D products from various metallic materials, and finished products were demonstrated, which were manufactured by laser 3D prototyping (LLC «Laser Additive Technologies of Ukraine») and in electron beam units (PJSC «NVO «Chervona Hvilya», PWI).

Proceedings of LTWMP-2019 Conference will be published by the end of 2019. The Proceedings of the previous eight LTWMP Conferences can be ordered from «Avtomaticheskaya Svarka» Editorial Board or received in the public domain in PWI publishing house site at the following link: http://patonpublishinghouse.com/eng/proceedings/ltwmp.
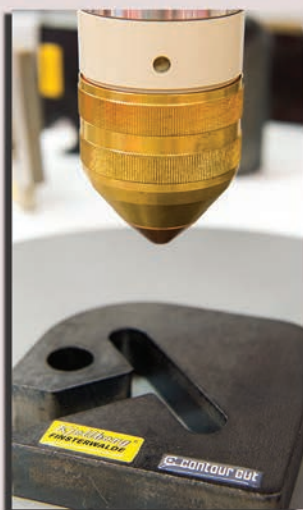
Friendly, hospitable and creative atmosphere of the Conference contributed to development of useful discussions, and establishing business contacts. Conference participants unanimously supported the proposal to conduct the following tenth International Conference on beam technologies in welding and materials processing (LTWMP-2021) in September 2021 in Odessa, Ukraine.

Organizing Committee of LTWMP-2019 Conference expresses gratitude and appreciation to PJSC «NVO «Chervona Hvilya», High Energy Technologies Companies, Chinese-Ukrainian Paton Institute of Welding, PWI «Titanium» Center, PWI Electron Beam Welding Center, and PWI International Center for Electron Beam Technologies for their assistance in conducting the Conference.

Dr. A.T. Zelnichenko

Calendar of October*

OCTOBER 1, 1934   Presidium of the USSR AS appointed E.O. Paton (1870–1953) as a director of Electric Welding Institute. To recognize welding as a reliable technological process it was necessary to carry out complex investigations of mechanics of welded structures, processes of metallurgy and materials science of welding, arc discharge physics; it was a need in development of apparatuses, materials and new welding technologies. These are the purposes, which made a basis for establishment by the initiative of E.O. Paton the first in the world practice Institute, which in the next years won leading grounds in development of welding engineering and technologies.

OCTOBER 2, 1934   First fly of training, two-seater low-wing aircraft AIR-9 with M-11 engine of Yakovlev DTB, piloted by pilot Yu.I. Piontkovsky. On July 4, 1937, pilots Irina Vishnevskaya and Ekaterina Mednikova made a woman international record for light aeroplanes of the first category. They reached 6518 m height. The fuselage of the plane is truss, welded of steel tubes and additionally braced. Such a decision was very unusual for that time, but significantly simplified plane production.

OCTOBER 3, 1967   Experimental rocket airplane «North American X-15A-2» gained the speed of 7273 km/h that is 6/72 times higher the sound velocity. First and for the 40 years single in the history piloted hyperacoustic air vehicle-plane performed suborbital piloted space flights. The peculiarity of airplane «North American X-15» was wide application of welding in its production. Thus, around 70–80 % of welded structures were in the airplane structure.

OCTOBER 4, 1957   First artificial Earth satellite was launched. Work of designers and manufacturers during satellite production was carried out simultaneously due to constricted terms. The main difficulty was in manufacture of spherical semi-shells by hydrodrawing, their welding with frame and polishing of the outer surfaces, even minor scratches were not allowed on them; welding of welds should be tight and was X-ray controlled, and tightness of assembled container was checked by helium leak detector.

OCTOBER 5, 1929   Birthday of N.P. Lyakishev (1929–2006), researcher-metallurgist, academician of the RAS and NAS of Ukraine. He developed a series of sparsely-alloyed cold-resistant steels with good weldability for main gas pipelines of northern designation and technological processes of their commercial production. He initiated implementation in the metallurgy of the process of direct iron production. In 1975–1984 he was a director of I.P. Bardin TsNIIchermet; in 1987–2004 he was a director of A.A. Baykov Institute of Metallurgy and Materials Science.

OCTOBER 6, 1893   Birthday of Meghnad Saha (1893–1956), Indian physicist and astronomer, member of the Royal Society of London (1927). The scientific works of M. Saha refers to thermodynamics, static physics, astrophysics, theory of propagation of radio waves, nuclear physics. An important scientific basic for development of arc welding was a theory on plasma ionization. To characterize the process of ionization M. Saha in 1921 proposed the equitation, named after that by his name. In development of this equation in 1924 I. Langmuir derived the formulae for determination of the level of ionization of vapors of substance evaporating from heated surfaces.

OCTOBER 7, 1934   Akulov N.S. (1900–1976), Soviet physicist, academician, specialist in the field of ferromagnetism developed in 1934 the first magnetic flaw detector. He studied influence of magnetic fields on different characteristics of ferromagnetic metals. He was awarded with the USSR State Prize for application of developed theory of ferromagnetism in metal flaw detection.

OCTOBER 8, 1936   Birthday of V.N. Zamkov (1936–2005), a well-known scientist in the field of metallurgy and welding of titanium alloys. Among the works of V.N. Zamkov it is necessary to note the development of a new method of argon-arc welding of titanium over a flux layer, which allowed fundamentally changing titanium welding technology, and thus, solving the problem of increase of welded joint quality. Under his direct leaders there were developed fundamentally new consumables for welding, namely fluxes and flux-cored wires.

OCTOBER 9, 1950   USSR State Prize was awarded to B.I. Medovar, R.I. Lashkevich (PWI), G.K. Slysh, A.M. Garagulya, P.I. Sobolev (Khartsyzsk Pipe Plant) for development of a new high-performance method of automatic twin arc welding of large diameter pipes. Method of automatic twin arc welding of pipes promoted rapid development of domestic pipe production.
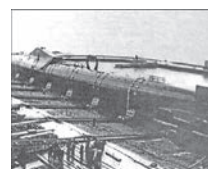
OCTOBER 10, 1731   Birthday of Henry Cavendish (1731–1810), British physicist and chemist. In 1766 Cavendish published the first important work on chemistry «Artificial air», where he informed about discovery of «combustible air» (hydrogen). He extracted (1766) carbon dioxide and hydrogen in pure form, accepting the latter as phlogiston, determined the main composition of air as a mixture of nitrogen and oxygen. He derived nitrogen oxides. These discoveries were an important constituent for next development of technology of autogenous welding.

OCTOBER 11, 1963   Howaldtswerke-Deutsche Werft Company in Kiel lied down a keel Otto Hahn, one of the fourth ever built merchant ships with nuclear power system. It was set afloat in 1964. In 1968 38-megawatt nuclear reactor of the ship was launched and seal trial was started. In October of the same year Otto Hahn was certified as merchant and research ship. In order to secure a crew it was decided to weld a reactor block in special large compartment. At that particularly rigid requirements were made to the welds and for this multiple tests of their quality were carried out.

OCTOBER 12, 1940   Soviet pilot V. Kokkinaki started testing of the second variant of single-seat plane Il-2, Soviet attack aircraft designed at DTB-240 under the leadership of Ilyushin S.V. Being the main attack power in the Soviet aviation, Il-2 attack aircraft played outstanding role in the Second World War. It was the war-plane of the most mass production in the history of air construction. In total there were produced 36 thou. The fuselage of the aircraft was all-metal or mixed type. The front part represented itself welded shell (armored hull) of stamped sheets of armor of 4–6 mm thickness, joined by riveting and welding. Developed high-performance technology of combined welding of elements of structure of Il-2 and Yak-7 of hardened steel was honored with Stalin Prize in 1946.

OCTOBER 13, 1941   State Defense Committee made a decision on construction of two plants in Barnaul, one of them on production of tank T-50. Tank hull was welded of armour sheets of 45 mm thickness, except for bottom and top (20 mm). In welded faceted turret 45 mm gun of 1934 year type and coaxial with it machine-gun of 7.62 mm bore were located. Sheet of the hull of T-50 were joined by welding and located under high tilting angles. To 1942 the engineering drawings for hull of homogenous armour of 40 mm thickness optimized for semi-automatic welding were prepared.

OCTOBER 14, 1948   The first in the history of aviation supersonic flight took place in 1947. It was done by pilot Charles Yeager on «Bell X-1» plane with liquid rocket which was launched from carrier aircraft Boeing-B29 and gained 2600 km/h velocity. Airframe was made of high-strength aluminum, fuel tanks were welded of steel. Welding was also used in manufacture of airframe parts.

OCTOBER 15, 1992   Publication of one of the patents of B.I. Medovar (1916–2000), leading scientist in the field of welding and metallurgy, academician, representative of the Paton school. Starting from 1960 he was developing the theoretical fundamentals of materials science and metallurgy of austenite steel welding. He was dealing with the problems of surfacing, remelting and casting. He is one of co-authors of technology of electroslag welding. Starting from 1979 he was a head of the works on development of new class of structural metallic materials obtained by electroslag remelting method.

OCTOBER 16, 2104   The last model of new generation of iMac computers was issued. The main peculiarity of it was strikingly thin body. In presentation it was mentioned in passing about some revolutional welding technology, which allowed making the body significantly thinner. It emerged that for joining the parts of new iMac the technology of rotation friction welding was used. As a result it was possible to get smoother and stronger joint, which provides the possibility to make the part thinner at that this process uses less energy than traditional joining technologies. Thanks to this thickness of body edge in Apple compurer is only 0.5 cm.

OCTOBER 17, 2001 Day of death of P.I. Sevbo (1900–2001), a well-known designer and scientist, representative of the Paton school, which for a long time was a head of design bureau of the E.O. Paton Electric Welding Institute. During the Second World War the personnel of the bureau under P.I. Sevbo leadership rapidly developed and implemented tens of specialized apparatuses and machines for automatic welding of armour hulls of T-34 tank. In the post-war years P.I. Sevbo actively worked on development and improvement of welding equipment for many braches of industry. He developed a series of projects related with complex automation of welding production.

OCTOBER 18, 1888 Method of metal-arc welding developed by N.G. Slavyanov was tested on public in presence of state commission in welding of crankshaft steam-engine. This date is considered as a birthday of Russian electric welding. The first in the world welding shop (so called electric casting factory with electric generator) was organized at the plant and since 1889 the record started to be kept «Record on works carried using electric casting of mining engineer Slavyanov at Perm cannon plant». Certificates on quality of performed works after part operation was mandatory attached to the record.

OCTOBER 19, 1958 Opening of the First International Exhibition in Brussels, where one of the main sights was Atomium. One the symbols of Brussels is a huge steel construction located on North-West, on Heysel park hill. It was designed by architect André Waterkeyn and constructed under the leadership of André and Michel Polak. By the idea of Waterkeyn its structure symbolizes beginning of new age, i.e. age of science, exploration of space and peaceful usage of nuclear energy. These unusual structure consists of 9 spheres «atoms» and presents a model of crystal of ferrum enlarged 165 bln times. Atomium can be considered as an anthem of welded structures of the XX century.

OCTOBER 20, 1480 Birthday of Vannoccio Biringuccio (1480–1539), Italian alchemist, metallurgist and architect. He was studying alchemy, metallurgy and casting for a long time in Italy, Czechia and Austria. He was a well-known in Europe casting craftsman and dealt with manufacture of military equipment in Florentine Republic. Here in 1529 Biringuccio casted one of the largest for that time cannons of more that 6 t weight and 6.7 m length. In his ten-volume work «Pyrotechnics» he describes, in particular, creation of butt joint using forge welding with the help of silver, broken glass and other materials. This was the way for joining swards and other types of weapon.

OCTOBER 21, 1954 Birthday of I.V. Krivtsun, leading scientist in the field of theoretical investigations and mathematical modelling of physical phenomena in low-temperature technological plasma, academician, representative of the Paton school. He developed such novel hybrid processes as laser-microplasma welding of metals of small thicknesses, laser-plasma powder surfacing and spraying of ceramic materials, laser-plasma deposition of diamond and diamond-like coatings. For practical implementation of indicated technological processes it was developed a series of integrated laser-arc plasmatrons, which have no analogues in the world practice. I.V. Krivtsun is the author of more than 270 research works, four monographs and ten patens.

OCTOBER 22, 1967 During the International Exhibition in 1967 the visitors were able to see the largest in the world open air geodesic dome, known as Montreal biosphere. The dome was constructed using approximately 65000 parts, including 13 km of extruded aluminum tubes welded in hexagon. It has no inner bearing elements and almost all 80 tons structures stands on five pylons filled with concrete.

OCTOBER 23, 1953 First public performance of the largest for that time helicopter YH-16 Transporter. It was piloted by Harold Peterson and George Callahan and became the first in the world helicopter with two gas turbine engines. Length of heavy transport helicopter made 24 m, diameter of two main rotor — 25 m. Such a dimensions were explained by technically set duration of flight, i.e. 2250 km. For the first time high-frequency resistance welding was used in construction of the helicopter.

OCTOBER 24, 1804 Birthday of Wilhelm Eduard Weber (1804–1891), German scientist-physicist. The main works of scientist belong to the field of magnetic phenomena and electricity. He determined an absolute system of electric measurements. The unit of measurement of magnetic flux is named after him. It was stated in 1881 at International Electric Congress in Paris.

CALENDAR OF OCTOBER

OCTOBER 25, 2005   Start of operation of airliner A380, wide-body passenger plane, the largest serial airliner in the world. According to the designers, the most complex problem in development of plane was the problem of weight reduction. Seat capacity is 525 passengers in the cabin of three classes and 835 passengers in one class configuration. Progressive welding technologies and improved aluminum alloys were used for reduction of plane weight. For lower panels of fuselage laser welding of stringers and skin was used that significantly reduced amount of fasteners.

OCTOBER 26, 1972   Sikorsky I.I. (1889–1972) died. He was a world-known aircraft designer of Ukrainian origin. First serially produced helicopter of his design Sikorsky R-4 Hoverfly flied for the first time on January 13, 1942. Its fuselage was framed and welded of steel tubes. Whole fuselage had linen skin. The cabin was with Plexiglas windows and aluminum aprons between them.

OCTOBER 27, 1984   Official opening of through traffic on Baikal-Amur mainline (construction in 1938–1984) of 3819 km length. Nowadays there is reconstruction of mainline, including laying of continuous track using alumothermic welding.

OCTOBER 28, 2013   Zumvalt class missile destroyer was set afloat. Zumvalt destroyer is the key part of the SC-21 program of USA Navy. Program started in 1991 was directed on development of a family of universal ships of new generation. Destroyers of this series are the multipurpose and designed for attacks of enemy on shore, counter-air missions and fire support from sea. Development of this type of ship is one of the recent achievements of military equipment. Arc welding having increased requirements to weld quality was widely used in this project realization.

OCTOBER 29, 1955   Battle ship Novorossiysk (until 1948 ship of Italian Navy «Giulio Cesare») went down in Sevastopol harbor. 829 people died. In May 1955 it was included in the Black Sea Navy Fleet and regardless declining ages (44 years) it became the most powerful ship in USSR. Repair was carried out in Sevastopol with wide application of welding.

OCTOBER 30, 1961   The most high-capacity explosive device in the history of humanity was exploded in Novaya Zemlya. AS of USSR headed the development of bomb AN602. Capacity of explosion is 575 megatons in TNT equivalent.

OCTOBER 31, 1935   First pilot variant of DI-6 plane (CDB-11), Soviet two-seat fighter was given by the plant-manufacturer for ground and plant tests. In the process of manufacture of this fighter atomic-hydrogen welding was used for the first time in the USSR for welding of wing spars. Fuselage of DI-6 is framed and welded of steel tubes with light outer cage, coated from the back side with linen. The wings are two-spar and welded of tubes. Later on the plane started to be produced with welded fuel tanks.